START-UP STRATEGIES FOR ENHANCED METHANE PRODUCTION FROM CATTLE MANURE IN BIOELECTROCHEMICAL SYSTEMS

A THESIS SUBMITTED TO
THE GRADUATE SCHOOL OF NATURAL AND APPLIED SCIENCES
OF
MIDDLE EAST TECHNICAL UNIVERSITY

BY

AMIN GHADERIKIA

IN PARTIAL FULFILLMENT OF THE REQUIREMENTS
FOR
THE DEGREE OF MASTER OF SCIENCE
IN
ENVIRONMENTAL ENGINEERING

DECEMBER 2022

Approval of the thesis:

START-UP STRATEGIES FOR ENHANCED METHANE PRODUCTION FROM CATTLE MANURE IN BIOELECTROCHEMICAL SYSTEMS

submitted by **AMIN GHADERIKIA** in partial fulfillment of the requirements for the degree of **Master of Science** in **Environmental Engineering, Middle East Technical University** by,

Prof. Dr. Halil Kalıpçılar
Dean, Graduate School of **Natural and Applied Sciences** _____

Prof. Dr. Bülent İçgen
Head of the Department, **Environmental Engineering** _____

Assist. Prof. Dr. Yasemin Dilşad Yılmazel Tokel
Supervisor, **Environmental Engineering, METU** _____

Examining Committee Members:

Prof. Dr. Filiz B. Dilek
Environmental Engineering, METU _____

Assist. Prof. Dr. Yasemin Dilşad Yılmazel Tokel
Environmental Engineering, METU _____

Prof. Dr. F. Dilek Sanin
Environmental Engineering, METU _____

Prof. Dr. Deniz Çekmecelioğlu
Food Engineering, METU _____

Assist. Prof. Dr. N. Işık Semerci
Energy Systems Engineering, Ankara University _____

Date: 22.12.2022

I hereby declare that all information in this document has been obtained and presented in accordance with academic rules and ethical conduct. I also declare that, as required by these rules and conduct, I have fully cited and referenced all material and results that are not original to this work.

Name Last name: Amin Ghaderikia

Signature:

ABSTRACT

START-UP STRATEGIES FOR ENHANCED METHANE PRODUCTION FROM CATTLE MANURE IN BIOELECTROCHEMICAL SYSTEMS

Ghaderikia, Amin
Master of Science, Environmental Engineering
Supervisor: Assist. Prof. Dr. Yasemin Dilsad Yilmazel Tokel

December 2022, 122 pages

Bioelectrochemical methane production, known as electromethanogenesis, provides an emerging technology for carbon recycling via the conversion of carbon dioxide to methane with the additional benefit of simultaneous organic waste reduction. Bioelectrochemical conversion reactions in an electromethanogenic microbial electrolysis cell (MEC) are catalyzed by electro-active biofilm on the electrodes; hence, biofilm formation has a key role in system performance. In this study, the objective was to evaluate the impacts of different start-up strategies on the performance of methane production from a complex waste, cattle manure in bioelectrochemical reactors. At first, the focus was on the performance of an electromethanogenic MEC and designed experiments for providing a comparative analysis of the impact of biofilm formation upon feeding a simple substrate, acetate (ACE), and a complex waste, cattle manure (CM). To this purpose, single chamber MECs were operated with an applied voltage of 0.7 V on a fed-batch mode. Upon biofilm formation on the sole carbon source (ACE or CM), a selected number of MECs (ACE_CM and CM_ACE) were subjected to cross-feeding during the test period. Even though the difference in the current production rate between the ACE_CM and CM_CM reactors was 20% in favour of the ACE_CM, cross-feeding

lowered methane production. The results showed that there was around 20% higher methane production rate (131.6 ± 2 mL/L-d) when CM was used as the sole feed. Evidently, microbial community analysis showed that the primary substrate shapes the community of the bioelectrodes and cross-feeding does not have a significant impact on the microbial community. Based on this knowledge, the second set of experiments was designed to investigate the impact of the use of biofilm attached electrodes formed via CM addition, and the amendment of a carbon-based conductive material, granular activated carbon (GAC), on the integrated system of anaerobic digestion – microbial electrolysis cell (AD-MEC). AD-MEC systems are a combination of MECs and conventional AD reactors and have recently been used for enhanced methane production from waste materials, however, there is limited information on the start-up procedures. Further, the choice of reactor medium (buffer) is significant in the performance of bioelectrochemical systems; therefore, in this work, the performance of AD-MEC reactors fed with CM using two different buffer solutions, 100 mM phosphate-buffered saline (PBS) solution and a salt media without phosphate has been compared. Using the salt buffer solution in the AD reactor resulted in a 4 times higher net methane yield and 5.8 times lower lag time than the same reactor with 100 mM PBS media. The highest methane production rate of 12.03±0.01 mL/d and methane yield of 318.1±1.4 mLCH_4/g volatile solids added (VS_{added}) were attained in the presence of salt medium with the amendment of biofilm-attached GAC, named, BioGAC when bare electrodes were used in AD-MEC. The yield attained in AD-MECs was around 25% higher than conventional AD.

Keywords: Anaerobic Digestion (AD), Microbial Electrolysis Cell (MEC), AD-MEC, Biofilm Formation, Bioelectrode

ÖZ

BİYOELEKTROKİMYASAL SİSTEMLERDE SIĞIR GÜBRESİNDEN ÜRETİLEN METANI ARTTIRMAK İÇİN BAŞLANGIÇ STRATEJİLERİ

Ghaderikia, Amin
Yüksek Lisans, Çevre Mühendisliği
Tez Yöneticisi: Dr. Öğr. Üyesi Yasemin Dilşad Yılmazel Tokel

Aralık 2022, 122 sayfa

Elektrometanojenesis olarak bilinen biyoelektrokimyasal metan üretimi, karbondioksitin metana dönüştürülmesi yoluyla karbon geri dönüşümü için gelişmekte olan bir teknoloji sağlamakta ve aynı zamanda organik atık azaltımı gibi ek bir fayda sağlamaktadır. Elektrometanojenik mikrobiyal elektroliz hücresindeki (MEH) biyoelektrokimyasal dönüşüm reaksiyonları, elektrotlar üzerindeki elektro-aktif biyofilm tarafından katalize edilir; dolayısıyla biyofilm oluşumu sistem performansında kilit bir role sahiptir. Bu çalışmada amaç, farklı başlatma stratejilerinin biyoelektrokimyasal reaktörlerde karmaşık bir atık olan sığır gübresinden metan üretiminin performansı üzerindeki etkilerini değerlendirmektir. İlk olarak, elektrometanojenik bir MEH'in performansına odaklanılmış ve basit bir substrat olan asetat (ASE) ve karmaşık bir atık olan sığır gübresi (SG) beslemesi üzerine biyofilm oluşumunun etkisinin karşılaştırmalı bir analizini sağlamak için deneyler tasarlanmıştır. Bu amaçla, tek hazneli MEH'ler beslemeli yığın modunda 0,7 V uygulanan voltajla çalıştırılmıştır. Tek karbon kaynağı (ASE veya SG) üzerinde biyofilm oluşumu üzerine, seçilen sayıda MEH (ASE_SG ve SG_ASE) test süresi boyunca çapraz beslemeye tabi tutulmuştur. ASE_SG ve SG_SG reaktörleri arasındaki mevcut üretim hızındaki fark ASE_SG lehine %20 olmasına rağmen,

çapraz besleme metan üretimini düşürmüştür. Sonuçlar, SG tek besleme olarak kullanıldığında yaklaşık %20 daha yüksek metan üretim oranı (131,6 ± 2 mL/L-d) olduğunu göstermiştir. Mikrobiyal komünite analizi, birincil substratın biyoelektrotların topluluğunu şekillendirdiğini ve çapraz beslemenin mikrobiyal topluluk üzerinde önemli bir etkisi olmadığını göstermiştir. Bu bilgiye dayanarak, ikinci deney seti, SG ilavesiyle oluşturulan biyofilm bağlı elektrotların kullanımının ve karbon bazlı iletken bir malzeme olan granül aktif karbonun (GAK) anaerobik çürütme - mikrobiyal elektroliz hücresi (AÇ-MEH) entegre sistemi üzerindeki etkisini araştırmak üzere tasarlanmıştır. AÇ-MEH sistemleri, MEH'ler ve geleneksel AÇ reaktörlerinin bir kombinasyonudur ve son zamanlarda atık maddelerden iyileştirilmiş metan üretimi için kullanılmaktadır, ancak başlatma prosedürleri hakkında sınırlı bilgi bulunmaktadır. Ayrıca, reaktör ortamının (tampon) seçimi biyoelektrokimyasal sistemlerin performansında önemlidir; bu nedenle, bu çalışmada, 100 mM fosfat tamponlu salin (PBS) çözeltisi ve fosfat içermeyen bir tuz ortamı olmak üzere iki farklı tampon çözeltisi kullanılarak CM ile beslenen AD-MEC reaktörlerinin performansı karşılaştırılmıştır. AD reaktöründe tuz tampon çözeltisinin kullanılması, 100 mM PBS ortamlı aynı reaktöre göre 4 kat daha yüksek net metan verimi ve 5,8 kat daha düşük gecikme süresi ile sonuçlanmıştır. En yüksek metan üretim hızı 12,03±0,01 mL/gün ve metan verimi 318,1±1,4 mLCH_4/g eklenen uçucu katı madde ($UKM_{eklenen}$), AÇ-MEH'de bakir elektrotlar kullanıldığında BiyoGAK olarak adlandırılan biyofilm bağlı GAK ilaveli tuz ortamı varlığında elde edilmiştir. AÇ-MEH'lerde elde edilen verim, geleneksel AÇ 'ye göre yaklaşık %25 daha yüksektir.

Anahtar Kelimeler: Anaerobik Çürütme (AÇ), Mikrobiyal Elektroliz Hücresi (MEH), AÇ-MEH, Biyofilm Oluşumu, Biyoelektrot

Dedication

To all women in my country…

Women, Life, Freedom

ACKNOWLEDGMENTS

I want to start by sincerely thanking my supervisor, Assist. Prof. Dr. Yasemin Dilşad Ylmazel Tokel, for her advice, debates, and insights during the project.

I also like to express my gratitude for the funding that the Office of Sponsored Research at METU granted for this study under grant number 10776.

I would like to express my gratefulness to Prof. Dr. Tuba Hande Ergüder Bayramoğlu, Prof. Dr. Bülent İçgen and Prof. Dr. İpek İmamoğlu for allowing me to use the facilities of their laboratories.

To Feride Ece Kutlar, I owe a tremendous debt of gratitude for the unwavering support she has given me from the very beginning to the very end. I am deeply grateful to the people in METU environmental engineering department especially, Mert Şanli, Aslı Onursal, Aykut Kaş, Berivan Tunca, Yasin Odabaş, Berkan Öden, Nihan Kalaycıoğlu, Rayan Harb, Irmak Subaşı and Danial Rahim for their comments, friendship, and support. In closing, I would want to express my gratitude to my parents and brother, who have been there for me during this entire process.

TABLE OF CONTENTS

LIST OF TABLES

TABLES

LIST OF FIGURES

FIGURES

LIST OF ABBREVIATIONS

ABBREVIATIONS

AD: Anaerobic digestion

AC: Activated carbon

ACE: Acetate

AD-MEC: anaerobic digestion - microbial electrolysis cell integration

BES: Bioelectrochemical systems

CE: Coulombic efficiency

CM: Cattle manure

COD: Chemical oxygen demand

CR: COD removal

CV: Cyclic voltammetry

DIET: Direct interspecies electron transfer

EET: Extracellular electron transfer

GAC: Granular activated carbon

GC: Gas chromatography

HMIET: Hydrogen mediation of interspecies electron transfer

IET: Interspecies electron transfer

MEC: Microbial electrolysis cell

MES: Microbial electrosynthesis

MFC: Microbial fuel cell

MMEC: Electromethanogenic microbial electrolysis cell

NHE: Normal hydrogen electrode

OTU: Operational taxonomic units

PBS: Phosphate buffer saline

PCR: Polymerase chain reaction

SAO: Syntrophic acetate-oxidizing

SEM: Scanning electron microscopy

sCOD: Soluble chemical oxygen demand

SHE: Standard Hydrogen Electrode

TCD: Thermal conductivity detector

TS: Total solids

VFA: Volatile fatty acid

VS: Volatile solids

CHAPTER 1

INTRODUCTION

The production of manure has increased as a result of industrial ranching, and its disposal has become a significant environmental and public health challenge. On the other hand, livestock manure is high in organic matter and can be used as a renewable energy source (Syed et al., 2022). Utilization of animal manure through anaerobic digestion (AD) technology is a sustainable method for energy production in the form of methane gas (CH_4) serving also the purpose of pollution reduction (L. Zhao et al., 2021). There are four stages to AD: i) hydrolysis, where hydrolytic bacteria break down organic matter into monomeric substances ii) acidogenesis, where fermentative bacteria further break down the monomeric organic substances and form carbon dioxide (CO_2), volatile fatty acids (VFAs), and other by-products iii) acetogenesis, at which acetogens produce acetic acid along with CO_2 and hydrogen (H_2), and iv) methanogenesis, which is the final step of the AD process where methanogens use the products of the previous steps such as acetate and H_2 to produce CH_4 (Mir et al., 2016). The hydrolysis step in the AD process is considered to be the limiting stage for complex wastes and in the literature, it is reported that physical and chemical pretreatment can speed up the hydrolysis phase (Bao et al., 2020). However, these pretreatment methods can sometimes produce inhibitory compounds and are most energy intensive hence should carefully be selected (Bougrier et al., 2006). Besides that, since methanogens have a slow metabolic rate, changes in environmental conditions such as organic loading rate, operation temperature, and operation pH can easily affect the metabolic rate and the balance between acetogens and methanogens (Feng et al., 2020). The mentioned drawbacks in the AD process highlight the need for innovative technologies to overcome these concerns and improve their stability and efficiency.

Bioelectrochemical systems (BES) are promising energy production technologies that convert chemical energy in organic matters into direct energy in the form of electricity or other value added products. Microbial fuel cells (MFC) and microbial electrolysis cells (MEC) are the most common BES reactors. MEC was initially developed to produce hydrogen gas from organic materials, but it has since been used to produce other value-added products such as CH_4, ethanol, hydrogen peroxide, etc. MECs are unique and promising options for long-term CH_4 production. In a MEC, electro-active microorganisms are grown as a biofilm on electrodes, and a small voltage (0.2–0.8 V) is typically applied to drive the bioelectrochemical reactions (Zakaria & Dhar, 2019). Methanogen enrichment on the cathode of MECs leads to CH_4 production in a process known as electromethanogenesis (Cheng et al., 2009). It may take place (i) via direct electron transfer and reduction of CO_2 to CH_4 or (ii) via indirect electron transfer and conversion of abiotically formed cathodic hydrogen to CH_4 (Cheng et al., 2009). Organics oxidation by exoelectrogens on the anode surface of the MEC provides the electrons necessary for CO_2 reduction.

Electro-active microorganisms that colonize the electrodes of MECs are key to the success of these systems. Exoelectrogens and electrotrophs are the two most frequent forms of electroactive microorganisms. Exoelectrogens are the type of microorganisms that can transmit electrons outside of the cell. Electrotrophs, on the other hand, are microorganisms that are capable of directly accepting electrons from the environment outside of the cell (Lovley, 2011). One of the most important exoelectrogens available on the anode surface of MECs, which can oxidize a broad range of organics, is *Geobacter* (Lovley, 2011). Furthermore, *Geobacter* species can transfer electrons directly to other species through their electrically conductive pili and outer surface c-type cytochromes (Rotaru, Shrestha, Liu, Markovaite, et al., 2014; Rotaru, Shrestha, Liu, Shrestha, et al., 2014). The mechanism is called direct interspecies electron transfer (DIET). According to Liu and colleagues, *Geobacter* species can execute DIET in the presence of conductive materials, even in the absence of electrically conducting pili and outer surface c-type cytochromes (F. Liu et al., 2012). Conductive materials provide environmental advantages to

microorganisms by allowing them to reduce their DIET investments (Z. Zhao et al., 2016a). The effects of carbon-based conductive materials, including granular activated carbon (GAC), biochar, graphite, and metal-based conductive materials like stainless steel, have been studied in many studies to improve the efficiency of AD systems. The results demonstrated improved CH_4 yield and production rate while decreasing lag time, effect of inhibitory compounds and VFA accumulation in the AD system (Kutlar et al., 2022).

Anaerobic digestion–microbial electrolysis cell (AD-MEC) is a novel hybrid technology that has recently emerged to improve CH_4 production and overcome the limitations of AD (Zakaria & Dhar, 2019). Electromethanogenesis may be incorporated into conventional AD systems by providing a pair of electrodes with external energy in the form of applied voltage (Zakaria & Dhar, 2019). Several studies have shown that combining AD-MEC in a single process can improve CH_4 output, kinetics, and increase process stability (Ying Chen et al., 2016; J. G. Park et al., 2019; Q. Yin et al., 2016). However, it is stated that in the AD-MEC integrated system, the bulk solution has a much larger share of CH_4 production than the electrode surface (W. Wang et al., 2022). Therefore, creating other pathways such as DIET with the help of conductive materials can be a good option to further improve the CH_4 production performance of AD-MECs (Feng, Song, & Ahn, 2018; Feng, Song, Yoo, et al., 2018). Labarge and colleagues improved their MEC performance by using GAC that had been pre-biofim formed by different substrates, which decreased the start-up time and boosted the rate of CH_4 production (LaBarge et al., 2017a). Moreover, Ren and colleagues showed that adding conductive material such as graphite can improve the stability of the AD-MEC system (Ren et al., 2018).

Phosphate buffer saline (PBS) concentrations ranging from 10 mM to 100 mM are used as the reactor medium in most AD-MEC and other bioelectrochemical (MEC/MFC) reactors (Bo et al., 2014; Ying Chen et al., 2016; Dou et al., 2018; Siegert, Li, et al., 2015). PBS solution has two key functions in a bioelectrochemical system. It adjusts the pH level in a way that is suitable for the growth of microorganisms and increases the conductivity of the solution, which leads to better

mass transfer and electrochemical processes (Ou et al., 2017). However, the high phosphorus concentration in the buffer solution can have an adverse effect on the CH_4 production performance of the AD-MEC. Few studies investigated the effect of phosphorus concentrations on AD and showed the inhibitory effect of phosphorus on the mesophilic AD process (Mancipe-Jiménez et al., 2017; R. Wang et al., 2015). Wang and colleagues stated that orthophosphate concentrations lower or higher concentrations than 414 g P/m^3 slow down the CH_4 production processes in AD (R. Wang et al., 2015). Although this promising technique, the AD-MEC, has been studied for the factors affecting the performance of its systems (e.g., electrode materials, reactor configuration, and applied voltage), little to no research has been devoted to investigating the effect of PBS solution and possible inhibition to AD. Also, Inhibition brought on by PBS may go undetected in some studies since control reactors like open circuits (no voltage) or conventional AD along with AD-MEC systems have not been operated.

1.1 Aim of the Study

In this thesis, the aim was to enhance biomethane production from cattle manure (CM) using an integrated AD-MEC reactor. To this purpose, we investigated the impacts of various start-up strategies on the CH_4 production performance of bioelectrochemical reactors. In this study, CM was chosen as a substrate since its production has recently skyrocketed as a result of modern animal agriculture, its improper handling causes various environmental problems, and it is rich in organic content (Huang et al., 2022). Further, currently, it is a commonly used feed of full-scale AD plants (Y. Li et al., 2021).

The experimental study consisted of two major start-up strategies (Figure 1.1). In the first part of this study, we investigated the potential of using CM as a substrate in electromethanogenic MECs. We focused our efforts on the role of biofilm formation in terms of the performance of electromethanogenic MECs that are fed with CM. To the best of our knowledge, this is the first report of a comparative analysis of biofilm formation by simple substrate (acetate) vs. complex waste (CM) on

electromethanogenic MECs. In the second part of this thesis, we attempted to determine the impacts of using biofilm attached electrodes, amendment of GAC, and voltage application on boosting CH_4 generation and the effectiveness of AD-MEC systems for treating CM. In addition, we looked at how 100 mM PBS and salt medium without phosphate affected AD-MEC performance (Figure 1.1).

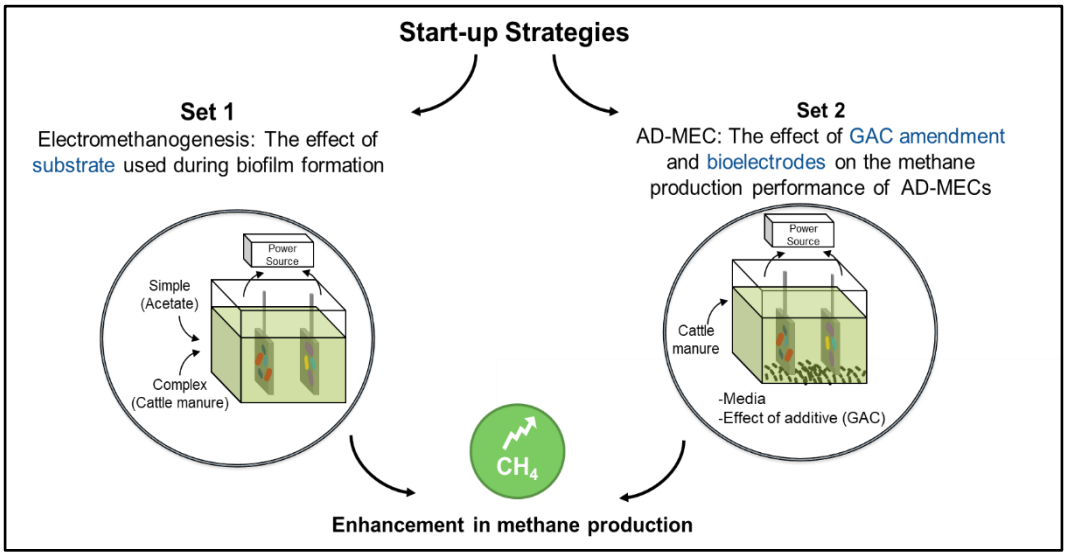

Figure 1.1 Aim of the study

1.2 Scope of the Study

This thesis contains two sets of experiments. In the first experimental set, the performance of electromethanogenic MECs fed with CM was evaluated. During the biofilm formation stage, two different substrates, namely acetate, and filtered manure were used, and then a comprehensive comparison of MEC performances was conducted. To this purpose, single chamber MECs of 25 mL were fabricated in our laboratory and operated with an applied voltage of 0.7 V under mesophilic conditions.

As for the second set of experiments, the impact of the amendment of a carbon-based conductive material (*i.e.*, GAC) to AD-MEC integrated systems was investigated. In this set, the single chamber reactor size was increased to 130 mL with an active volume of 65 mL. Based on the results of the first experimental set, filtered manure

was used for biofilm formation. Upon biofilm formation, biofilm attached electrodes, *i.e.*, bioelectrodes and biofilm attached GAC, bioGAC, were used in the AD-MEC set. AD-MEC reactors were operated for two cycles: first with 100 mM PBS buffer solution, and then with a salt solution to assess the impact of the reactor medium on the performance.

CHAPTER 2

LITERATURE REVIEW

2.1 Anaerobic Digestion (AD)

AD technology is a sustainable method for energy production in the form of CH_4 gas and pollution reduction (Zhao et al., 2021). Various microorganisms work together in AD to reproduce and generate energy for metabolic processes by digesting organic compounds in the absence of oxygen. At the end of the anaerobic process, biogas is produced as a result of these actions. There are four phases to AD: i) hydrolytic bacteria break down organic matter into monomeric organic substances ii) fermentative bacteria further break down the monomeric organic substance and form CO_2, VFAs, and other byproducts iii) acetogenesis by acetogens to produce acetic acid along with CO_2 and hydrogen iv) methanogenesis is the final step of the AD process in which methanogens use the products of the previous steps and produces CH_4 (Mir et al., 2016). The steps of AD are shown in Figure 2.1.

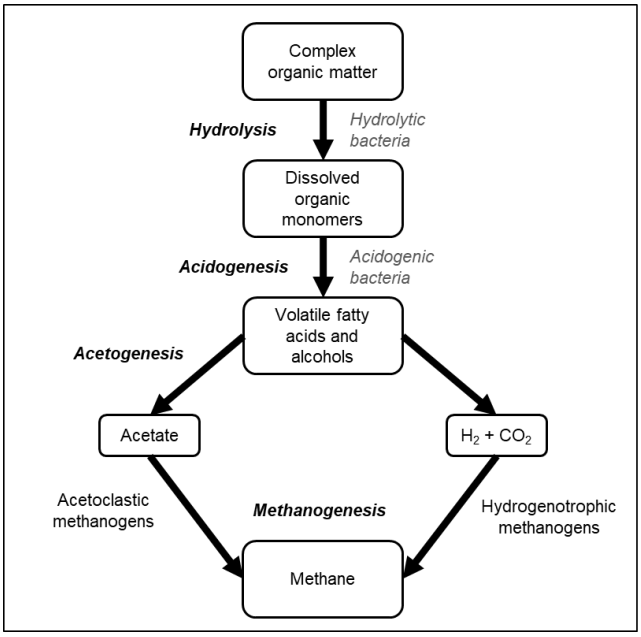

Figure 2.1 Stages of AD

2.1.1 Electron transfer mechanisms in AD

The successful operation of the AD process requires a good understanding of interactions between different microorganisms involved in the different stages of the AD process (Martins et al., 2018). The transport of electrons between bacteria and archaea is necessary for the syntrophic interactions that occur between them for CH_4 production. It has been demonstrated that CH_4 can be produced in two different ways during the process of methanogenesis: (1) through the conversion of acetate to CH_4 by acetoclastic methanogens, and (2) through the transfer of electrons from VFAs to CO_2 to produce CH_4. This second process is carried out mostly by hydrogenotrophic archaea, which use the hydrogen that is produced as a byproduct of fermentative bacteria's oxidation of VFAs as an electron carrier. Hydrogen mediation of interspecies electron transport is the name given to this mechanism (HMIET) (Bryant et al., 1967) (Figure 2.2). Although other electron carriers like formate are capable of acting as mediators during interspecies electron transfer (IET), the poor diffusion of these intermediates causes the AD process to move at a slower rate due to diffusion (De Bok et al., 2002). On the other hand, DIET, a fundamentally novel notion that is an alternative to HMIET, was discovered around a decade ago (Kutlar et al., 2022). Energy is preserved during classical respiration via electron translocation from an electron giver (organic substrate) to a terminal electron acceptor (e.g., oxygen) diffused into the cell. However, in DIET, electron transfer processes occur outside the cell between the electron donor and acceptor, called extracellular electron transfer (EET) (Logan et al., 2019). Microorganisms that have c-type cytochromes and pili are capable of DIET (Figure 2.2). However, most fermentative bacteria and methanogens lack these conduits (Martins et al., 2018). Recently, it has been shown that conductive materials such as GAC, and carbon cloth can substitute c-type cytochromes and pili to perform DIET (Rotaru, Shrestha, Liu, Markovaite, et al., 2014) (Figure 2.2). Moreover, several researches showed that conductive material amendment in AD results in several advantages as increase in CH_4 yield, CH_4 production rate and tolerance to inhibitory compounds, and decrease in VFA accumulation and lag phase compared to conventional AD (Kutlar et al., 2022).

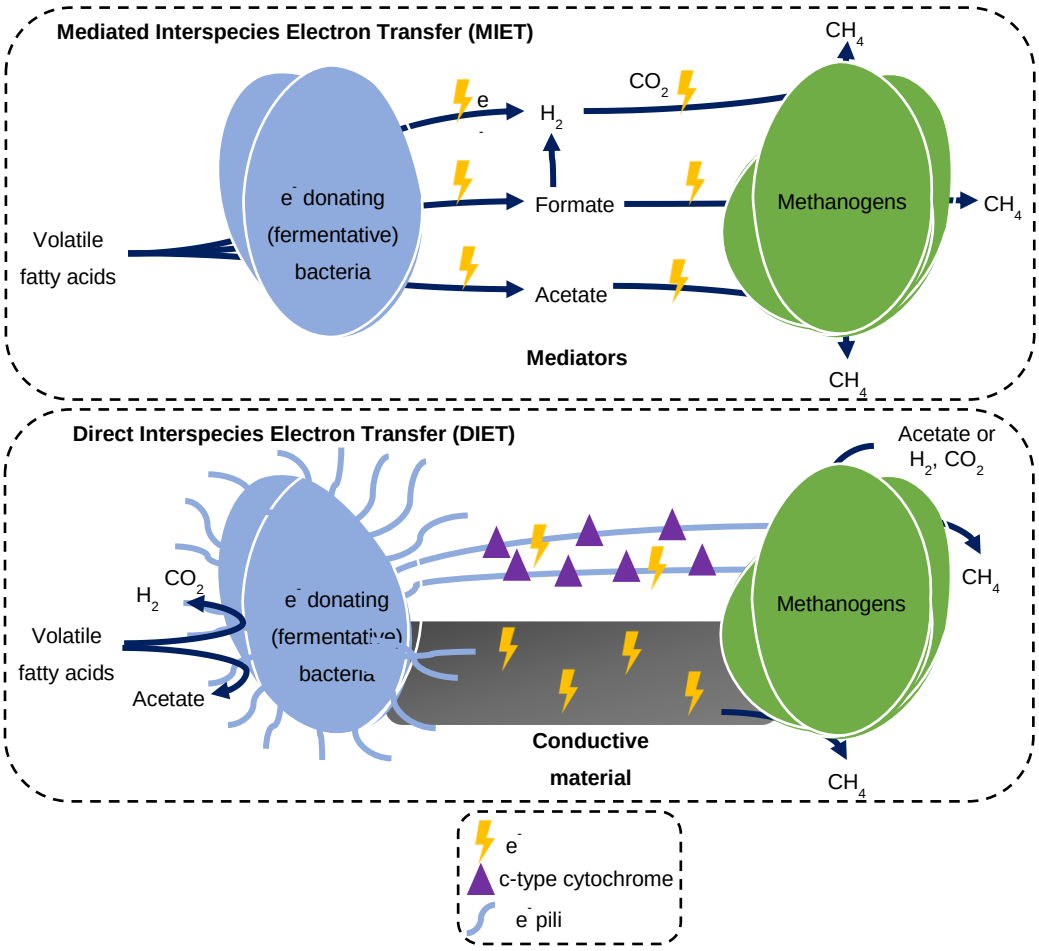

Figure 2.2 Electron transfer mechanisms

2.1.2 Limitations of AD

The hydrolysis stage of the AD process is believed to be the limiting stage, and the AD process can be sped up by both physical and chemical pretreatment. On the other hand, these pretreatment procedures can occasionally be difficult and pricey to implement in practice (Bougrier et al., 2006). Alterations in environmental circumstances such as loading rate, temperature, and pH may readily influence the metabolic rate balance between acetogens and methanogens. This is due to the fact that methanogens have a slow metabolic rate (Feng et al., 2020). The AD process has a number of problems, some of which have been mentioned. These shortcomings

highlight the need for novel technologies that may overcome these issues and increase the stability and efficiency of the process. The activation of DIET by the use of conductive material in AD reactors is one approach that may be taken to circumvent these limitations. In the study by Ryue and colleagues, 25 g/L GAC was added to the AD reactor treating food waste in mesophilic conditions. The results showed two times increase in CH_4 yield and a 1.26 times enhancement in CH_4 production rate compared to the control reactor (Ryue et al., 2019). The addition of biochar for the anaerobic treatment of dairy manure in a psychrophilic condition also showed a 28% enhancement in CH_4 production yield and a 20% enhancement in production rate compared to the control (Jang et al., 2018). In the study comparing the effect of biochar and activated carbon addition on the mesophilic AD of piggery waste. The bioreactors amended with biochar produced higher CH_4, had a higher kinetic constant and removed more COD than the control and activated carbon reactors. Biochar-added reactors had a 6.9% higher maximum CH_4 output and kinetic constant, and 3% higher COD removal efficiency. Compared to the control, activated carbon only slightly improved AD (Herrmann et al., 2021). An additional strategy for overcoming the constraints of AD systems is the integration of AD systems with BES, which is a topic that will be covered in the next section.

2.2 Bioelectrochemical Systems (BES)

BESs are promising and relatively new technologies that combine electrochemistry with microbial activity (Hamelers et al., 2010). In BESs, microorganisms attach to one or both electrodes to perform oxidation on the anode and/or reduction on the cathode. Biofilm-attached electrodes are called bioelectrodes (Hamelers et al., 2010). There are two types of BES electron-producing MFCs and electron-consuming microbial electrosynthesis (MES). That is, because of cathodic reactions, BESs can be categorized. In MFCs, electrical energy production occurs. On the other hand, in MES, electrical energy is used to obtain products such as hydrogen, CH_4, and ethanol. There are many applications of BESs. Wastewater treatment is one example of the application of BESs.

2.2.1 Microbial Electrolysis Cell (MEC)

MEC originated from microbial electrosynthesis systems. MEC was developed to produce hydrogen gas from organic materials (Logan et al., 2008). The system must be anaerobic to enrich anaerobic microorganisms to occur in reactions. For hydrogen production, biofilm formation on an anode (bioanode) surface is needed. These microorganisms are called exoelectrogens, microorganisms that donate electrons to a solid surface and protons to the solution (Logan et al., 2008). As a result of this electron donation, the current is produced. *Geobacter sulfurreducens* is one of the well-known examples of exoelectrogens (Bond & Lovley, 2003). Organics are oxidized on the surface of an anode by exoelectrogens. Protons and electrons are transported to the cathode. With the help of external voltage application, hydrogen is produced abiotically (Figure 2.3). MECs are a very promising technology since while organics are removed, valuable products such as hydrogen can be produced by low energy input (Logan et al., 2008).

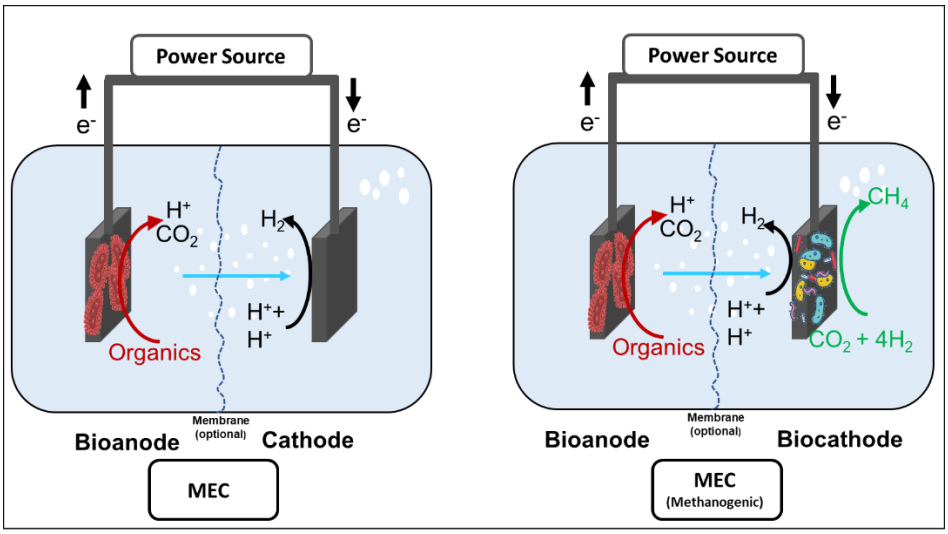

Figure 2.3 Hydrogen producing MEC and methanogenic MEC

MECs may also consist of a biofilm-formed cathode (biocathode) (Cheng et al., 2009). By biocathode, CH_4 can be harvested from MEC systems. They are called electromethanogenic MECs (MMECs). Anode mechanisms are the same for both systems. For MMEC, produced electrons are utilized by electrotrophs on the cathode

surface to produce CH_4. Moreover, abiotic hydrogen production can still occur with protons transferred from the anode in MMEC. CH_4 production is not thermodynamically feasible; therefore, external voltage application is needed for MMEC. The schematic representation with all mechanisms in the MMEC systems is given in Figure 2.4.

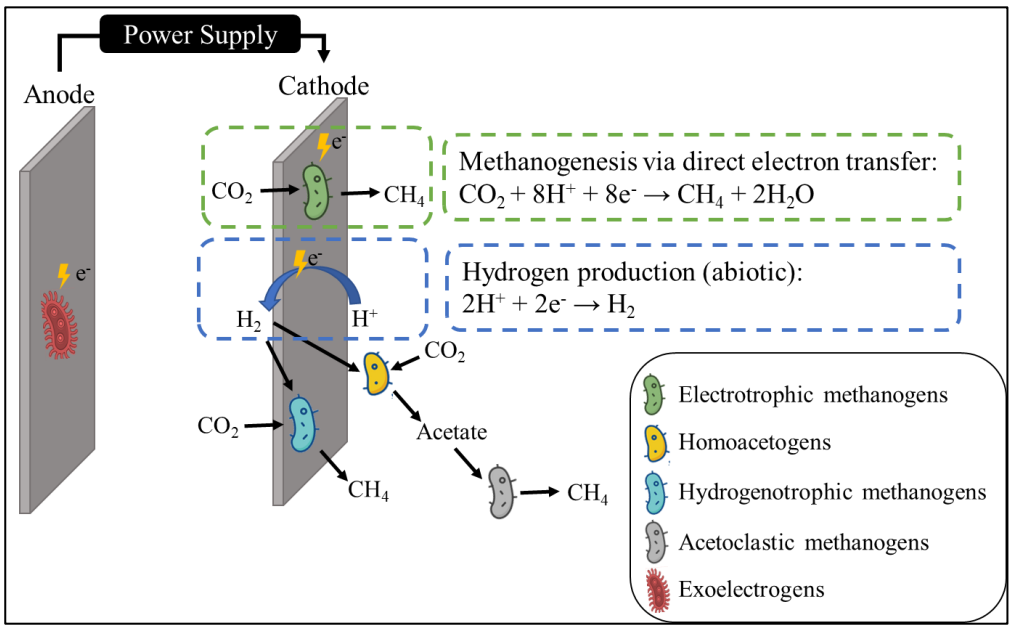

Figure 2.4 The schematic representation of the electromethanogenic MEC (MMEC)

On the anode, oxidation is performed by exoelectrogens. Oxidation of one mole acetate at the anode chamber provides 8 electrons for methanogens on the biocathode as given in Eq. 2.1 (Cheng et al., 2009).

$$CH_3COO^- + 4H_2O \rightarrow 2HCO_3^- + 9H^+ + 8e^- \quad \text{(Eq 2.1)}$$

There are two mechanisms for electromethanogenesis on the cathode:

(i) Direct extracellular electron transfer in which microorganisms directly get electrons from the cathode surface and use them to reduce CO_2 to CH_4.

$CO_2 + 8H^+ + 8e^- \rightarrow CH_4 + 2H_2O$ (E = -0.24 V vs. Normal hydrogen electrode (NHE) (Eq 2.2)

(ii) Indirect extracellular electron transfer, in which either electrochemically or bio-electrochemical, hydrogen evolution happens in the cathode, then the produced hydrogen and CO_2 are utilized to produce CH_4.

$2H^+ + 2e^- \rightarrow H_2$ (E = -0.41 V vs. NHE) (Eq 2.3)

$CO_2 + 4H_2 \rightarrow CH_4 + H_2O$ (Eq 2.4)

The hydrogenotrophic methanogens can only utilize abiotically produced hydrogen. On the other hand, other methanogens may perform direct or indirect methanogenesis. Based on the energy required for driving the reactions, CH_4 production by direct extracellular electron transfer is an energy-efficient process, as the energy needed for the hydrogen evolution process has a lower potential (E = -0.41 vs. NHE) (Cheng et al., 2009). Low voltage (0.2 - 0.8 V) is applied for CH_4 production in MMECs (Amrut Pawar et al., 2020). That is why CH_4 production takes place through which pathways (direct or indirect) it has still remained unknown (Liang et al., 2009).

MMECs studies have been gaining attention over time when the interaction between microorganisms and electrodes has been started to investigate. As shown in Figure 2.5, the number of studies between 2013 and 2022 increased dramatically. Even if the number of studies is increasing, more research focusing on biocathode formation, electron transfer mechanisms, and microorganisms attached to the electrode surface is needed.

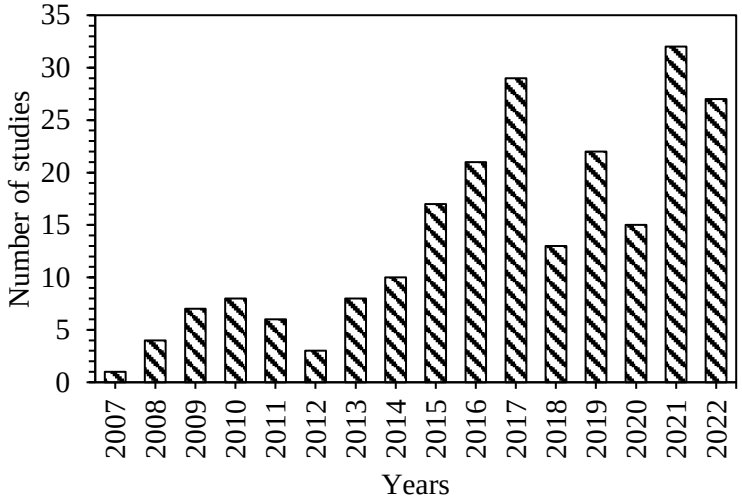

Figure 2.5 Scientific publications investigating MMECs published from 2013 to 2021. This data was extracted from the Scopus database using the keywords "microbial electrolysis cell", and "methane" (Search date: 27 July 2022).

The performance of MMECs can be affected by four main parameters as configuration, electrodes, applied voltage, and substrate. Studies investigated MMECs are summarized in Table 2.1 featuring main parameters as configuration, electrodes, applied voltage, and substrate.

Configuration	Applied Voltage (V)	Anode	Cathode	Substrate	Biocathode microbial community	CH_4 production rate	Reference
D (300 ml)[b]	0.7 +201 (SHE)	Graphite fiber brush Carbon plate	Carbon cloth Carbon plate	Acetate	*Methanobacterium palustre* (86.7%) *Methanoregula boonei* *Methanospirillum hungatei*	not stated	(Cheng et al., 2009)
D (270 ml)	0.65 0.9	Glassy carbon rod	Carbon plate	Mixture of fatty acids and alcohols	not stated	400 (mmole/m^2d)	(Villano et al., 2010)
D (860 ml)[b]	+0.5 (SHE)	Graphite granules	Graphite granules	Acetate	Mixed hydrogenophilic methanogenic culture	0.018 (L/Ld)	(Villano et al., 2011)
D (250 ml)[b]	0.6 0.8	Carbon sheets	Carbon sheets	Dog food	*Methanosarcina sp* (60%) *Methanoculleus sp.* (30%) *Methanobacterium sp* (10%)	8.23 (L/Ld) 7.995(L/Ld)	(Sasaki et al., 2011)
D (150 ml) [b]	-0.59 (SHE)	Graphite granules	Graphite granules	Acetate	*Methanobacterium* (93%) *Methanobrevibacter* (5%) Others (3%)	0.09 (mmole/Ld)	(Marshall et al., 2012)
D (300 ml)b	0.7 +201 (SHE)	Graphite fiber brush Carbon plate	Carbon cloth Carbon plate	Acetate	*Methanobacterium palustre (86.7%)* *Methanoregula boonei* *Methanospirillum hungatei*	not stated	(Cheng et al., 2009)
D (270 ml)	0.65 0.9	Glassy carbon rod	Carbon plate	Mixture of fatty acids and alcohols	not stated	400 (mmole/m^2d)	(Villano et al., 2010)

Table 2.1 Summary of electromethanogenic MEC studies (continued)

Configuration	Applied Voltage (V)	Anode	Cathode	Substrate	Biocathode microbial community	CH_4 production rate	Reference
D (860 ml)b	+0.5 (SHE)	Graphite granules	Graphite granules	Acetate	*Mixed hydrogenophilic methanogenic culture*	0.018 (L/Ld)	(Villano et al., 2011)
D (250 ml)b	0.6	Carbon sheets	Carbon sheets	Dog food	*Methanosarcina sp (60%)* *Methanoculleus sp. (30%)* *Methanobacterium sp (10%)*	8.23 (L/Ld)	(Sasaki et al., 2011)
D (150 ml) b	-0.59 (SHE)	Graphite granules	Graphite granules	Acetate	*Methanobacterium (93%)* *Methanobrevibacter (5%)*	0.09 (mmole/Ld)	(Marshall et al., 2012)
S (250 ml)	0 0.5 0.75 1 1.25 1.5	Plain carbon felt	Plain carbon felt	Acetate	*Methanomicrobia (91%)* *Methanocorpusculum bavaricum(77%)* *Methanobacteria (0.2%)* *Thermoplasmata (8.8%)*	40 40 170 185 450 275 (mmole/m^2d)	(Kobayashi et al., 2013)
D (860 ml) b	+0.2 (SHE)	Graphite granules	Graphite granules	Acetate	not stated	0.28 (L/Ld)	(Villano et al., 2013)
S (250 ml)	0.75	Plain Carbon felt	Plain Carbon felt	Acetate	not stated	386 (mmole/m^2d)	(Kuramochi et al., 2013)
S (10 ml)	1	Plain carbon paper	Carbon paper	Acetate	*M. thermautotrophicus*	87.9 (mmole/m^2d)	(Hara et al., 2013)

Table 2.1 Summary of electromethanogenic MEC studies (continued)

Configuration	Applied Voltage (V)	Anode	Cathode	Substrate	Biocathode microbial community	CH_4 production rate	Reference
S (250 ml) D (300 ml)	0.7 +0.2 (SHE)	Plain carbon cloth	Plain carbon cloth	Sodium acetate	not stated	not stated	(Fu et al., 2015a)
S (25 ml)	0.6	Graphite fiber brush	Carbon cloth coated with Pt/C catalyst	Pretreated WAS	*Methanocorpusculum (96%)*	0.23 (L/Ld)	(Sun, et al., 2015)
D (860 ml) b	+0.2 (SHE)	Graphite granules	Graphite granules	Synthetic solution	*Methanobrevibacter arboriphilus Methanosarcina mazei*	47.7± 4.8 (meq /day	(Zeppilli et al., 2015)
D (150 ml) b	0.6	Carbon felt brush	Graphite coated carbon black + Nafion binder	Water splitting	not stated	not stated	(Siegert, Yates, et al., 2015)
S (1300 ml)	1.2	Carbon fiber brush	Carbon cloth powder + platinum	Acetate	*Methanobrevibacter (97%)*	not stated	(Rago et al., 2015)
S (500 ml)	0.7	Carbon cloth	Ni-foam	Sodium acetate	not stated	0.17 (L/Ld)	(Hou et al., 2015)
S (5 ml)	0.7	Graphite plate	Graphite plate	Sodium acetate	*Methanobacterium (95%)* *Methanobrevibacter (5%)*	0.2 (L/Lm^2) 0.27 - 0.2 (L/Lm^2)	(Siegert, Li, et al., 2015)

Table 2.1 Summary of electromethanogenic MEC studies (continued)

Configuration	Applied Voltage	Anode	Cathode	Substrate	Biocathode microbial community	CH_4 production rate	Reference
S (3000 ml)	1	Carbon felt	Stainless steel	Sodium acetate wastewater	not stated	0.0014(L/Ld) 0.008 (L/Ld)	(Moreno et al., 2016)
D (400 ml)	0.4 0.6 0.8 1 2	Carbon felt	Carbon felt	Sodium acetate - saccharose	not stated	0.03 (L/Ld) 0.075 (L/Ld) 0.104 (L/Ld) 0.07 (L/Ld) 0.065(L/Ld)	(Ding et al., 2015)
D (860 ml)[b]	-0.1 -0.2 +0.2 (SHE)	Graphite granules	Graphite granules	Sodium acetate	not stated	4.2 9.7 12 (mmole/Ld)	(Villano et al., 2016)
D (260 ml)[b]	0.9 1 1.1 1.3 1.4	Platinum (Pt)	Carbon stick inside graphite felt tube	Water splitting	*Methanobacterium* (86.7%)	6.4 (ml/Ld) 14.4 (ml/Ld) 44.2 (ml/Ld) 58.3 (ml/Ld) 80.9 (ml/Ld)	(Zhen et al., 2016)
D (155 ml)[b]	-0.2 (SHE)	Ruthenium mixed metal oxide	Carbon brushes	Methanol VFA mix Acetate Hydrogen Wastewater	not stated	25 ± 9.7 (M) 22 ± 11 (MAP) 22 ±9.3 (H) (nmol/cm3.d)	(LaBarge et al., 2017a)
S (30 ml)	0.3 0.7	G (brush)	C cloth (Pt catalyst layer)	Sodium acetate	not stated	0.18 (L/Ld) 0.09 (L/Ld)	(W. Liu et al., 2018)

Table 2.1 Summary of electromethanogenic MEC studies (continued)

Configuration	Applied Voltage (V)	Anode	Cathode	Substrate	Biocathode microbial community	CH_4 production rate	Reference
D (260 ml)[b]	0.9	Platinum (Pt)	Carbon stick, CS-carbon cloth, CS-Ti wire, CS-carbon fiber , CS -graphite felt	Water splitting	not stated	20.1 (ml/Ld) 47.4 (ml/Ld) 29.9 (ml/Ld) 24.1 (ml/Ld) 75.7 (ml/Ld	(Zhen et al., 2018)
S (1000ml)	0.8	Carbon brush	carbon cloth coated with Pt/C	Acetate	*Methanobacterium* (96.21%) [alcaliphilum 71.03%]	7.1 (mmole/m^3d)	(Cai et al., 2018)
S (100 ml)	0.6	Graphite rod	Graphite rod	Water splitting	*Methanobacterium sp.* (81.4%), *Methanoculleus sp.* (18.6%)	.47 ± 0.03 (mL/ daycm^2)	(Giang et al., 2018)
S (130 ml)	0.8	Graphite brush	Carbon cloth with a Pt catalyst layer	Acetate	*Methanobacteriaceae, Methanobrevibacter,*	0.093 (L/L·d)	(X. Li et al., 2019)
D (550 ml) [b]	-0.7 (SHE)	Graphite rod	Graphite rod	(H_2 / CO_2) Methanol	*M. maripaludis* *M. vannielii* *M. petrolearia* *M. submarinus* *M. congolense* *M.mazei*	8.81 8.76 7.49 7.90 4.12 (mmol/m^2d)	(Mayer et al., 2019)
D (370 ml) [b]	-0.1 (SHE)	Carbon fiber brush	Graphite rod	Primary sludge-based blackwater	not stated	0.021 eq/L/d	(Deaver et al., 2022)

Reactor configuration

The reactor design in MECs can affect current density through internal resistance, which effects on CH_4 production rate (Villano et al., 2016). Although the working principles of BESs are the same, different types of reactors design, have by studied up to now. Generally, these reactor designs can be classified into two-chamber and single chamber MEC.

In two-chamber MECs, the anode and cathode chambers are separated by a cation exchange membrane. Due to this separation, two different media or substrates can be used in two-chamber MECs. Two-chamber reactors are widely used in different types of chamber shapes such as H-type, disc-shape, cubic, and rectangular (Blasco-Gómez et al., 2017). The problem with double chamber MECs is their complexity, which makes it difficult for scaling up. The main reason for this complexity is the ion-exchange membrane, which causes potential loss and pH gradient across the membrane. The pH gradient causes a decrease in the anode chamber and an increase in the cathode chamber, which leads to a performance loss of BES (Blasco-Gómez et al., 2017). Single chamber MECs are developed to solve the problems related to double chamber MECs by removing the membrane. In contrast to MFCs, MECs are completely anaerobic, and removing the membrane does not introduce oxygen to the system. Due to their low cost and operation advantages, single chambers are real alternatives compare to double chamber ones. Single chamber MECs have been developed in different shapes using different commercially available materials like glass serum bottles, plastic cubes, glass tubes, and plexiglass cylindrical chambers.

Electrode types

Electrodes are one of the important parts of MECs. Different types of materials, such as metals or carbon-based materials, have been used as electrodes (Siegert, Yates, et al., 2015). There are important features of electrodes to be able to use in MMEC systems. The electrodes should have (Amrut Pawar et al., 2020):

- High electrical conductivity,
- Chemical stability,

- Anti-corrosiveness,
- Good biocompatibility,
- Low resistance,
- Large surface area,
- Strong mechanical strength,
- Fouling resistance
- Scalability preferably with ease of construction
- Low cost.

According to desired features, an optimization of the electrodes should be done considering the cost to obtain an efficient MMEC.

Among all different kinds of materials, Platinum, due to its excellent catalytic capabilities, shows the highest hydrogen evolution production performance, which results in a higher CH_4 production rate (Villano et al., 2010). However, due to its scarcity and high price, it is not economically feasible to use platinum cathodes in large scale MMECs. However, in some studies, cheaper electrode materials like stainless steel or carbon-based material have been coated with platinum powder (R. Sun et al., 2015). Metal material such is Ni and steel also have been used as cathodes. Ni-based materials are resistance to corrosion and also have good catalytic capabilities (Hou et al., 2015). Stainless Steel mesh or brush is also good electrode material due to providing high surface area for methanogens and low cost (Moreno et al., 2016). Some other metals such as Ti also have been used as cathode materials.

Carbon-based materials also have been applied as electrodes due to their electrical conductivity and also high biocompatible property. These materials provide a high surface area for the growth of microorganisms, and since they have high porosity. Microorganisms can easily attach to this type of electrode and form a biofilm. The performance of different shapes of carbon-based electrodes such as carbon mesh, carbon paper, carbon brush, graphite plate, and graphite felt, graphite granules have been studied up to the present time. For example, graphite brush has been used in many studies, since brush materials have a huge surface area compared to plate

electrodes (Table 2.1). Since single material does not compensate for all the necessities for catalytic activities, many modifications to the shape and structure of cathode materials have been studied and research is still going on. For example, in order to increase catalytic activity and decrease cathodic overpotential, a combination of different metallic materials with carbon-based materials has been used. Cost and applicability in larger-scale MMEC are important concerns for cathode material and shape selection. The performance of different cathode materials applications on MECs has been summarized in Table 2.1.

Voltage application

Besides reactor design and electrode selection, there are other operational parameters such as applied voltage, temperature, and hydraulic retention time which effects the performance of MMECs (Amrut Pawar et al., 2020). As explained before, CH_4 production in MMECs takes place by applying a voltage to the system. The applied voltage directly affects microorganisms' distribution, growth, and CH_4 production. A wide range of studies reported applied voltage against Ag/AgCl or standard hydrogen electrodes (SHE) using a potentiostat. The standard electrode potential of Ag/AgCl against SHE is 0.197 V (Macaskill & Bates, 1978). The power supply was used in other studies that reported voltage as only in V. Effect of different voltages in the range of 0.3 to 1.5 V has been investigated in different studies as summarized in Table 2.1. However electrical input at $E_{app} > 1.1\,V$ is so large that it is not recommended (Ding et al., 2015). The applied voltage should be optimized according to electrodes, microbial activity, microbial community, and substrate. However, increasing the voltage application will increase the cost of the operation. Therefore, an economic analysis considering the voltage application needed for MMEC should be done to determine the feasibility of the process.

Substrate type

Among the CH_4 production pathways given in Figure, the CO_2 reduction pathway determines the overall performance of BES, as it is considered the major pathway which drives CH_4 production (Amrut Pawar et al., 2020). CO_2 can be provided to the

system directly in the form of gas or as bicarbonate in media. On the other hand, the electron needed for CO_2 reduction can be provided abiotically by water splitting or biotically by oxidation of organic material on an anode. The minimum energy required for water splitting is 1.2 V, which is the reason why this method is not economically feasible. However, in lab-scale studies, water splitting can be performed (Siegert, Yates, et al., 2015). Biotically oxidation of organic matter takes place by exoelectrogens such as *G. sulfurreducens, and G. metallireducens* (Bond & Lovley, 2003). Different types of simple compounds like acetate, glucose, or complex source of organics such as different types of wastewaters (synthetic, municipal, refinery, brewery, etc.), waste activated sludge, have been used as substrates in MMECs. Table 2.1 shows the summary of studies that investigate the effect of the different substrates in terms of CH_4 production rate.

Simple substrates have higher current production due to their easy biodegradability for microorganisms, which leads to better performance for CH_4 production. Among studies between 2009 and 2022, 83% of the studies were conducted with simple substrates (Figure 2.6). However, the main idea behind MECs is waste treatment and sustainable CH_4 production. That's the reason why complex substrates have been thoroughly investigated in MECs. However, only 17% of the studies were conducted with complex substrates. Therefore, there is a gap in the literature. Studies with different kinds of complex substrates should be investigated in future studies.

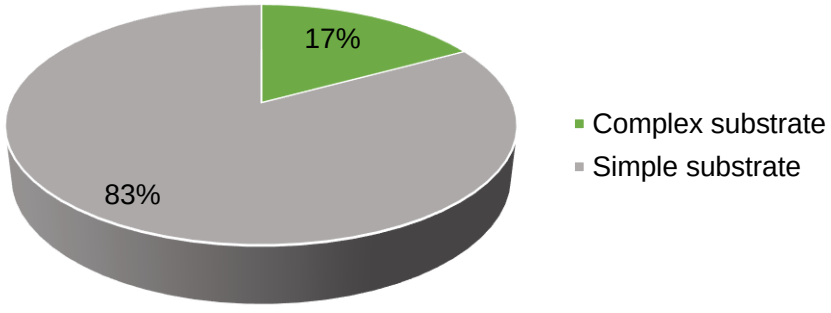

Figure 2.6 Distribution of studies among the researches in Table 2.1 with regard to substrates as simple and complex.

2.3 AD-MEC Integrated System

The AD process presents various challenges, some of which were discussed in section 2.1.2. These deficiencies bring to light the requirement for the development of innovative technologies that have the potential to solve these problems while also improving the process's consistency and effectiveness. Numerous possible solutions, including co-digestion, waste pretreatment, and parameter modification, have been proposed to address the abovementioned issues. In addition, the incorporation of conductive materials into the AD system in the form of additives, such as GAC, biochar, and others, has been documented to enhance the process (Wang and Lee, 2021).

The novel technique of electromethanogenesis also is implemented into traditional AD systems by inserting a pair of electrodes as an anode and a cathode and supplementing the system with an external energy source in the form of an applied voltage. In the literature, these systems are known as AD-MEC coupled systems (Cai et al., 2016). The research conducted in recent years on increasing biomethane recovery from wastewater through AD-MEC integrated systems has significantly grown (Huang et al., 2022). According to the findings of these investigations, AD-MEC coupled systems have several advantages over conventional digesters, including improvements in kinetics, CH_4 productivity, and reactor stability (Chen et al., 2016; Choi et al., 2017; Park et al., 2019). The fact that the AD-MEC system can reduce reliance on the acetoclastic methanogenesis pathway is the most significant advantage offered by this technology. The electroactive bacteria on the anode surface of these systems can oxidize the organic materials and directly transfer the electrons to the anode surface with extracellular electron transport. Later, methanogens on the cathode surface can convert these electrons to CH_4 via direct or indirect CH_4 production pathways (Cheng et al., 2009).

Because of all of the benefits of using an AD-MEC system, using such a system is the most advanced option for accelerating the process of organic decomposition and producing biomethane. In spite of the fact that AD-MEC systems are typically

portrayed as a simple technology for the generation of biomethane, there are a variety of factors that influence the performance of these systems. Therefore, over the last five years, researchers have been studying the AD-MEC system from a variety of perspectives, such as the configurations of AD-MEC systems, performance enhancement strategies, operational parameters' effects, and so on. Table 2.2 provides a synopsis of many different research projects that investigated the generation of CH_4 using AD-MEC reactors.

Table 2.2 Summary of CH_4 production studies with AD-MEC reactors

Substrate	T (°C)	Voltage (V)	CH_4 content	CH_4 production yield	CH_4 production enhancement with respect to control	Reference
Acetate	35	0.8	-	59.2 mLCH_4/g VS	42%	(L. Wang et al., 2019)
Dextrin/peptone	22	2	88.5%	-	-	(Dou et al., 2018)
Ethanol	35	0.1	-	280.83 mL CH_4/g COD	15.69%	(M. Sun et al., 2020)
Food Waste	35	0.3	70.2%	255.3 mL CH_4/g COD	43%	(An et al., 2020)
Food Waste	35	1.2	-	326 mL CH_4/g COD	120%	(Choi & Lee, 2019)
Incineration leachate	35	0.7	-	-	44.3%	(Gao et al., 2017)
Swine manure	35	0.7	-	0.6 mL CH_4/g VS	18.5%	(Yu et al., 2019)
Swine manure	35	0.9	-	0.52 mL CH_4/g VS	Negative	(Yu et al., 2019)
Waste activated sludge	20-25	0.8	-	808 mL CH_4 (cumulative)	97%	(Bao et al., 2020)
Waste activated sludge	35	0.6		1363 mL CH_4 (cumulative)	15.2%	(Z. Zhao et al., 2016b)

Wang et al. (2019) studied the effect of different cathode materials on CH_4 production in the AD-MEC system. They used copper, nickel, and stainless steel as the cathode in their single-chamber reactors and supplemented them with acetate under 0.8 applied voltage. The results revealed that reactors with nickel cathode showed maximum CH_4 production yield compared to stainless steel and copper electrode. AD-MEC reactors equipped with nickel electrodes enhanced the amount

of CH_4 produced by up to 40% compared to conventional AD reactors. To evaluate the effect of voltage application and biofilm on the performance of the AD-MEC system, Dou and colleagues used a dextrin/peptone mixture as a substrate in AD-MEC reactors. They applied different voltages between 0.5 to 2 V vs. Ag/AgCl. The results showed that reactors with 2 V vs. Ag/AgCl achieved 88.5% CH_4 content which was the highest. The better performance of reactors with 2 V vs. Ag/AgCl applied voltage was due to water electrolysis and hydrogen production in these reactors (Dou et al., 2018). In the AD of food waste, the characteristics of bioelectrochemical CH_4 generation were investigated with the use of a carbon-modified copper foam electrode (An et al., 2020).

The operation of the digester, as well as aspects of its performance, such as CH_4 output, process stability, and electrochemical characterization, were analyzed. The results showed that the reactor with 0.3 V applied voltage at 35 degrees celsius showed a 43% enhancement in CH_4 production compared to conventional AD control with 70.2% CH_4 content. In another study for treating food waste in the AD-MEC system, the reactor was incubated at 35 degrees Celsius, and 1.2 V voltage was applied. The CH_4 production rate was 326 ml CH_4/g COD which was 120% higher than the control reactor (Choi and Lee, 2019). Gao and his colleagues investigated the potential of using incineration leachate as a substrate in the AD-MEC system. According to their findings, AD-MECs are more successful in treating leachate from municipal solid waste incineration, and their use should be taken into consideration when planning the construction of new treatment facilities (Gao et al., 2017). In a study for treating swine manure using AD-MEC reactors, different voltages (0.3, 0.5, 0.7, and 0.9) were applied to the system at 35 degrees Celsius. The highest CH_4 production rate was achieved when 0.7 V voltage was applied to the reactor with 0.6 ml CH_4/g VS, which increased the CH_4 production by 18.5% compared to the control reactor. Interestingly, the 0.9 V voltage application negatively affected CH_4 production compared to the control reactor (Yu et al., 2019).

The effect of different pretreatment methods on CH_4 production with an AD-MEC integrated system has been investigated by researchers. Bae et al. improved waste-

activated sludge's CH_4 production by ultrasound and alkali pretreatment. Their study showed that AD-MEC reactors increased CH_4 output by three times compared to control AD. AD-MEC integrated reactors produced 808 ± 8 mL of CH_4, up 97.0% ± 1.85% from control AD reactors (410 mL) (Bao et al., 2020).

It has been demonstrated that adding additives into AD-MEC may increase CH_4 production, and current research pertaining to this topic is described in Table 2.3. GAC that had been pre-biofilm formed with various substrates, such as methanol, hydrogen, acetate, and so on, was afterward processed and fed to AD-MEC reactors that treated bog sediment to produce CH_4. The findings indicated an increase in CH_4 output and a reduction in the lag time between reactor startup and operation. (LaBarge et al., 2017). In another study that looked into the impact that additives have on AD-MEC reactors, 20 mM magnetite was added to AD-MEC reactors that were treating dairy wastewater under mesophilic conditions. According to the findings, there was a 288% increase in CH_4 production compared to its control reactor (Baek et al., 2020). Incorporating biochar into MEC increased CH_4 output by 24.7% and VS removal by 17.9%, as reported by Yin et al. (C. Yin et al., 2019). Microorganisms that bond to the surface of conductive materials facilitate DIET, while additives like nitrate serve as electron acceptors to boost the efficiency of the anode's oxidation process. (Peng et al., 2019) increased waste-activated sludge decomposition by 55.9% with the addition of 1 g/L nitrate to the AD-MEC reactor. In the study by (Xing et al., 2021), coconut-shell-derived bio-based carbon was used as an additive for the co-digestion of cow manure and aloe peel waste. The reactors were incubated at 36 ℃, and 0.6 V voltage was applied. The results showed a 120.68% improvement in CH_4 yield.

Table 2.3 Additives effect on AD-MEC performance.

Substrate	Additive	Additive dosage	Temperature (ºC)	Voltage (V)	Performance enhancement	Reference
Bog sediment	GAC	-	31	−0.6 (cathode, vs. SHE)	Start-up time improvement	(LaBarge et al., 2017b)
Glucose	AC	1 g/L	35	0.5	5.8% increased CH_4 production	(Feng et al., 2020)
Glucose	Magnetite	20mM	35	0.8	12.9% increased CH_4 production	(Vu et al., 2020)
Lignite	AC	3 g/L	35	0.33	3.3% increased CH_4 production	(Piao et al., 2019)
Lignite	AC	3 g/L	35	0.67	26.7% increased CH_4 production	(Piao et al., 2019)
Waste activated sludge	Biochar	1 g/g DM	55	0.6	44.4% increased CH_4 production	(C. Yin et al., 2019)
Waste activated sludge	Nitrate	1 g/L	35	0.8	8.9% increased CH_4 production	(Peng et al., 2019)
Cow manure and aloe peel waste co-digestion	CBC*	0.15 wt.%	36	0.6	CH_4 yield improvement by 120.68%	(Xing et al., 2021)
Dairy wastewater	Magnetite	20mM	35	0.6	288% increased CH_4 production	(Baek et al., 2020)

* coconut-shell-derived bio-based carbon

CHAPTER 3

MATERIALS AND METHODS

3.1 Preparation of Inoculum, Substrate, and Medium

3.1.1 Set 1: Electromethanogenesis

The inoculum used in this set was collected from the mesophilic municipal digester at the Eskisehir Metropolitan Municipality Wastewater Treatment Facility in Turkey. CM sample was taken from the feed tank of a biogas plant in Polatli, Turkey. CM sample was sequentially filtered through 1000-µm and 600-µm mesh filters to remove large particles for easier injection into the MECs. The inoculum and filtered CM samples were kept at 4 ± 2 ºC before use. The characteristics of filtered CM and AD seeds are shown in Table 3.1.

Table 3.1 Characteristics of filtered CM and AD seed used in Set 1

Parameter	Filtered CM	Anaerobic Digester Seed
pH	7.0	7.1
COD (mg/L)	64650 ± 1961	26395 ± 455
Soluble COD (mg/L)	19043 ± 342	-
sCOD/COD (%)	29.5	-
Acetic Acid (mg/L)	4307 ± 83	-
PO_4-P (mg/L)	23.9 ± 1	-
NH_4-N (mg/L)	1800 ± 86	-

The medium consisted of PBS, trace elements, sodium bicarbonate, and vitamin solution. PBS (100mM, pH = 7.0) was prepared by mixing 9.94 g/L of $NaH_2PO_4.H_2O$, 5.5 g/L of $Na_2HPO_4.H_2O$, 310 mg/L of NH_4Cl, and 130 mg/L of KCl (Siegert, Li, et al., 2015). The trace element solution was prepared with the

composition provided in Table 3.2, sterilized via autoclave, and purged with nitrogen (N_2) gas for 10 mins. It was added at a dosage of 40 mL/L to the medium. Vitamin solution contained all the necessary vitamins as given in Table 3.3 and it was added to the medium at a dosage of 40 mL/L (Siegert, Li, et al., 2015). 25 g/L sodium bicarbonate was separately prepared and transferred into an autoclaved-anaerobic empty bottle via filter sterilization. A sodium acetate solution of 8.2 g/L (10 mM) was prepared similarly by autoclaving and purging. PBS, trace element, vitamin, and bicarbonate solutions were merged inside the anaerobic chamber (Plas Labs 818-GB, MI, USA) forming the reactor media. This solution was divided into two bottles for the addition of substrates; 10 mM acetate was added to one media bottle and filtered CM, containing an adjusted amount of soluble chemical oxygen demand (sCOD) equivalent to the 10 mM acetate (640 mg sCOD/L), was added to the other media bottle.

Table 3.2 Chemical composition of trace element solution

Chemical composition	**g/L**
Nitrilotriacetic acid	1.5
MgSO4.7H2O	3
NaCl	1
MnSO4.H2O	0.5
$NiCl_2.6H_2O$	0.2
$CoCl_2$	0.1
$CaCl_2.2H_2O$	0.1
$FeSO_4.7H_2O$	0.1
$ZnSO_4$	0.1
$AlK[SO_4]_2$	0.01
$CuSO_4.5H_2O$	0.01
$Na_2MoO_4.2H_2O$	0.01
H_3BO_3	0.01

Table 3.3 Chemical composition of vitamin solution

Chemical composition	mg/L
Pyridoxine HCl	10
Thiamin HCl	5
Riboflavin	5
Nicotinic acid	5
Calcium pantothenate	5
Vitamin B12	5
p-aminobenzoic acid	5
Thioctic acid	5
Biotin	2
Folic acid	2

3.1.2 Set 2: Anaerobic Digestion - Microbial Electrolysis Cell (AD-MEC) integration

The inoculum used in this set was collected from the mesophilic municipal digester at the Eskisehir Metropolitan Municipality Wastewater Treatment Facility in Turkey. CM was collected from the feed tank of a biogas plant located in Polatli, Turkey. Before use, CM was mixed for 15 minutes to get a more homogeneous composition. The inoculum and CM were maintained at 4 ± 2 ºC until they were used in the experiments. The characteristics of CM and AD seed is given in Table 3.4.

Table 3.4 Characterization of inoculum and CM used in Set 2

Parameters	Inoculum	CM
TS (mg/L)	34,000 ± 6	124,000 ± 1,400
VS (% of TS)	56 ± 0.1	78 ± 0.04
COD (mg/L)	13,000 ± 8	146,800 ± 3,100
sCOD/TCOD (%)	3.9 ± 0.2	15.1 ± 0.8
pH	7.55	7.84

Two different mediums were used in this set. The first medium was PBS (100mM, pH 7.0, containing NaH_2PO_4.H2O 9.94 g/L, $Na_2HPO_4.H_2O$ 5.5 g/L, NH_4Cl 310 mg/L, KCl 130 mg/L) (Siegert, Li, et al., 2015). The second medium (pH 7.0, containing $MgSO_4.7H_2O$ 0.5 g/L, $CaCl_4.2H_2O$ 0.15 g/L, NaCl 5.5 g/L, NH_4Cl 310

mg/L, KCl 130 mg/L) was a modification the first medium but without phosphate and named as the salt medium in the rest of the thesis. The trace element solution was added at a dosage of 40 mL/L (Table 3.2.) and then the combined medium was sparged with N_2 gas for 10 mins before being autoclaved. 2.5 g/L sodium bicarbonate solution and vitamin solution (Table 3.3) were separately prepared and transferred in the autoclaved-purged empty container after filter sterilization. Vitamin solution was added at the same dosage as the trace element solution (40 mL/L). All components of the medium were merged inside the anaerobic chamber (model no: 818-GB, Plas Labs, MI USA).

3.2 Reactor Construction

3.2.1 Set 1: Electromethanogenesis

Single chamber MECs with a total volume of 25 mL (active volume of 15 mL) were fabricated as described elsewhere (Kas & Yilmazel, 2022). Graphite blocks (Eren Karbon Grafit San. Tic. Ltd. Sti, Istanbul, Turkey) of the following dimensions: 2 cm (L), 1 cm (W), and 0.3 cm (D) were used as both anode and cathode. Pretreatment of cut graphite blocks was performed in four steps: (i) polishing with 400-grit type sandpaper, (ii) sonication, (iii) soaking in 1 N HCl overnight, and (iv) rinsing three times with deionized water. The pretreated electrodes were connected to an 8 cm long titanium wire with an inner diameter of 0.08 cm (Timed metal, Turkey) that is also cleaned with the same sandpaper. Electrodes with more than 0.5 Ω contact resistance between graphite block and titanium wire were discarded. Two electrodes per reactor (anode and cathode) were fixed in the thick butyl rubber stopper and then pushed into the serum bottles. After crimp sealing the bottles, all reactors were purged using N_2/CO_2 (80/20) for 10 mins to sustain anaerobic conditions and autoclaved at 121 ºC for 15 mins. The reactor configuration is given in Figure 3.1.

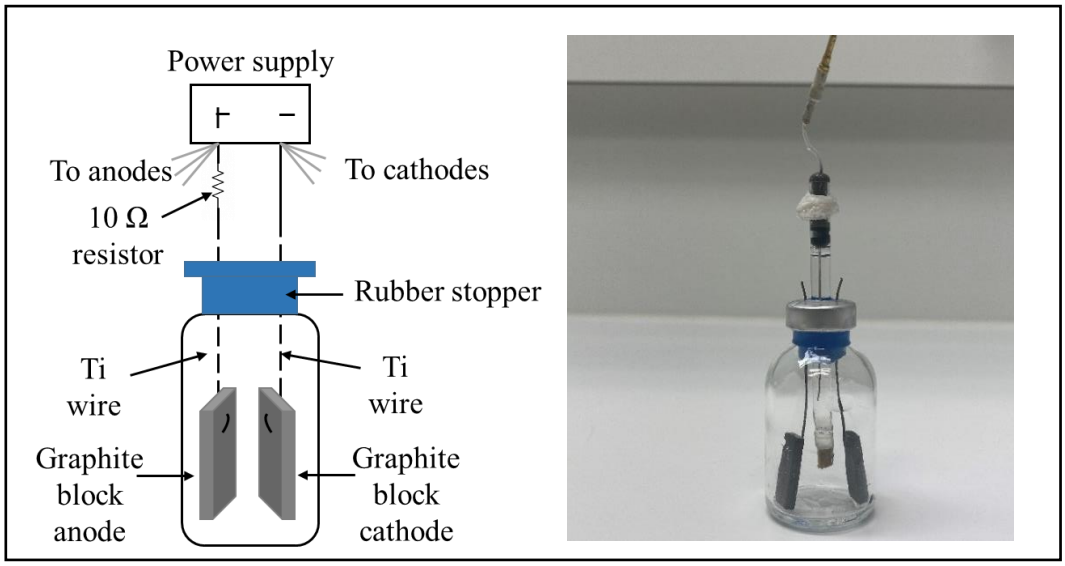

Figure 3.1 Reactor configuration used in Set 1

3.2.2 Set 2: Anaerobic Digestion - Microbial Electrolysis Cell (AD-MEC) integration

Serum bottles with two side ports and a total volume of 130 mL were used in the experiments. Both anode and cathodes were isomolded graphite blocks with dimensions of 2.5×2.5×0.3 (total surface area of 15.5 cm^2) connected to 12 cm titanium wire (0.1 cm diameter; Timed metal, Turkey). After electrode preparation, they were fixed in the thick neoprene stopper (40 mm diameter) at approximately 1 cm distance, then pushed into the serum bottles. The reactor configuration is given in Figure 3.2. GAC was used as the conductive material in the experiment. GAC particles were thoroughly washed with deionized water and dried overnight in an oven at 80 ^oC. The pre-biofilm formation of electrodes and GAC started with twelve reactors containing 40 g/L GAC.

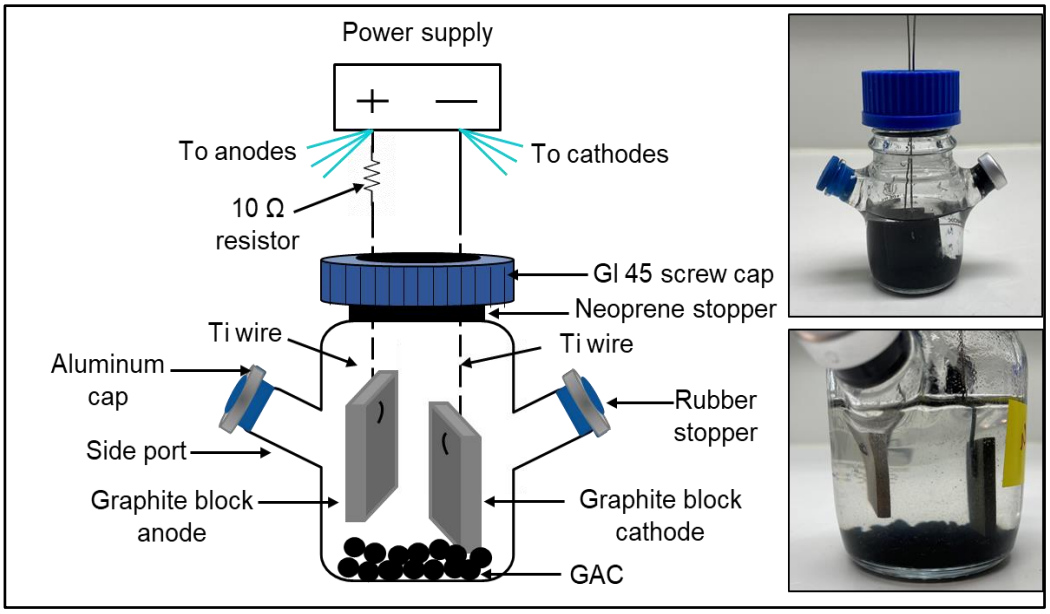

Figure 3.2 Reactor configuration used in Set 2

3.3 Experimental Design and Reactor Operation

The start-up strategies for CH_4 production enhancement using two different sets of experiments were established in this study. In the first set of the experiment (set 1), the effect of two different substrates namely, CM and acetate as the complex and simple substrates on the biofilm formation for electromethanogesis cells were examined. In the second phase of the experiment (set 2), the pre-biofilm formation of electrodes and GAC using CM as substrate was performed and used in AD-MEC reactors to determine which parameters (electrode surface area, GAC, electrode, and GAC pre-biofilm formation, and voltage application) have the most impact on boosting CH_4 generation and the effectiveness of AD-MEC systems for treating CM.

3.3.1 Set 1: Electromethanogenesis

The experiments consisted of two stages: (1) biofilm formation, and (2) test period (Figure 3.3). In the first stage, MECs were divided into three groups; the first group was inoculated with AD seed and fed with ACE, the second group was inoculated

with AD seed and fed with CM, and the last group labeled as Blank did not receive any AD seed and fed with CM. Blank reactors were operated as a control to observe the impact of native microorganisms present in the CM. All the reactors except the Blank group were then inoculated with AD seed (10% v/v). In the first stage, the objective was to provide an environment suitable for biofilm formation on the electrodes; hence, reactors were operated by injecting substrate (either ACE or CM) into the reactors without any liquid removal. During this stage, when the current reached its peak point and then dropped below 0.05 mA a new cycle was started through the injection of the corresponding substrate (ACE or CM). After several cycles when the current production in all the reactors became stable, the second stage named as test period was started. The difference between the biofilm formation and test period in terms of MEC operation is that during the test period when the current dropped below 0.3 mA a new cycle was started by replacing the total reactor content with new media. To keep the MECs anaerobic, between each cycle, the reactor headspace was purged using an N_2/CO_2 (80/20) gas mixture for 10 mins after medium exchange.

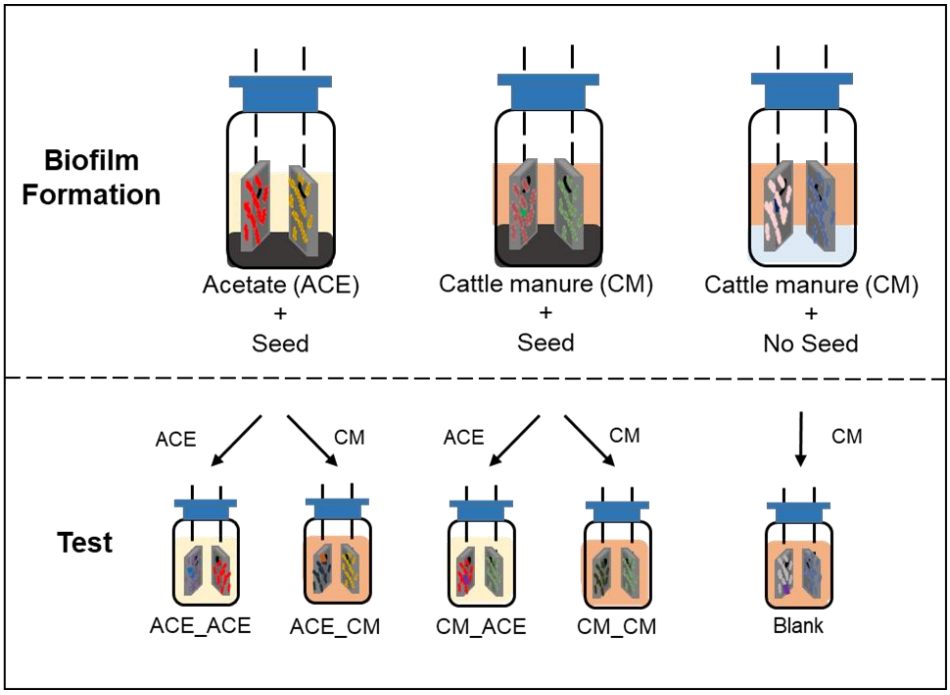

Figure 3.3 Experimental design of Set 1

During the test period all reactors, except the controls, were fed with CM to compare the impact of acclimation substrate on the reactor performance. To provide a baseline and serve as a positive control, half the reactors from both the first group (ACE fed during biofilm formation) and the second group (CM fed during biofilm formation) were fed with ACE during the test period. Hence, MECs that were fed with ACE during biofilm formation was divided into two ACE_ACE and ACE_CM, indicating that the former reactor received ACE during both biofilm formation and the test period, while the latter received ACE during the biofilm formation but was switched to CM during the test period (Figure 3.3). The described sequential feeding approach used in this study is referred to as cross-feeding (Ivanov et al., 2013). Similarly, CM fed MECs were divided into two as CM_CM and CM_ACE, where CM_ACE are the cross-fed reactors. The Blank reactors were kept on CM during the test period. All MECs were operated in triplicate. Also, each group had two extra reactors running for destructive tests such as SEM. Open circuit controls were also run in the same condition except for voltage application to determine any background CH_4 production. During the test period, after two cycles sCOD concentration of MECs was increased. The positive controls (ACE_ACE and CM_ACE) were run for about 48 days in total at two concentrations (600 and 1200 mg/L sCOD). The test reactors (ACE_CM and CM_CM) and the Blanks were run for around 60 days at four concentrations (600, 1200, 1800, and 2400 mg/L sCOD) until we observed the same amount of CH_4 as in positive controls.

Anodes of all MECs were connected to the positive terminal and cathodes to the negative terminal of the power supply. The positive leads had a 10 Ω resistor, and a multimeter (Keysight Technologies, 34972A LXI, USA) was used to record the voltage at 10 min intervals. MECs were incubated at 35 ºC without mixing, and 0.7 V was applied to the reactors using a power supply (Marxlow, RXN-1502D, China) (Figure 3.4).

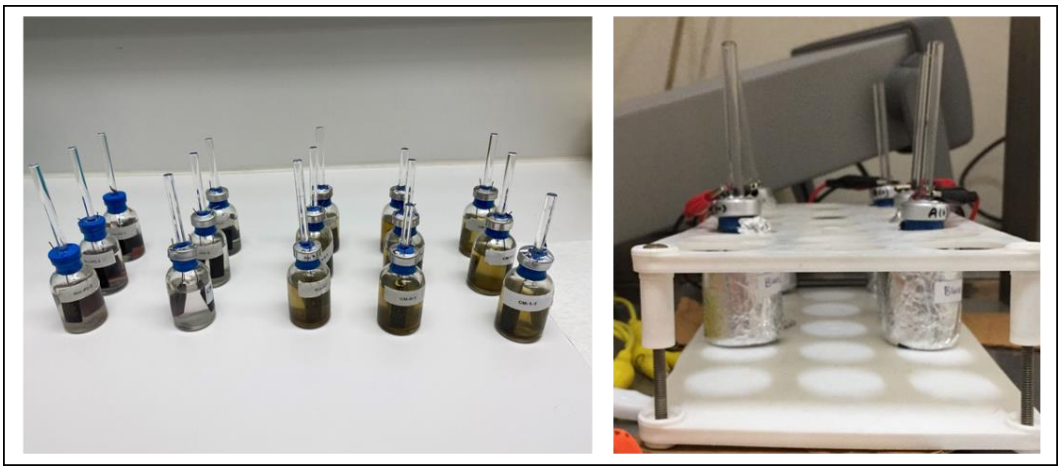

Figure 3.4 Reactors during the Set 1 operation

3.3.2 Set 2: Anaerobic Digestion - Microbial Electrolysis Cell (AD-MEC) integration

Similar to Set 1 experiments, in Set 2 there were two stages in total. The first stage was named Biofilm Formation and the second stage was named AD-MEC Operation. The experimental design of Set 2 is given in Figure 3.5.

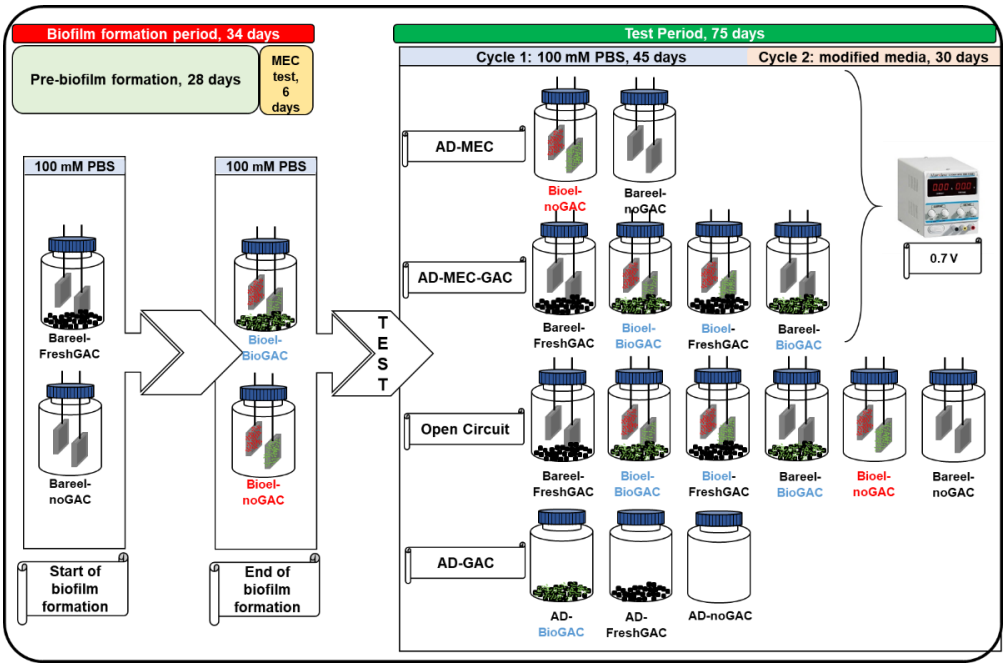

Figure 3.5 Experimental design of Set 2

Stage 1: Biofilm Formation Period

All reactors were filled with 59.5 mL of 100 mM PBS growth medium containing filtered cattle manure (1200 mg/L sCOD) as substrate and 6.5 mL inoculum (10% v/v) inside the anaerobic chamber.

The reactors were connected to the power supply (Marxlow, RXN-1502D, China) under 0.7 V voltage and incubated at 35 ºC without mixing (Table 3.5). The current produced was monitored using a multimeter (Keysight Technologies, 34972A LXI Data Acquisition, U.S.A.). During the pre-biofilm formation period, the reactors were operated by injecting substrate (filtered CM) without any sampling or opening of the reactors. Filtered CM (1200 mg/L) was injected into the reactors and the current was monitored. When the current density dropped under 0.08 mA/cm^2, fresh filtered CM was injected into the reactors. After a few times substrate injections, all of the reactors' current production became stable; therefore, pre-biofilm formation of electrodes and GACs was considered complete.

Table 3.5 Experimental design during biofilm formation (pre-biofilm formation)

Reactor	**Feed (filtered CM)**	**AD Seed**	**Electrode**	**GAC**	**Applied Voltage (V)**
Bareel	+	+	+	-	+
Bareel-FreshGAC	+	+	+	+	+

After completion of the pre-biofilm formation stage, all the reactors were emptied and then filled with fresh medium (100 mM PBS) and 1200 mg/L filtered cattle manure as the substrate to perform the MEC test. At this point, no inoculum was added and hence most activity can be attributed to the colonized biofilm on the electrodes considering the negligible impact of native microorganisms present in the filtered CM. Two batch cycles of the MEC test were done for all of the reactors, which was similar to the operation of reactors during the test period of Set 1. The amount of CH_4 produced by the reactors as well as their current production was measured.

To compare the performances of reactors after scaling up the data of Set 1 and Set 2 were compared as the active volume of the reactor in Set 1 was increased from 15 mL to 65 mL in Set 2. After running two batch cycles of the MEC test, all of the reactors were emptied, and the bio-electrodes and bio-GACs were carefully moved to new reactors within the anaerobic chamber so that the AD-MEC test could begin.

Stage 2: Test Period

In the Test Period, the experiment contained sixteen types of reactors in duplicate. These sixteen types of reactors were divided into three main groups: i) AD-GAC, ii) AD-MEC, and iii) AD-MEC-GAC.

The AD-GAC groups were made up of three different types of reactors: AD-noGAC, AD-FreshGAC, and AD-BioGAC. The AD-GAC group's major purpose was to examine the impact of the addition of both fresh GAC and biofilm attached GAC (BioGAC) on conventional AD reactor performance. The AD-MEC group included two reactor types: Bioel-noGAC, Bareel-noGAC, and their open circuit (OC) control. The goal of operating these reactors was to assess the effects of biofilm attached electrodes (Bioel) vs. bare electrodes (Bareel) on AD-MEC. Again, corresponding OC controls were set without external voltage to investigate the influence of electrode surface area on AD-MEC performance. The AD-MEC-GAC group had four different combinations of Bareel-FreshGAC, Bioel-FreshGAC, Bareel-BioGAC, Bioel-BioGAC, and their OC controls. Also, blank reactors were set up without cattle manure as the substrate to investigate the CH_4 production from seed (Table 3.6). The experimental design is shown in Figure 3.5 and Table 3.6.

Table 3.6 Experimental design for Set 2

Reactor		Feed	Seed	Electrode	GAC	Applied Voltage (V)
Blank		-	+	-	-	-
AD-GAC	AD-noGAC	+	+	-	-	-
	AD-FreshGAC	+	+	-	Fresh	-
	AD-BioGAC	+	+	-	Bio	-
AD-MEC	Bioel-noGAC	+	+	Bio	-	0.7
	Bareel-noGAC	+	+	Bare	-	0.7
	OC-Bioel-noGAC	+	+	Bio	-	-
	OC-Bareel-noGAC	+	+	Bare	-	-
AD-MEC-GAC	Bareel-FreshGAC	+	+	Bare	Fresh	0.7
	Bioel-BioGAC	+	+	Bio	Bio	0.7
	Bioel-FreshGAC	+	+	Bio	Fresh	0.7
	Bareel-BioGAC	+	+	Bare	Bio	0.7
	OC-Bareel-FreshGAC	+	+	Bare	Fresh	-
	OC-Bioel-BioGAC	+	+	Bio	Bio	-
	OC-Bioel-FreshGAC	+	+	Bio	Fresh	-
	OC-Bareel-BioGAC	+	+	Bare	Bio	-

Except for the blank reactors, all reactors had a total active capacity of 65 mL filled with 100 mM PBS growth medium and a mixture of inoculum (AD seed) and substrate (CM) with an F/M ratio of 1 (Table 3.7). The blank reactors contained only AD seed and growth medium (Table 3.6). The GAC dosage of 40 g/L was kept constant in this study.

Table 3.7 Initial composition of the reactors with 100 mM PBS

Reactor	Seed	Feed	Initial VS (mg/L)	F/M ratio
Blank	+	-	9000±175	-
Test reactors	+	+	19200±400	1

Following pH and conductivity measurements for all reactors within the anaerobic chamber, the headspace of all reactors was flushed for 10 mins with N_2/CO_2 (20/80 %) gas and then operated at 35 ºC in duplicate without shaking or stirring. When the

cumulative CH_4 production increase dropped to below 3%, the operation ended. Once the operation with 100 mM PBS was completed, the reactors were emptied and refilled with fresh feed, seed, and salt growth medium filled into the reactors. The bare electrode reactors also received new bare electrodes and fresh GAC reactors received fresh GAC.

Since high phosphate concentration due to 100 mM PBS media has inhibition potential, salt media was also used in the AD-MEC operation (Carliell-Marquet & Wheatley, 2002). The salt media was developed according to the growth medium of some well-known methanogens: *Methanosaeta pelagica* (DSMZ DSMZ: Deutsche Sammlung von Mikroorganismen und Zellkulturen (German Collection of Microorganisms and Cell Cultures) 1329) medium, *Methanobacterium* (DSMZ 119*)* medium, *Methanogenium* medium (DSMZ 141), *Methanosarcina* (DSMZ 120) medium, and *Methanoculleus sp.* (DSMZ 141b). Common salts were chosen among these medias to increase the conductivity of the medium. These salts are $MgSO_4.7H_2O$, $CaCl_2.2H_2O$, and NaCl. The concentrations of salts according to the growth medium are given in Table 3.8. Since NH_4Cl and KCl do not contain phosphate, these salts were kept the same with 100 mM PBS media.

Table 3.8 Salt concentrations in different methanogenic mediums

Medium	**$MgSO_4.7H_2O$ (g/L)**	**$CaCl_2.2H_2O$ (g/L)**	**NaCl (g/L)**
Methanosaeta pelagica	-	0.15	20
Methanobacterium	0.4	0.05	0.4
Methanogenium	3.45	0.14	18
Methanosarcina	0.5	0.25	2.25
Methanoculleus sp.	3.45	0.14	6

The concentrations of the selected salts were chosen to be within the range of the medium given in Table 3.8. Furthermore, the ion concentration due to the salt media was computed and compared to the literature to eliminate any inhibition (Table 3.9)

(Ye Chen et al., 2008). Furthermore, the conductivity of the salt solution was equalized to 100 mM PBS (8 mS/cm). As a result of these factors, the salt concentrations in the medium were selected as 0.5 g/L $MgSO_4.7H_2O$, 0.15 g/L $CaCl_2.2H_2O$, and 5.5 g/L NaCl.

Table 3.9 A summary of possible inhibitory compounds in AD

Chemical	Effect
Ammonia	As ammonia concentrations were increased in the range of 4051–5734 mg NH_3–N/L, acidogenic populations in the granular sludge were hardly affected while the methanogenic population lost 56.5% of its activity.
Sulfide	The levels reported in the literature for inhibition of MPB also vary, with IC50 values of 50–125 mg H_2S/L at pH 7–8 for suspended sludge and 250 mg H_2S/L and 90 mg H_2S/L at pH 6.4–7.2 and pH 7.8–8.0, respectively.
Aluminum	After being exposed to 1000 mg/L $Al(OH)_3$ for 59 days, the specific activity of methanogenic and acetogenic microorganisms decreased by 50% and 72%, respectively.
Calcium	Ca^{2+} was moderately inhibitory at a concentration of 2500–4000 mg/L but was strongly inhibitory at a concentration of 8000 mg/L.
Magnesium	Cultures could be adapted to 300 mM (7.2 mg/L) Mg^{2+} without a change in growth rate, but growth ceased at 400 mg/L Mg^{2+}.
Potassium	It was observed that 0.15 M (5850 mg/L) K^+ caused 50% inhibition of acetate-utilizing methanogens. The inhibition could be at the acidogenic stage.
Sodium	The optimal growth conditions for mesophilic hydrogenotrophic methanogens reportedly occurred at 350 mg Na^+/L. Na^+ concentrations range from 3500 to 5500 mg/L to be moderate and 8000 mg/L to be strongly inhibitory to methanogens at mesophilic temperatures.

The initial composition of the reactors with the salt medium is given in Table 3.10. Moreover, the reactor operation during Set 2 is shown in Figure 3.6.

Table 3.10 Initial composition of the reactors with salt medium

Reactor	Seed	Feed	Initial VS (mg/L)	F/M ratio
Blank	+	-	8200±160	-
Test reactor	+	+	16500±300	1

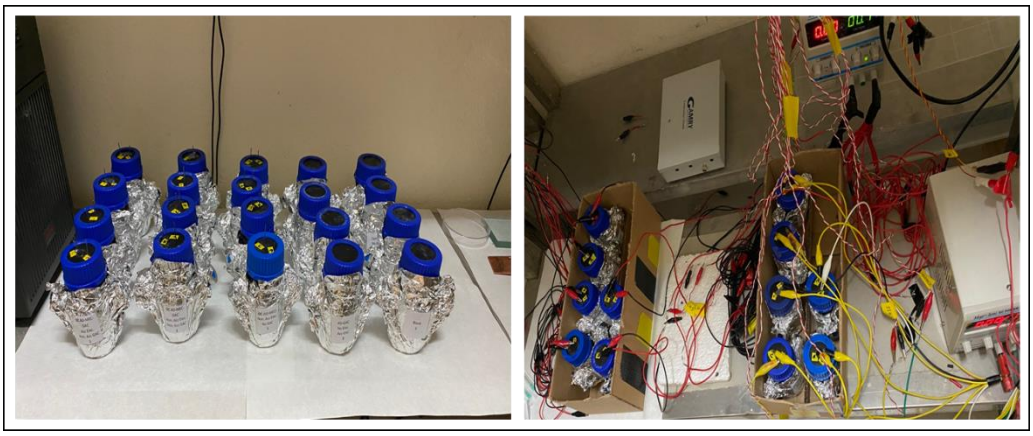

Figure 3.6 Reactors during the set 2 operation

3.4 Analytical Methods

Standard methods were used to determine COD (Method 5220 B), TS (Method 2540 B), and VS (Method 2540 E) (*APHA, Standard Methods for the Examination of Water and Wastewater*, 1999). Determination of orthophosphate (PO_4-P) and ammonium nitrogen (NH_4-N) was performed via the amino acid colorimetric method (Hach Method 8178) and the Nessler colorimetric method (Hach Method 8038) using a spectrophotometer (Hach Company, DR9200, USA), respectively. pH was measured with a portable pH meter (Ohaus, Starter300, U.S.A.). A portable conductivity meter was used to test conductivity (Hach, sensION 5, U.S.A.). Biogas production was measured using a gas-tight glass syringe at the end of each cycle. To analyze the CH_4 content of biogas, 150 µL of the sample was injected into a gas chromatograph (Thermo Scientific, TRACE GC Ultra, USA) equipped with a thermal conductivity detector (TCD) and two columns connected in series (CP-Moliseve 5A and CP-Porabond Q). Oven, injector, and detector temperatures were set as 35 ºC, 50 ºC, and 80 ºC, respectively. Helium was used as carrier gas at a constant pressure of 100 kPa.

Calibration curve for determination of biogas composition

The calibration equation was obtained by the use of 5-point duplicate injections of standard gas with volumes ranging from 50 µL to 250 µL of standard gas. The

standard gas was a mixture of hydrogen, N_2, CO_2, and CH_4. The composition of the mixture was, 50% hydrogen, 30% CO_2, 10% N_2, and 10% CH_4. In Table 3.11 and Figure 3.7, an example of how to calibrate for CH_4 can be seen.

Table 3.11 CH_4 gas calibration for GC-TCD

Injection Volume	Trial	Peak Area	Mean	Standard Dev.	Coefficient of Variation (%)
50	1	698710	691688	9930.60	1.44
	2	684666			
100	1	1314449	1308597	8275.97	0.63
	2	1302745			
150	1	1936349	1935039.5	1851.91	0.1
	2	1933730			
200	1	2562074	2583951.5	30939.45	1.2
	2	2605829			
250	1	3243900	3297415	75681.63	2.3
	2	3350930			

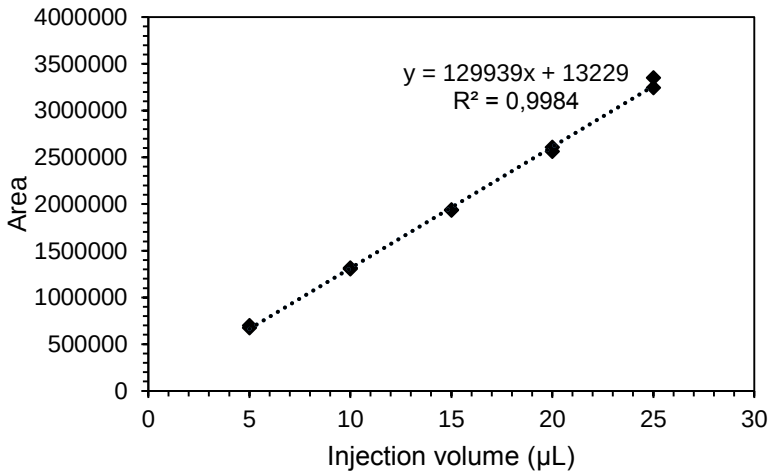

Figure 3.7 CH_4 gas calibration curve and equation

3.5 Calculations

Current Generation

In both Set 1 and Set 2 to monitor current production due to oxidation of organics, the voltage across the external resistor (R_{ex}: 10 Ω) connected to the anode electrode is continuously monitored using the data acquisition unit and calculated as given in Eq. 3.1 (Kas & Yilmazel, 2022) for Set 1 and 2.

$$I = \frac{V}{R_{ex}} \quad \text{(Eq. 3.1)}$$

The produced current was normalized by dividing it into anode total surface area (A) immersed in the reactor electrolyte. This normalized current is called current density (J) and is calculated using Eq. 3.2.

$$j\left(\frac{A}{m^2}\right) = \frac{I}{A} \quad \text{(Eq. 3.2)}$$

3.5.1 Set 1: Electromethanogenesis

Coulombic efficiency (CE)

The ratio of measured electrons from current and electrons that are available from substrate removal describes CE and is calculated as in Eq. 3.3 (Guo et al., 2017).

$$CE(\%) = \frac{\int_0^t Idt}{\frac{\Delta S \times V \times F \times b_O}{M_O}} \times 100 \quad \text{(Eq. 3.3)}$$

where ΔS is the substrate (COD) removed (mg/L), V is reactor active volume, F is Faraday constant (96485 C/mole of e^-), b_O is the mole of electrons that can be produced from the oxidation of organic matter by 1 mole O_2 (4 mole e^- /mole O_2), and M_O is the molar mass of oxygen (32 g/mole). An example calculation of the parameters is given in Appendix B.

Charge accumulation graph

The moles of electrons (Coulombs) that transferred from the anode are calculated below (Eq. 3.4).

$$C = \int_{t=0}^{t} Idt \quad \text{(Eq. 3.4)}$$

where I is the measured current and dt (s) is the interval over which data are collected. Summing up all the moles of electrons during specific time interval provides charge accumulation graph as equation below (Eq. 3.5) (Guo et al., 2017). An example calculation of the parameters is given in Appendix B.

$$charge\ accumulation = \sum_{1}^{n} \int_{t=n-1}^{t=n} Idt \quad \text{(Eq. 3.5)}$$

Gompertz Fitting to Charge Accumulation

The charge accumulation graph of reactors was fit by the modified Gompertz equation (Eq. 3.6) to interpret the charge accumulation rate and other relevant parameters for different reactors.

$$P = P_{\infty} \times exp\left\{-exp\left[\frac{Y_m \times e}{P_{\infty}}(\lambda - t) + 1\right]\right\} \quad \text{(Eq. 3.6)}$$

where P is cumulative coulombs transferred (C), P_{∞} is coulombs transferred potential (C), Y_m is the maximum specific coulombs transfer rates (C/d), and λ is the lag phase period to start coulombs transfer (days) (Fujikawa et al., 2004). An example calculation of the parameters is given in Appendix B.

3.5.2 Set 2: Anaerobic Digestion - Microbial Electrolysis Cell (AD-MEC) integration

Change in energy recovery efficiencies

Change in energy recovery efficiencies relative to the AD control was calculated as below (Huang et al., 2022):

$$\text{Change in energy efficiency} = \frac{W_{CH4_{AD-MEC}} - W_{PS}}{W_{CH4_{AD}}} \quad \text{(Eq. 3.7)}$$

where $W_{CH4_{AD-MEC}}$ is the energy recovery as CH_4 from the AD-MEC system (kJ).

$W_{CH4_{AD}}$ is the energy recovery as CH_4 from the control AD (kJ).

W_{PS} (kJ) is the energy added by the power source. It is corrected for losses across the external resistor (R_{ex} = 10 Ω) and calculated as (Call & Logan, 2008; Cheng & Logan, 2007).

$$W_{ps} = \sum_1^n IE_{PS}\Delta t - \sum_1^n I^2 R_{ex}\Delta t \quad \text{(Eq. 3.8)}$$

where E_{PS} = 0.7 V is the voltage applied using the power source, Δt (s) is the time increment for n data points measured during a batch cycle.

Gompertz Fitting to Methane Production

The modified Gompertz equation was used to estimate the trend of CH_4 production in reactors as below:

$$G = G_\infty \times exp\left\{-exp\left[\frac{X_m \times e}{G_\infty}(\omega - t) + 1\right]\right\} \quad \text{(Eq. 3.9)}$$

where G is cumulative CH_4 production (mL), G_∞ is CH_4 production potential (mL), X_m is the maximum specific CH_4 production rate (mL/d), and ω is the lag phase period to produce CH_4 (days) (Fujikawa et al., 2004). An example calculation of the parameters is given in Appendix B.

3.6 Statistical Analysis of Set 1: Electromethanogenesis

The Statistical Analysis System (SAS version 9.4 SAS, Cary, NC) was used to analyze the COD removal and C_E of MECs in Set 1. General linear model (GLM) analysis was used to determine differences between the averages of the groups, and Duncan's multiple comparison test was used to determine differences between the groups. *P* values < 0.05 were considered statistically different.

3.7 Cyclic Voltammetry

Cyclic Voltammetry (CV) is a strong and widespread electrochemical method used to study molecular species reduction and oxidation (Fricke et al., 2008). We apply different voltages to the reactors and measure the current. The largest current indicates the voltage with the most oxidation, and the lowest current indicates the reduced peak voltage (Figure 3.8). In both Set 1 and Set, 2 CV analysis was conducted using the same protocol. To analyze the activity of bioelectrodes CV with a standard three-electrode system was performed in each reactor (Scan range of -0.7 to 0 V vs. Ag/AgCl (3 M NaCl), scan rate 1 mV/S, equilibrium time 99 s) using a potentiostat (Gamry, Interface 1010B, USA). CV was performed on both anode and cathode after ten days from the start of biofilm formation and at the end of the test period. CV was also performed on a sterile bare anode and cathode with a sterile fresh anaerobic medium to provide an abiotic CV curve.

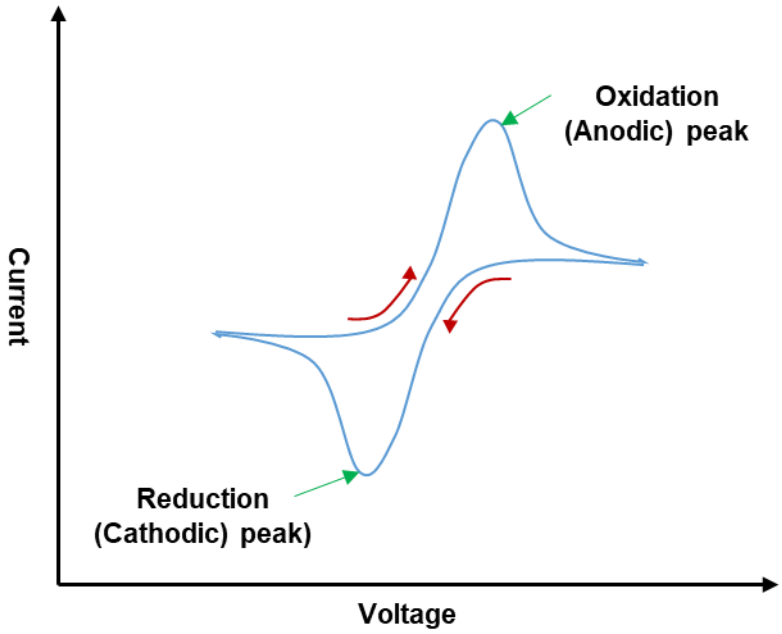

Figure 3.8 Example of cyclic voltammogram (Elgrishi et al., 2018)

3.8 Scanning Electron Microscopy (SEM) for Set 1 Electrodes

For SEM of bioelectrodes, samples were fixed with 4% paraformaldehyde (PFA) in 0.1 M phosphate buffer at pH 7.4 for 8 hours at 4°C as described elsewhere (Kas & Yilmazel, 2022). After three times washing with 0.1 M phosphate buffer, the samples were dehydrated in 25%, 50%, 75%, 95%, and 3x 100% EtOH. In order to increase the conductivity, before imaging, the samples were coated with a 15 nm gold-palladium coating. (Kas & Yilmazel, 2022). SEM was performed on day 10 of the biofilm formation stage for each MEC in Set 1.

3.9 Microbial Community Analysis in Set 1: Electromethanogenesis

The total genomic DNA isolation from the electrode surface and bulk solution was performed using GeneMATRIX Soil DNA Purification Kit (EURx, Poland) following the manufacturer's protocol. Isolated DNA sample concentrations and purities were checked by gel electrophoresis and NanoPhotometer P-Class (Titertek-Berthold, Germany). The metagenomic analysis was performed by the BM Laboratory Systems Company (Ankara, Turkey). The V3-V4 variable region (length of ~464 bp) of bacterial and archaeal 16S rRNA gene was used for metagenomic analysis using a set of primers: 341F (5′-CCTAYGGGRBGCASCAG-3′) and 785R (5′-GGACTACNNGGGTATCTAAT-3′) for bacteria, and archaea (Klindworth et al., 2013). During polymerase chain reaction (PCR) 28 cycles were performed. Cycles included the following steps: 95ºC for a duration of 3 mins, followed by 28 cycles of 95ºC for half a minute, 55ºC for half a minute, and 72ºC for a half minute, followed by the last step of elongation performed at 72ºC for 5 mins. After purification, the PCR products were used for another PCR reaction, where Illumina sequencing adapters and dual-index barcodes were attached to the amplicon target using KAPA HiFi HotStart Ready-mix PCR Kit (Kapa Biosystems, USA) and Nextera XT index kit (Illumina, San Diego, CA, USA) in accordance with the manufacturer's protocol. The second amplification program consists of the following steps: 95ºC for 3 min, followed by 8 cycles of 95ºC for half a minute, 55ºC for half

a minute, and 72ºC for half a minute, followed by a final elongation step at 72ºC for 5 mins. High-throughput sequencing was performed on Illumina Novaseq 6000 platform according to the standard protocols. All steps of the bioinformatics analysis were done on QIIME2 v2020.8 (Bolyen et al., 2019). The raw sequence reads were first checked and filtered using the q2-dada2 pipeline program by de-replication, de-noise procedures, and chimera removal (Callahan et al., 2016). q2-vsearch was used to cluster DNA sequence data into operational taxonomic units (OTUs) (Rognes et al., 2016). Taxonomic identification was achieved by aligning a representative sequence of each OTU using the Silva database (http://www.arb-silva.de). The overall community structure of bacterial and archaeal was determined based on biodiversity. Diversity indices of Shannon, Chao1, phylogenetic diversity and the observed richness were used to describe alpha diversity. An unweighted pair group method with arithmetic mean (UPGMA) clustering was used to assess the diversity between samples (beta diversity) based on the OTUs obtained from each sample. Both alpha and beta diversity indices were processed via the QIIME pipeline. Community analysis was performed for only Set 1.

CHAPTER 4

RESULTS AND DISCUSSION

4.1 Set 1: Electromethanogenesis

4.1.1 Current generation and charge accumulation

After the start-up of the MECs (t = 0) during the biofilm formation, current production in both ACE and CM fed reactors started approximately two days (Figure 4.1). The first peak in ACE fed MECs was recorded around day 4, and the peak of the CM fed reactors was recorded around day 8. On the other hand, the first peak of Blank reactors was recorded on day 30. When the coefficient of variation in the average peak current density of MECs over three consecutive cycles during the biofilm formation stage dropped to below 3%, the initial cycle of the three was accepted as the start of the stable current production in our study. Based on this, stable current production was started around day 15 for ACE fed MECs, day 20 for CM fed MECs, and day 25 for Blank MECs. During the biofilm formation period, the highest average peak current density of 0.30 ± 0.007 mA/cm^2 was recorded with the ACE fed reactors, which was around two times higher than the average peak current density (0.15 ± 0.005 mA/cm^2) recorded with the CM fed reactors. This may be due to the complex nature of the CM, leading to its slower utilization.

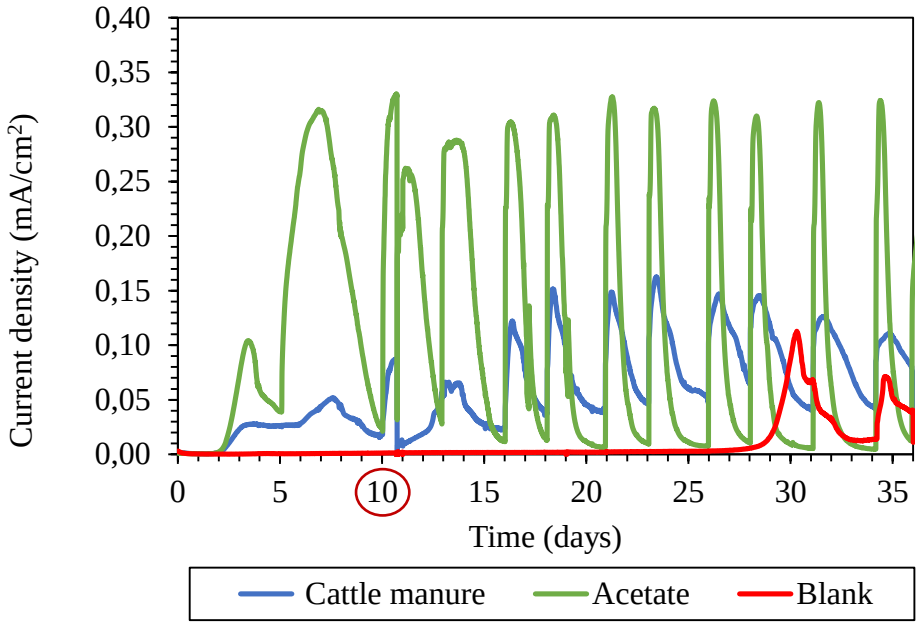

Figure 4.1 Current density graphs of MECs during A biofilm formation period (average of triplicate reactors is shown; a red circle on the x-axis (day 10) shows the time at which SEM was performed.)

Prior to stable current production in any of the reactors on day 10 of the biofilm formation stage, one reactor from each group was sacrificed for SEM imaging of electrode surfaces (Figure 4.2). Microorganisms with rod shape morphology and similar size, which are most likely exoelectrogens, were abundant on the anodes of both ACE fed MECs and CM fed MECs (Figure 4.2). Interestingly the cathodes of MECs fed with CM were also predominantly populated by rod shape microorganisms. Yet, on the cathodes of MECs fed with ACE mostly coccoidal shape microorganisms were observed. This suggests the presence of different types of microbial species on the cathodes as the cathode is a very selective environment (Zeppilli et al., 2015). As expected from very low current densities, there was no significant biofilm formation on the electrodes of Blank controls as of day 10.

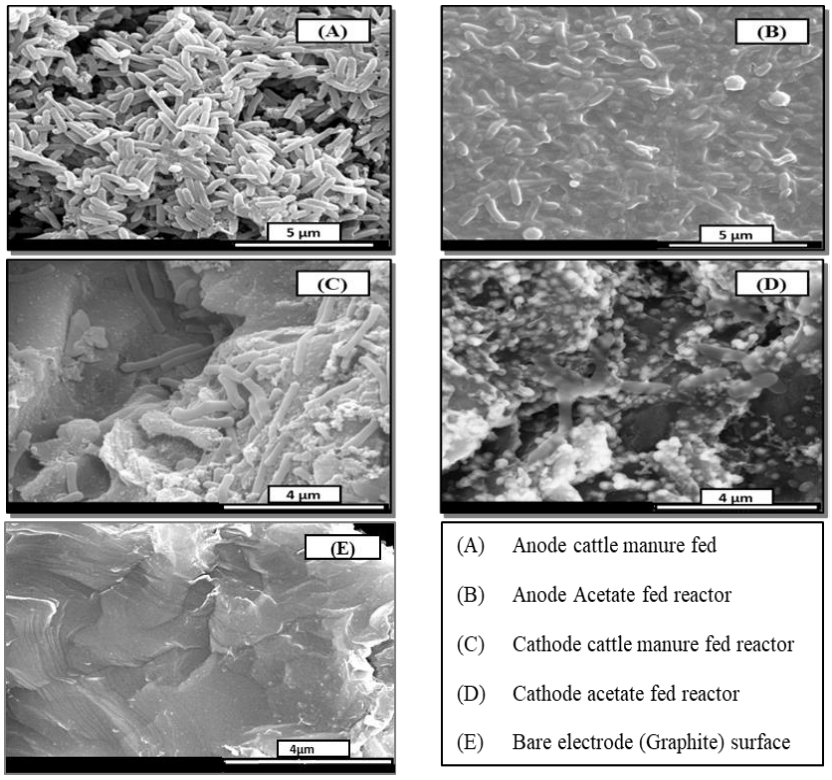

Figure 4.2 SEM images of bioelectrodes of A) anode of CM fed MECs, B) anode of ACE fed MECs, C) cathode of CM fed MECs, D) cathode of ACE fed MECs, E) Bare electrode

The current densities of the MECs during the test period are depicted in Figure 4.3 (see Appendix C for triplicate reactors). Among reactors fed with CM, namely, ACE_CM, CM_CM, and Blank, in most cycles of the test period, the highest current density was recorded with the ACE_CM reactors (Figure 4.3). Clearly, the current was improved due to the use of ACE. Similar to our results, a higher peak current was recorded with ACE during biofilm enrichment, and a lower current was produced upon switching to animal rendering waste in another recent work, where electrical current production in MECs was studied (Xie et al., 2021). During the test period, substrate concentration was gradually increased, and increasing the substrate concentration did not affect the peak current density; however, it had a direct relation with the cycle time (R^2 = 0.98; Figure 4.4). Among all reactors, ACE_ACE positive controls produced the highest peak current density of 0.41± 0.02 mA/cm^2 in the test

period, as expected (Figure 4.3). Siegert and others (2015) investigated the impact of different inoculation ratios of AD seed as inoculum (0.01% to 25% (w/v)) and similarly used acetate (10 mM) as the electron donor for both biofilm formation and test periods (Siegert, Li, et al., 2015). The recorded peak current densities in Mini MECs ranged from 0.22 – 0.28 mA/cm^2 when normalized to the whole immersed anode surface area (Siegert, Li, et al., 2015). The higher current densities recorded in our ACE_ACE MECs may be related to different inoculums, MEC materials, and higher operating temperatures of 35 ºC in our experiments (Siegert, Li, et al., 2015). During the test period, the cross-fed positive controls (CM_ACE) reached 0.34 ± 0.04 mA/cm^2, which was lower than single substrate ACE_ACE controls.

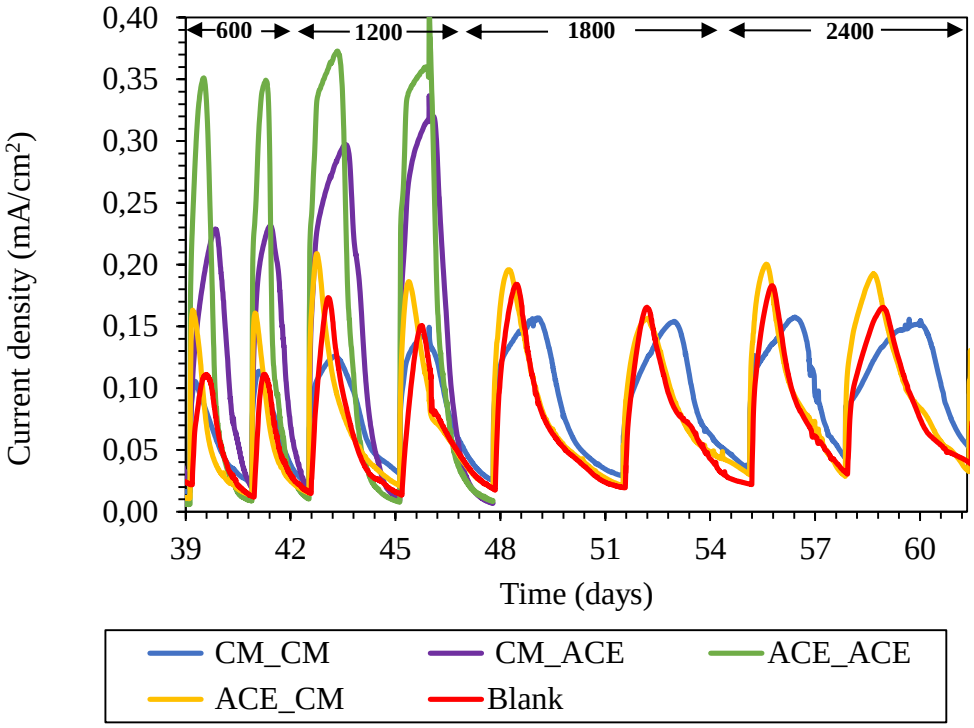

Figure 4.3 Current density graphs of MECs during the test period at different sCOD concentrations of 600, 1200, 1800, and 2400 mg/L (average of triplicate reactors is shown)

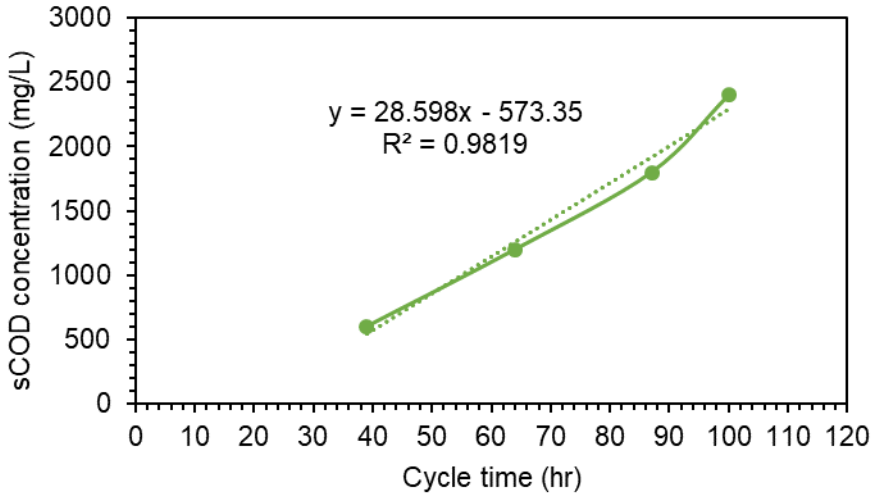

Figure 4.4 The relation between the sCOD added and cycle duration

Analyzing the charge accumulation profile is helpful for evaluating MEC performance and waste treatability (Ivanov et al., 2013). To this purpose, transferred coulombs through the circuit were computed by summing up the current output over time (Ivanov et al., 2013) and then analyzed using the modified Gompertz equation (Figure 4.5 and Table 4.1). The modified Gompertz fittings and experimental data of all reactors are shown in Appendix D.

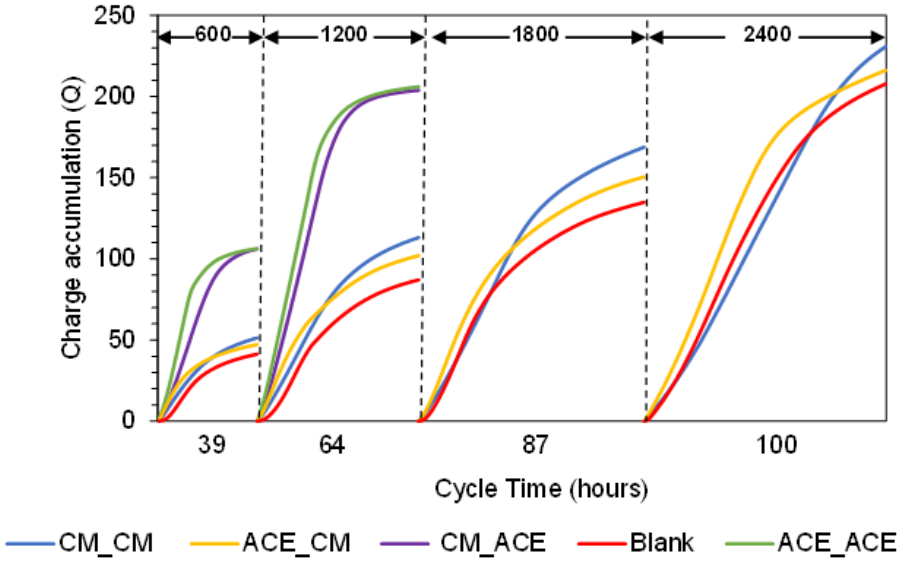

Figure 4.5 Charge accumulation curve during the test period at different sCOD concentrations of 600, 1200, 1800, and 2400 mg/L (Only the second cycle at each sCOD concentration is shown)

Table 4.1 Coulombs transferred rates (C/d) during the test period at different sCOD concentrations (Average of triplicate reactors)

sCOD concentration	**CM_CM**	**CM_ACE**	**ACE_ACE**	**ACE_CM**	**Blank**
600 mg/L	51.07	123.47	178.57	61.97	49.81
1200 mg/L	72.31	179.06	204.68	71.66	61.57
1800 mg/L	80.69			83.71	79.61
2400 mg/L	77.82			101.74	84.96

Total charge accumulation for CM_CM reactors in all sCOD concentrations was slightly higher compared to ACE_CM reactors. Yet, interestingly, Y_m in ACE_CM reactors at 600 and 2400 mg/L sCOD concentration was ~20% higher than CM_CM. The higher Y_m translates into less time requirement of ACE acclimated reactors to

reach their peak current and this is related to the microbial community on the anode of MECs. A similar observation was made for positive controls. During the test period, coulombs transferred in ACE_ACE and CM_ACE were both around 107 C at 600 mg/L sCOD concentration, which was almost doubled at 1200 mg/L sCOD concentration reaching 203.7 ± 5.8 C in CM_ACE and 208.6 ± 5.1 C in ACE_ACE (Figure 4.6A). Yet, the modified Gompertz fitting of charge accumulation profiles showed that ACE_ACE reactors had 36% higher Y_m (maximum specific coulombs transfer rate) compared to CM_ACE reactors at 600 mg/L sCOD concentration (Figure 4.5 and Table 4.1). At 1200 mg/L sCOD concentration, again there was faster charge accumulation in ACE_ACE reactors in comparison to CM_ACE reactors, yet the difference decreased to 15%. Feeding ACE during the biofilm formation stage favors more exoelectrogens as most are capable of utilizing ACE, which increases the rate of coulombs transfer. Our microbial community analysis also supported this, as Geobacter, the model exoelectrogen, was present in ACE acclimated reactors at a higher abundance (Logan et al., 2019).

4.1.2 Methane production

By increasing substrate concentration, CH_4 production in MECs also increased (Figure 4.6B). Mostly the highest CH_4 production for CM fed reactors was recorded with CM_CM reactors. With this reactor, there was 127.6 ± 8.82 mL/L (91.2 ± 6.6 mL/L-d) of CH_4 production at 600 mg/L sCOD and 530 ± 60 mL/L (150.2 ± 17.0 mL/L-d) at 2400 mg/L sCOD. Positive controls produced higher CH_4 than CM added reactors at the same sCOD level. For example, ACE_ACE reactors produced 267 ± 7 mL/L (with a rate of 200 ± 5 mL/L-d) of CH_4 at 600 mg/L of sCOD concentration and 518 ± 10 mL/L (with a rate of 230± 4 mL/L-d) of CH_4 at 1200 mg/L of sCOD. Since ACE is a pure, readily biodegradable substrate, CH_4 production in MECs fed with ACE was two times higher than in MECs fed with CM at the same sCOD concentration. This may stem from the presence of slow hydrolysis steps that are necessary to obtain suitable electron donors for exoelectrogenic bacteria when CM

is fed as a substrate. These results show that twice as much sCOD was needed for producing the same amount of CH_4 with CM.

CH_4 production of Blank reactors was mostly less than CM_CM reactors which were inoculated with AD seed. However, as time passed, the difference between the CH_4 production rate in Blank reactors and CM_CM reactors decreased from 45% at 600 mg/L sCOD to 10% at 2400 mg/L sCOD. The difference clearly stems from the inoculum. There is a longer time requirement for Blank reactors to establish an active layer of electro-active biofilm similar to AD seed inoculated reactors.

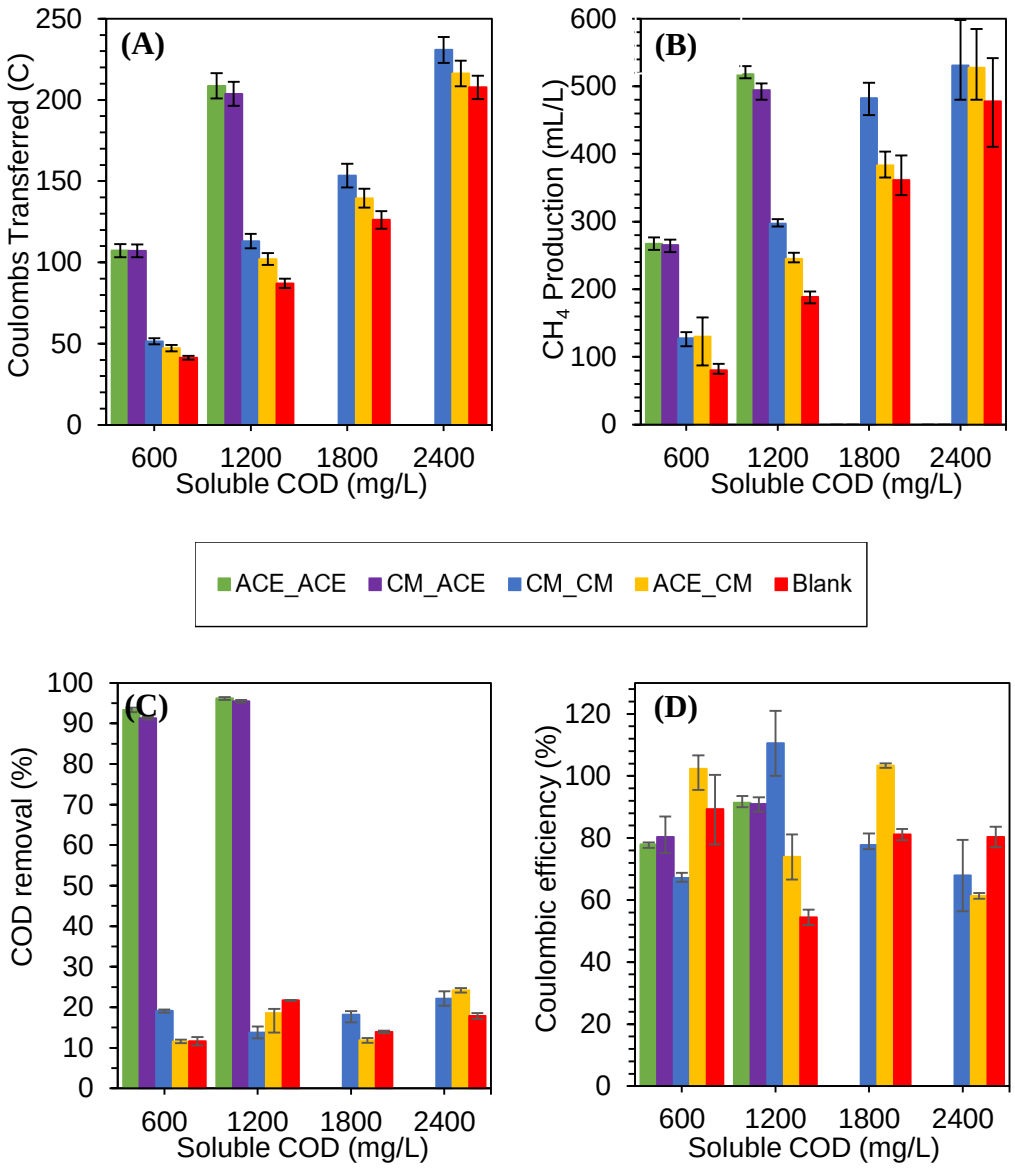

Figure 4.6 A) Coulombs transferred and B) CH_4 production C) COD removal D) CE during test period at different sCOD concentrations (average of triplicate reactors is shown; error bar indicates the variation between triplicate reactors)

When the CH_4 production of ACE_CM reactors and CM_CM reactors were compared, the total amount of CH_4 production in CM_CM reactors was higher or similar to the ACE_CM reactors in various sCOD levels. This may be indicative of a slight adverse impact of cross-feeding on the performance of electromethanogenic reactors. Hence, for electromethanogenic reactors, there is no need for starting up

the reactors with a simple substrate. It should be noted that among the CM fed reactors, peak current was higher in ACE_CM and Blank reactors in comparison to CM_CM, and this does not necessarily translate into the total amount of CH_4 production. On the other hand, total coulombs transferred are directly related to the amount of CH_4 production (Figure 4.5 and 4.6B). CH_4 production in open circuit controls was negligible (<0.1 mL).

4.1.3 COD removal and coulombic efficiency

The COD removal during each cycle is given in Figure 4.6C. As expected, there was lower organic removal in the case of complex waste in comparison to ACE. The average COD removal, including all cycles of the test period, was 18.3 ± 2.9% in the CM_CM reactor, 17.0 ± 5.2% in the ACE_CM reactors and 16.2 ± 3.2% in the Blank reactors. The charge accumulation trend of reactors fed with CM suggests that at the start of each batch cycle, exoelectrogens rapidly start to degrade the readily biodegradable portion of the substrate and produce current at a high rate. As time passed the current production rate decreased which may be explained by the reduced substrate degradation rate. Unlike reactors fed with ACE, the charge accumulation in these reactors did not reach a plateau because there was no complete depletion of the substrate (Figure 4.5). Regardless of the initial concentration, COD removal in positive controls which were fed with ACE averaged 94 ± 2%. Almost complete substrate depletion in ACE fed MECs also explains the plateau reached by the end of the cycle in the charge accumulation graphs of ACE fed MECs (Figure 4.5).

Among the ACE fed reactors (CM_ACE and ACE_ACE) there was a statistically significant difference in COD removals, only when MECs were fed with sCOD of 600 mg/L and no statistically significant difference in COD removals was observed when reactors were fed with sCOD of 1200 mg/L. Further, no statistically significant difference was found in the CEs of CM_ACE and ACE_ACE reactors in either sCOD of 600 mg/L or 1200 mg/L (Table 4.2 and 4.3). This can be interpreted as the

short-term impact of complex waste feed during biofilm formation in terms of organic removal.

Table 4.2 Summary table for statistical analysis for COD removal (CR, %) with respect to different COD concentrations

Reactor	COD600	COD1200	COD1800	COD2400
CM_CM	19.1±0.2^{c}	13.8±0.8^{d}	18.2±0.5^{a}	22.2±1.0^{a}
ACE_CM	11.5±0.4^{d}	18.5±0.6^{c}	11.8±0.3^{c}	24.2±0.3^{a}
ACE_ACE	93.2±0.3^{a}	96.3±0.2^{a}	-	-
CM_ACE	91.2±0.2^{b}	95.6±0.2^{a}	-	-
Blank	11.6±0.6^{d}	21.7±0.1^{b}	13.9±0.2^{b}	17.9±0.4^{b}

Means of three replicates (Mean ± Std. Errors). Values within a column followed by different lowercase letters are significantly different ($p < 0.05$).

Table 4.3 Summary table for statistical analysis for coulombic efficiency (CE, %) with respect to different COD concentrations

Reactor	COD600	COD1200	COD1800	COD2400
CM_CM	67.2±0.9^{c}	110.5±6.0^{a}	77.7±0.7^{c}	67.9±6.6^{ab}
ACE_CM	102.3±3.6^{a}	73.9±4.2^{c}	103.4±0.4^{a}	61.3±0.5^{b}
ACE_ACE	78.9±0.6^{b}	88.7±1.1^{b}	-	-
CM_ACE	81.4±3.5^{b}	88.4±1.3^{b}	-	-
Blank	89.3±6.4^{b}	54.5±1.4^{d}	81.1±1.0^{b}	80.3±1.9^{a}

Means of three replicates (Mean ± Std. Errors). Values within a column followed by different lowercase letters are significantly different ($p < 0.05$).

When ACE_CM and CM_CM were compared in terms of COD removals and CEs; there was a statistically significant difference between their COD removals at sCOD concentrations of 600, 1200, and 1800 mg/L (Table 4.2 and 4.3). Yet, no statistically significant difference was found between ACE_CM and CM_CM at sCOD of 2400 mg/L, which corresponds to an operation of more than 55 days. As opposed to

CM_ACE and ACE_ACE, a longer time was needed for ACE_CM and CM_CM reactors to show no statistically significant difference. Hence, if the aim is to feed MECs with a complex waste it is suggested that biofilm formation also started with the same complex waste.

Our results also clearly show that the biofilm formation protocol, i.e., the type of the primary substrate and the source of inoculum, does not significantly impact the COD removals during the test period, and it is mostly related to the complexity of the substrate.

4.1.4 Electrochemical analysis of the electrodes at different stages

The SEM images showing the presence of microorganisms on the anodes, and current production together imply that exoelectrogenic microorganisms were enriched in the MECs. As proof, CV curves of both ACE fed MEC anodes (dashed line in Figure 4.7A) and CM fed MEC anodes (dashed line in Figure 4.7B) showed a sigmoidal curve with clear oxidation peaks. However, as there was not sufficient biofilm on the anode of the Blank reactors, no such peak was observed on the anode of the Blank MECs (dashed line in Figure 4.7C). This is also consistent with the SEM images. The sigmoidal CV curve is typical for direct electron transfer and has been also observed with model exoelectrogens such as Geobacter (Fricke et al., 2008).

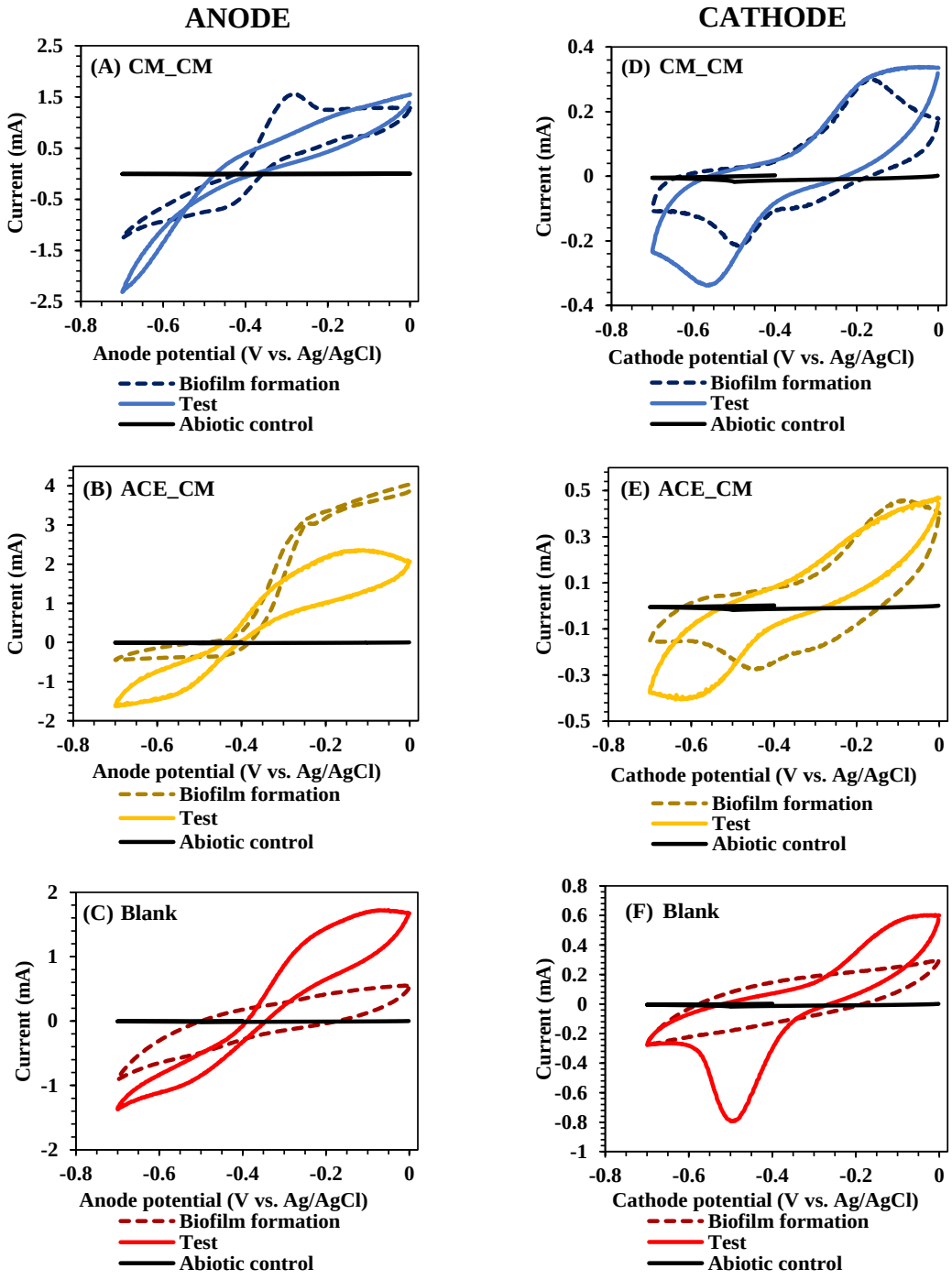

Figure 4.7 CV graphs of anodes of A) CM_CM, B) ACE_CM, C) Blank reactors and cathodes of D) CM_CM, E) ACE_CM, F) Blank reactors

CV curves of the CM_CM and ACE_CM cathodes both showed a reduction peak between the potential of −0.35 and −0.65 V vs. Ag/AgCl on day 10, and yet there was no such reduction peak in the Blank reactors. As biofilm formed in the Blank reactors by the end of the test period, the final CV of the Blank reactors also showed a similar reduction peak (straight line, Figure 4.7E) as in CM_CM and ACE_CM CVs. This is another proof of the late biofilm formation on the electrodes of the Blank reactors and the need for a longer time. CM_CM and ACE_CM cathodes showed a clear cathodic reduction peak between −0.35 and −0.65 V vs. Ag/AgCl with a midpoint potential around ca. −0.5 V vs. Ag/AgCl. The midpoint potential in the Blank reactors was around −0.4 V vs. Ag/AgCl. No appreciable peak was observed in the bare electrodes placed in the abiotic control. Similar CV curves to our work were obtained when thermophilic electomethanogenic biocathodes prepared in single chamber MECs were later used as cathodes in two-chamber MECs (Fu et al., 2015). The presence of the catalytic wave similar to our results with a midpoint potential of around −0.55 V vs. Ag/AgCl (-0.35 V vs. SHE) was observed in another study, indicating the presence of direct electron transfer mechanism in electromethanogenic MECs (Fu et al., 2015).

4.1.5 Archaeal community

The diversity of archaea on the CM_CM anode and CM_CM cathode appears to be similar except for minor differences. In the CM_CM anode biofilm, the unidentified species belonging to the genus *Methanoculleus* and *Candidatus methanogranum* were the most abundant archaea with rates of 45.4 % and 44.1 %, respectively (Figure 4.8).

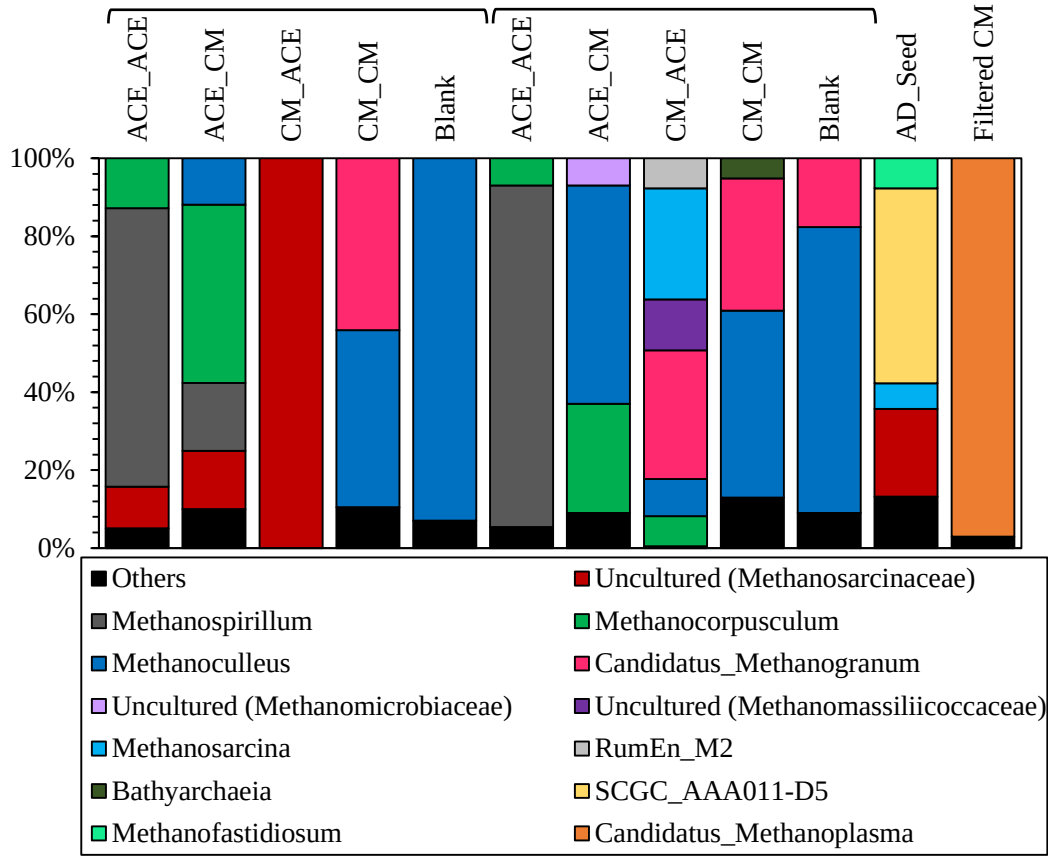

Figure 4.8. Microbial community structures based on the relative abundance of 16S rRNA sequences of AD seed, filtered CM, and biofilms of the electrodes in MECs at the archaeal genus level

In the CM_CM cathode biofilm, the same archaeal species were dominant with 47.9% and 33.9%, respectively. *Methanoculleus* is a hydrogenotrophic methanogen; hence capable of using H_2 released from the cathode surface for the reduction of CO_2 to CH4 (Eq. 2 and 3) (Cheng et al., 2009). On the other hand, members of the family Methanomethylophilaceae, including the genus *Candidatus methanogranum*, are methylotrophic methanogens using hydrogen-dependent reduction of methanol to CH_4 (H_2 + CH_3OH → CH_4 + H_2O) (Iino et al., 2013). Family Methanomethylophilaceae are among those methanogens that are mostly associated with the digestive tracts of animals, which explains their presence in CM-associated reactors (Cozannet et al., 2021). The existence of the genus *Methanoculleus* in

methanogenic communities of BES such as AD – MEC systems have been previously reported (Bo et al., 2014). However, the significant presence of the genus *Candidatus methanogranum* was rare to the best of our knowledge. It is clear that the microbial diversity that can form biofilms on the electrodes of Blank reactors comes only from CM. When the diversity of archaea in the anode and cathode of the Blank reactors was examined, it was revealed that communities of bioanode and biocathode were quite similar even though the ratios of the genera were different (Figure 48). The most abundant archaea in Blank reactors belong to the genus *Methanoculleus*, with a ratio of 92.9% at the anode and 73.4% at the cathode. When the archaeal diversity analysis of CM alone was examined, it was observed that *Candidatus methanoplasma* (97.0%) from the family *Methanomethylophilaceae* is the dominant species, which has also been detected in the archaeal microbiome of mesophilic biogas plants located in Italy that are fed cattle sewage and corn silage (Agrimonti et al., 2022). However, in anode and cathode biofilms of MECs that were fed with CM, the relative proportion of this genus decreased with the increase in the diversity during the electromethanogenesis process (Figure 4.8).

In the ACE_ACE cathode biofilm, *Methanospirillum* (87.6%), *Methanocorpusculum* (7.0%), and *Methanoculleus* (3.2% listed under others in Figure 4.8) stand out as the three dominant archaeal genera which are hydrogenotrophic (Demirel and Scherer, 2008). In addition to these, metagenome analysis of the biofilm on ACE_ACE cathode also identified the members of methylotrophic order *Methanomassiliicoccales*, hydrogenotrophic order *Methanomicrobiales*, as well as a well-known acetoclastic methanogen *Methanosaeta* in small proportions (Demirel and Scherer, 2008). Although ACE is the only substrate in the ACE_ACE reactor, acetoclastic methanogens appear to have a relatively small abundance in diversity, as noted above. Many studies reported that hydrogenotrophic methanogens are dominant in MEC cathode biofilms, whereas acetoclastic methanogens are less abundant (Dykstra and Pavlostathis, 2017). Our results are consistent with the results of previous studies. Here, the presence and activities of syntrophic acetate-oxidizing (SAO) bacteria on the electrodes should be

noted. SAO bacteria work in coordination with hydrogenotrophic methanogens to perform a two-stage conversion. In the first stage, SAO bacteria produce H_2 and CO_2 via the degradation of ACE, then these products are consumed by hydrogenotrophic methanogens to produce CH_4 (Westerholm et al., 2018). Recently it was reported that SAO bacteria replace acetoclastic methanogenesis during the anaerobic degradation of biowaste (Dyksma et al., 2020). The close association between these two groups makes the dominance of hydrogenotrophic methanogens clear, especially in cathode biofilms. When anode archaeal microbial community distribution is analyzed, we observe mostly similar distribution of archaeal microbial community to their respective cathodes especially in single substrate MECs of ACE_ACE, CM_CM, and Blank. In the case of cross-feeding of CM and ACE, differences between archaeal communities in the anodes and cathodes were observed. For example, the CM_ACE anode was populated with the *Methanosarcinaceae* family, while it was not present in the CM_ACE cathode. It is reported that this family is the most adaptable among all methanogens regarding the variety of the substrates they are capable of using; for instance, some can utilize methanol, multiple species can use hydrogen, some use acetate and there are also others capable of utilizing other substrates such as carbon monoxide (Oren, 2014).

4.1.6 Bacterial community

It was revealed that there was a highly diverse range of bacterial communities on the electrode biofilms when compared to the archaeal diversity, as shown by the higher contribution of others (<5% abundance) in Figure 4.9. 16s rRNA amplicon-based microbial diversity results identified over one hundred bacteria at the genus level. In general, it was observed that the dominant phylum on the anodes is Desulfobacterota, to which the genus Geobacter belongs. On the other hand, Firmicutes, to which the SAO bacteria species of the dominant phylum were present on the cathodes (Figure 4.9). In fact, Geobacter, the model exoelectrogens commonly found in MECs, was the most dominant genus in all anode biofilms (Figure 4.10).

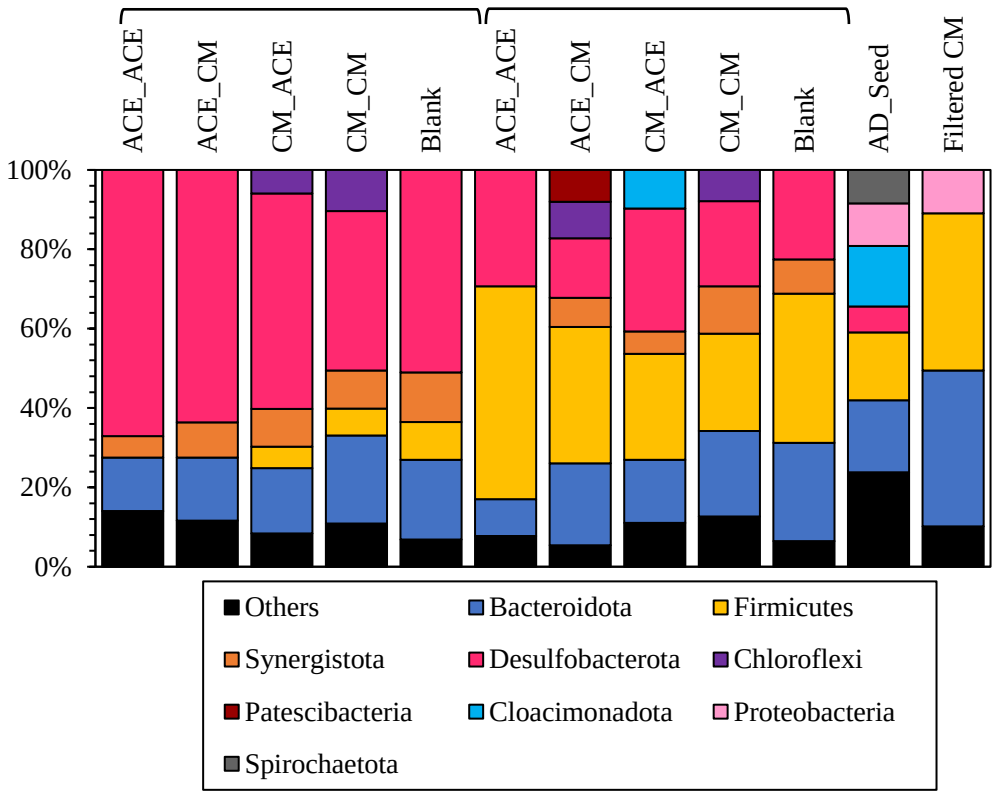

Figure 4.9. Microbial community structures based on the relative abundance of 16S rRNA sequences of AD seed, filtered CM, and biofilms of the electrodes in MECs at the bacterial phylum level

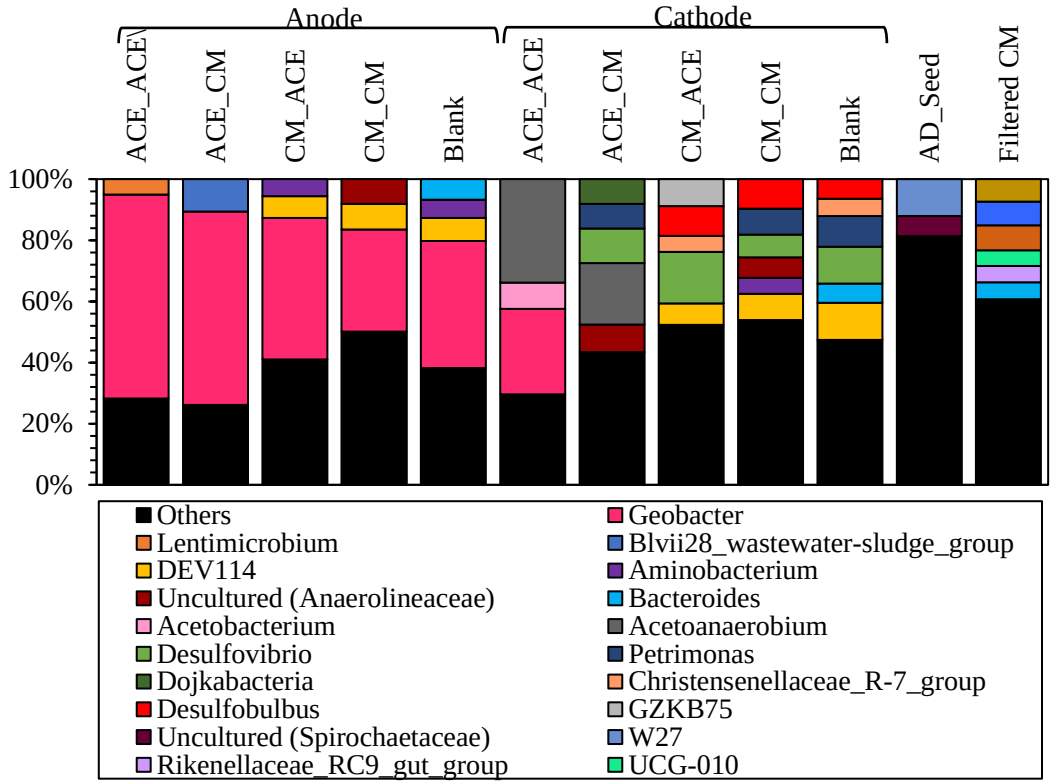

Figure 4.10. Microbial community structures based on the relative abundance of 16S rRNA sequences of AD seed, filtered CM, and biofilms of the electrodes in MECs at the bacterial genus level.

Further, the ratio of phylum *Bacteroidota* in biofilm samples taken from all electrodes is undeniable. It was present by 18.1% in AD seed and 39.3% in filtered CM. Its higher abundance in the CM sample played a role in its relatively higher abundance on the cathodes of MECs fed with CM. For example, Class *Bacteriodota* belonging to phylum *Bacteroidota* was present at 21.7% on the cathodes of Blank reactors, 19.1% on the cathodes of CM_CM reactors, 20.6% on the cathodes of ACE_CM reactors, 14.5% on the cathodes of CM_ACE reactors, and less than 10% (~9.3%) on the cathodes of ACE_ACE reactors. A similar observation was noted for the anodes; the lowest abundance was present in ACE_ACE anodes, among others. The presence of exoelectrogenic species belonging to the Class Bacteriodota on the anodes of bioelectrochemical reactors has also been reported in other studies (Kutlar

et al., 2022). In general, it was observed that the bacterial diversity distribution on the cathodes was proportionally more balanced than on the anodes, and anodes created a more selective environment for bacteria.

When the hierarchical clustering of the isolated DNA samples from both electrode surfaces of each MEC, the initial AD seed, and filtered CM was analyzed according to the UPGMA (Figure 4.11), and two distinct communities on anodes and cathodes were statistically distinguished as expected. Community cluster analysis proved that the primary substrate has critical importance in the formation of microbial biofilm on the electrodes and the impact of cross-feeding was not significant on the biofilm microbial population. In other words, after biofilm formation on the electrode surface is completed upon feeding the primary substrate, changing the substrate does not help to reshape the biofilm entirely, and the first settlers resist the biofilm. This explains why the performance of reactors decreased when the substrate was changed. A similar observation was reported recently by Harnish and Korth (2021), where they report that the microorganism that first colonized on the electrode occupies the surface and hence forms most of the biofilm community. In our work, during the biofilm formation stage, we did not add any CM to ACE fed reactors; hence microorganisms originating from CM may not have predominated in the biofilm of these MECs. For instance, among the anode microbial community, we observed that ACE_CM and ACE_ACE were related more closely than the cluster of CM_CM, CM_ACE, and Blank reactors, all of which received only CM during the biofilm formation stage (Figure 4.11). Detailed analysis of Figure 4.10 shows that Geobacter abundance on the anodes of CM_ACE and Blank reactors was relatively higher than CM_CM; hence they are clustered closely. When cathodes were analyzed, we observed that ACE_ACE cathodes were less similar to others; which can be explained by the fact that this reactor never received CM while all others received CM. For example, although not dominant a significant presence of Geobacter was observed in the ACE_ACE cathodes. This may be explained by DIET between Geobacter and Methanofastidiosum, which was recently reported to be possible in a recent study (König et al., 2022). Among CM receiving reactors, CM_CM and

CM_ACE were more closely related than the Blank cathode indicating the importance of the seed on cathodic biofilm formation.

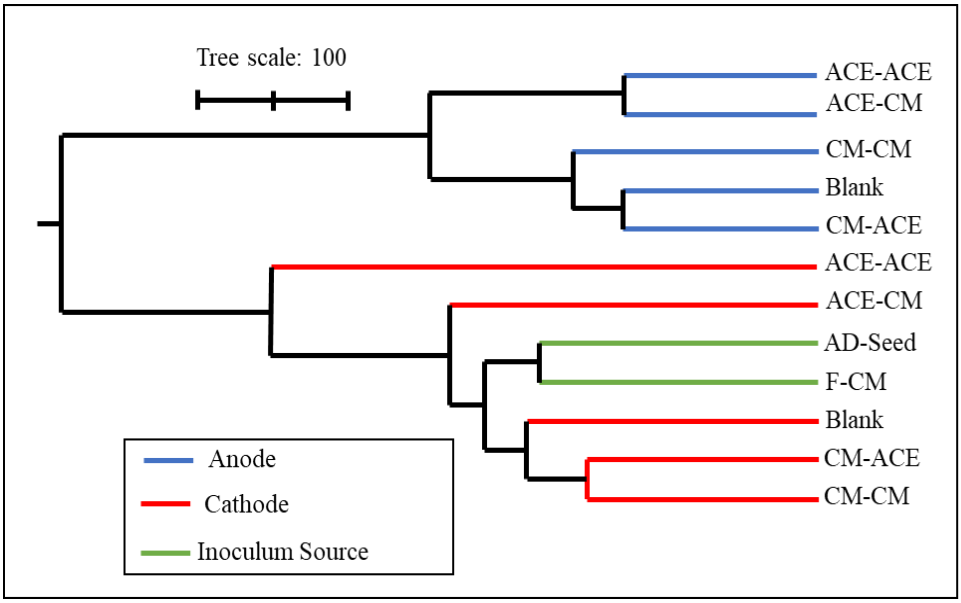

Figure 4.11. Microbial community structures based on the relative abundance of 16S rRNA sequences of AD seed, filtered CM, and biofilms of the electrodes in MECs the via hierarchical clustering tree

4.2 Set 2: Anaerobic Digestion - Microbial Electrolysis Cell (AD-MEC) integration

4.2.1 Biofilm Formation

Initial Current Production and Cyclic Voltammetry

The experimental design of the test period of biofilm formation in Set 2 is given in Table 3.5 and Figure 3.5. The current density during the first 28 days of the biofilm formation stage is shown in Figure 4.12. Around 4 days after the incubation of MECs, current production started in both MECs with GAC and MECs without GAC. The current production dropped after almost 8 days. Hence, the first cycle lasted

around 8 days. Once the current density dropped to below 0.08 mA/cm^2, a new cycle was started via injection of the substrate. Later on, based on the increase in the biofilm amount on the electrodes, the cycle time decreased to 4 days. In this stage, there were 4 cycles in total corresponding to 28 days of total operation time. The highest current density during this initial phase averaged at 0.189 ± 0.08 mA/cm^2 in MECs without GAC while the average peak current was around 0.216 ± 0.06 mA/cm^2 in MECs with GAC. At the end of day 28, CV was performed for both anodes and cathodes to monitor the presence of biofilm on the electrodes. The yellow lines in (Figure 4.13A and 4.13B) belong to the bare electrode as abiotic controls. No appreciable peak was observed in the bare electrodes placed in the abiotic control.

The cathodic and anodic peaks for MEC_noGAC and MEC_GAC are shown in Figures 4.13A and 4.13B. The cathodic and anodic peaks for MEC_noGAC and MEC_GAC are shown in Figures 4.13A and 4.13B. The CV results for anodes of MEC_noGAc and MEC_GAC showed a sigmoidal curve with clear oxidation peaks. The sigmoidal CV curve is characteristic of direct electron transfer, and it has been seen in the field with model exoelectrogens like Geobacter (Fricke et al., 2008). The cathode CV results for both MEC_noGAC and MEC_GAC showed a reduction peak between the potential of −0.35 and −0.65 V vs. Ag/AgCl with a midpoint around -0.5 V vs Ag/AgCl. Another research found a catalytic wave with a midpoint potential of −0.55 V vs. Ag/AgCl (-0.35 V vs. SHE) in electromethanogenic MECs, confirming direct electron transfer (Fu et al., 2015b).

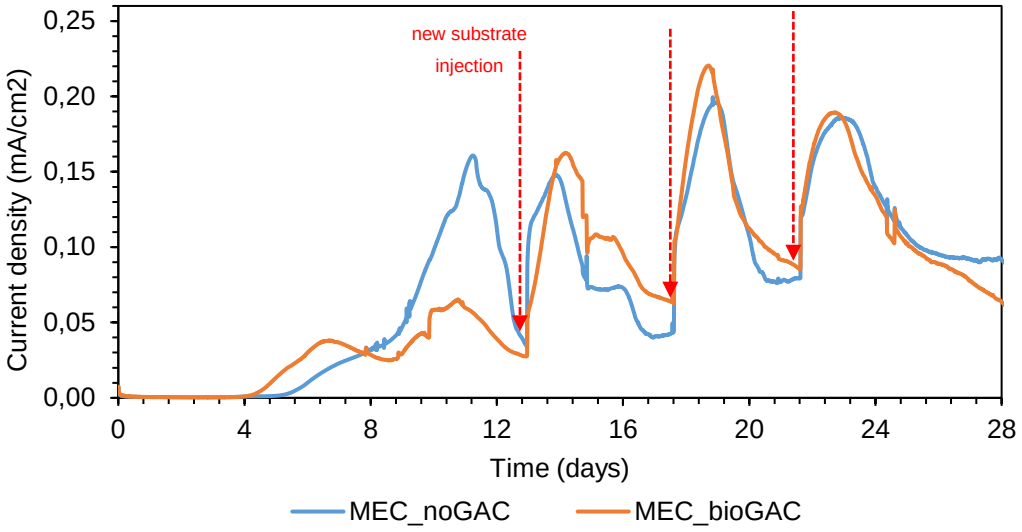

Figure 4.12 Current density graph during the biofilm formation stage until day 28

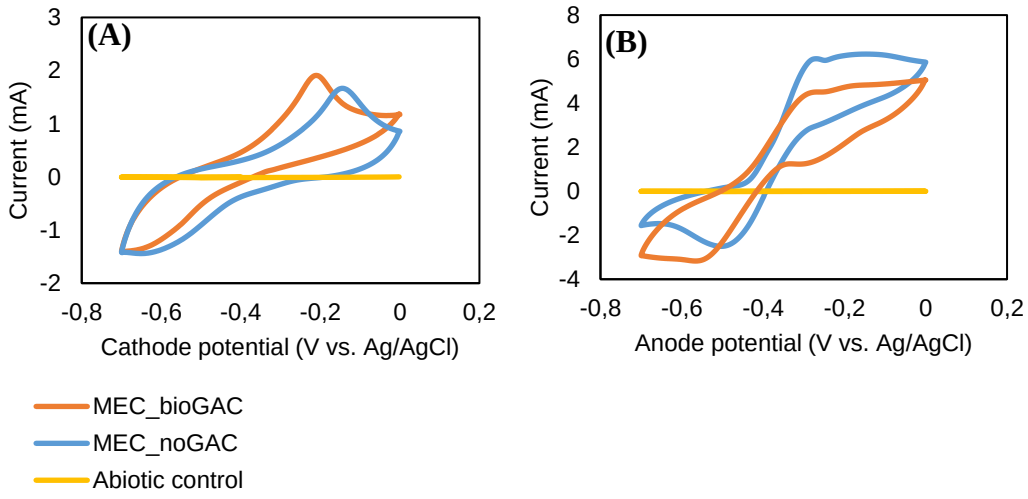

Figure 4.13 Cyclic voltammetry graph for A) cathode, B) anode after 28 days of operation

Performance of MEC test

Before completion of the biofilm formation stage, each of the MECs was operated for two more cycles in fed batch mode. This time as described in the Materials and Methods section, the reactor content was emptied and refilled to start a new cycle.

During the first MEC cycle, the MEC_noGAC produced an average of 277.9±35.3 mL/L of CH_4, while during the second cycle, they produced 297.9±17.9 mL/L (Figure 4.14A). On the other hand, the MEC_BioGAC produced 324.6±18.5 mL/L CH_4 during the first cycle and 395.3±26.2 mL/L CH_4 during the second cycle (Figure 4.14A). Even though the difference in the first cycle was not significant there was around 28% higher CH_4 production in the presence of BioGAC during the second cycle.

Coulombs transferred, current density, and charge accumulation graphs are shown in Figure 4.14B and Figure 4.15. Both the current densities and coulombs transferred were similar in the absence and presence of GAC, hence it may be concluded that the presence of GAC did not have a significant impact on the performance of exoelectrogenic microorganisms colonized on the anode surface. The position of the anode electrode within the MEC is a probable explanation for the identical current output in the MEC_GAC and MEC_BioGAC. There was no contact of GAC with the anode electrode, hence its impact on anodic biofilm may be lower.

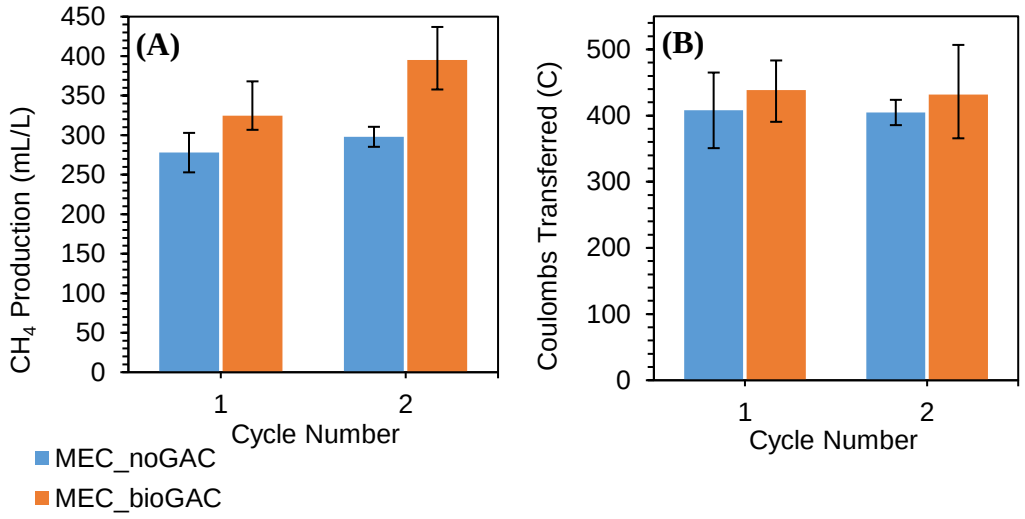

Figure 4.14 A) CH_4 production B) Total number of Coulombs transferred during fed-batch operation of MECs at the biofilm formation stage

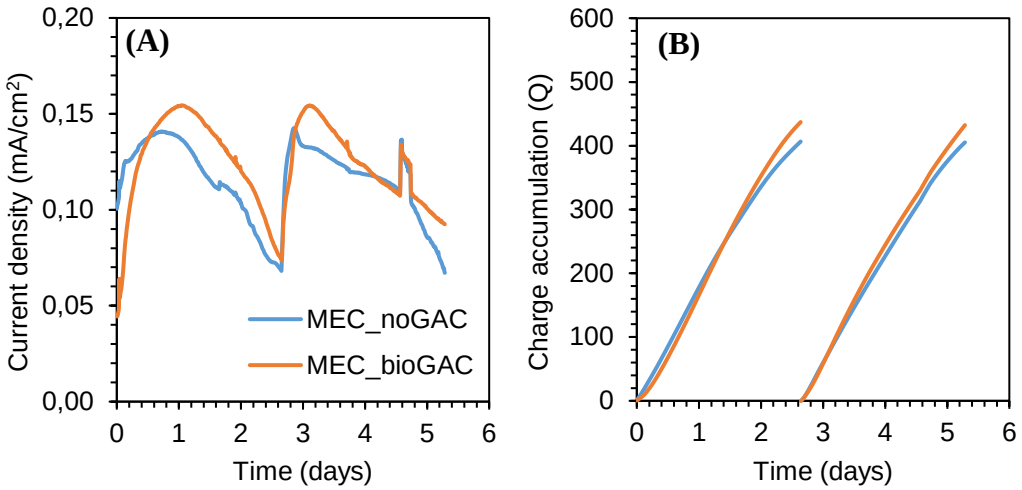

Figure 4.15. A) Current density B) Charge accumulation graph during fed-batch operation of MECs at the biofilm formation stage

Comparison of Set 1 and Set 2 Data

In order to see how scaling up the reactors from 15 ml to 65 ml active volume affects the MEC performance during the biofilm formation stage, we compared the results of CM_CM reactors from the first set of experiments with MEC_withoutGAC (Figure 4.16A and 4.16B). To do this, we have used the same sCOD (1200 mg/L) cycle data. We normalized the coulombs transferred to the surface area of the electrodes used in Set 1 and Set 2. The normalized coulombs transferred for 15 mL and 65 mL active volume were 25.13±0.9 and 26.20±0.1 C/cm^2, respectively. Also, the normalized CH_4 production in 15 mL active volume reactors of Set 1 averaged 297.22±4.64 mL/L, and CH_4 production in 65 mL active volume reactors of Set 2 averaged 287.9±10 mL/L. These results show that there was a similar performance of MEC batch cycles after scaling up the reactor size from 15 mL to 65 mL active volume. See Appendix B for the details of the calculations.

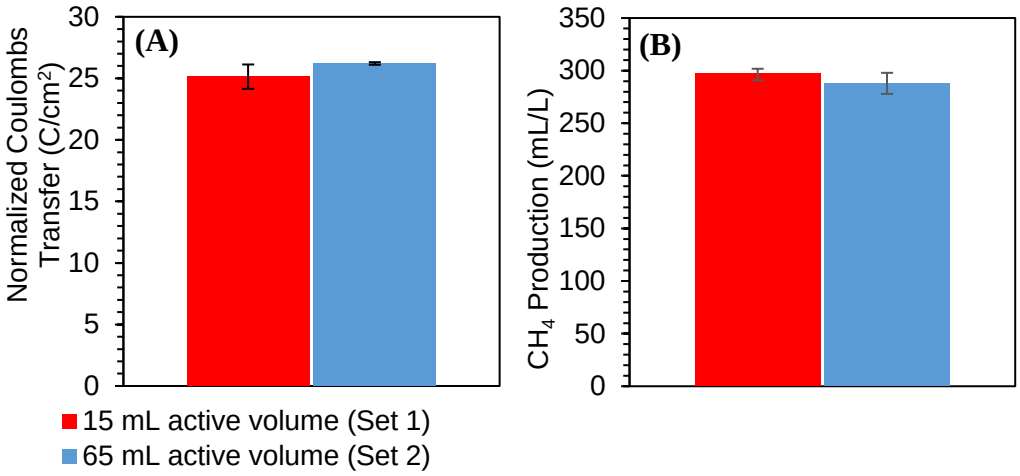

Figure 4.16. Comparison of Set 1 and Set 2 MEC performances in terms of A) Coulombs transferred B) CH_4 production with 1200 mg/L sCOD feed

4.2.2 Test Period

Methane production and organic removal

The experimental design of the test period of Set 2 is given in Table 3.7 and illustrated in Figure 3.5. The cumulative CH_4 production of the AD-GAC, AD-MEC, and AD-MEC-GAC groups is shown in Figure 4.17A-C. Moreover, cumulative CH_4, net CH_4 yield and production rate parameters (lag time, and maximum CH_4 production rate), equivalent CH_4 of current, and VS removal are summarized in Table 4.4 for 100 mM PBS and Table 4.5 for salt media. The modified Gompertz fittings and experimental data of all reactors are shown in appendix D for 100 mM PBS media and Appendix E for salt media. The lag time and maximum CH_4 production rate were calculated via modified Gompertz fitting to the cumulative CH_4 production and the equivalent CH_4 of current was calculated assuming all current is used for CH_4 production, *i.e.*, 100% cathodic recovery. An example calculation for all these parameters is provided in Appendix B.

When 100 mM PBS was used as the medium, the conventional AD (AD-noGAC) reactor produced 88.44 ± 1.7 mL CH_4 leading to around 49.9 ± 2.6 CH_4/g VS_{added} as

yield during 45 days. Upon extension of the batch cycle to 61 days, total cumulative CH_4 production was increased to 129.9 ± 1.2 mL corresponding to a net CH_4 yield of 112.6 ± 1.7 mL CH_4/g $VS_{added,}$ (Table 4.4). The long lag time of around 25 days as well as CH_4 production lower than Blank reactors is an indication of strong inhibition in the AD-noGAC reactors. In a study for evaluating the effect of phosphorus enrichment on digester performance, different concentration of phosphate (500, 1000, and 2000 mg/L) PO_4-P was added to AD reactors, The results demonstrated that reactors with 500 mg/L started CH_4 production after 11 days and on day 18 produced 85% of CH_4 which control reactor without phosphorus did produce. The reactors with 1000 and 2000 mg/L phosphorus produced the same as the control reactor after 46 and 71 days respectively (Carliell-Marquet & Wheatley, 2002). The PO_4-P concentration in 100 mM PBS is around 3000 mg/L which could be the reason for inhibition in the AD-noGAC reactor.

The cumulative CH_4 production and CH_4 yield for AD-FreshGAC during 45 days of operation were 130.9 ± 3.1 mL and 114 ± 4.6 mL CH_4/g $VS_{added,}$ respectively. Even though the cumulative CH_4 production and yields are similar, the presence of fresh GAC increased the CH_4 production rate by 70% and decreased the lag time by 62% when compared to conventional AD. Using conductive materials such as GAC boosts the CH_4 generation rate and reduces the lag time, by promoting DIET in the microbial consortium (Lovley, 2017; J. H. Park et al., 2018). As opposed to MIET electron transfer via DIET does not have the same diffusion constraints therefore the rate of conversion is higher (Lovley, 2017; J. H. Park et al., 2018). When bioGAC was amended (AD-BioGAC), the reactors produced 183.5 ± 2.3 mL cumulative CH_4 corresponding to a yield of 193.8 ± 3.4 mL CH_4/g VS_{added} during 45 days. Adding bioGAC in conventional AD reactors increased the CH_4 production rate by 63% in comparison to AD-noGAC. The lag time for conventional AD reactors without GAC amendment was around 25 days, which shows the inhibitory effect of 100 mM PBS medium on the AD process. However, using the bioGAC in the AD reactors dropped the lag time to 1.8 days. It is reported that the addition of GAC adsorbs the inhibitory compounds and hence improves AD performance (Aktaş & Çeçen, 2007; Poirier et

al., 2017). The better performance of AD-BioGAC reactors compared to AD-FreshGAC could be the microbial aggregation on GAC during the biofilm formation stage (Cayetano et al., 2022).

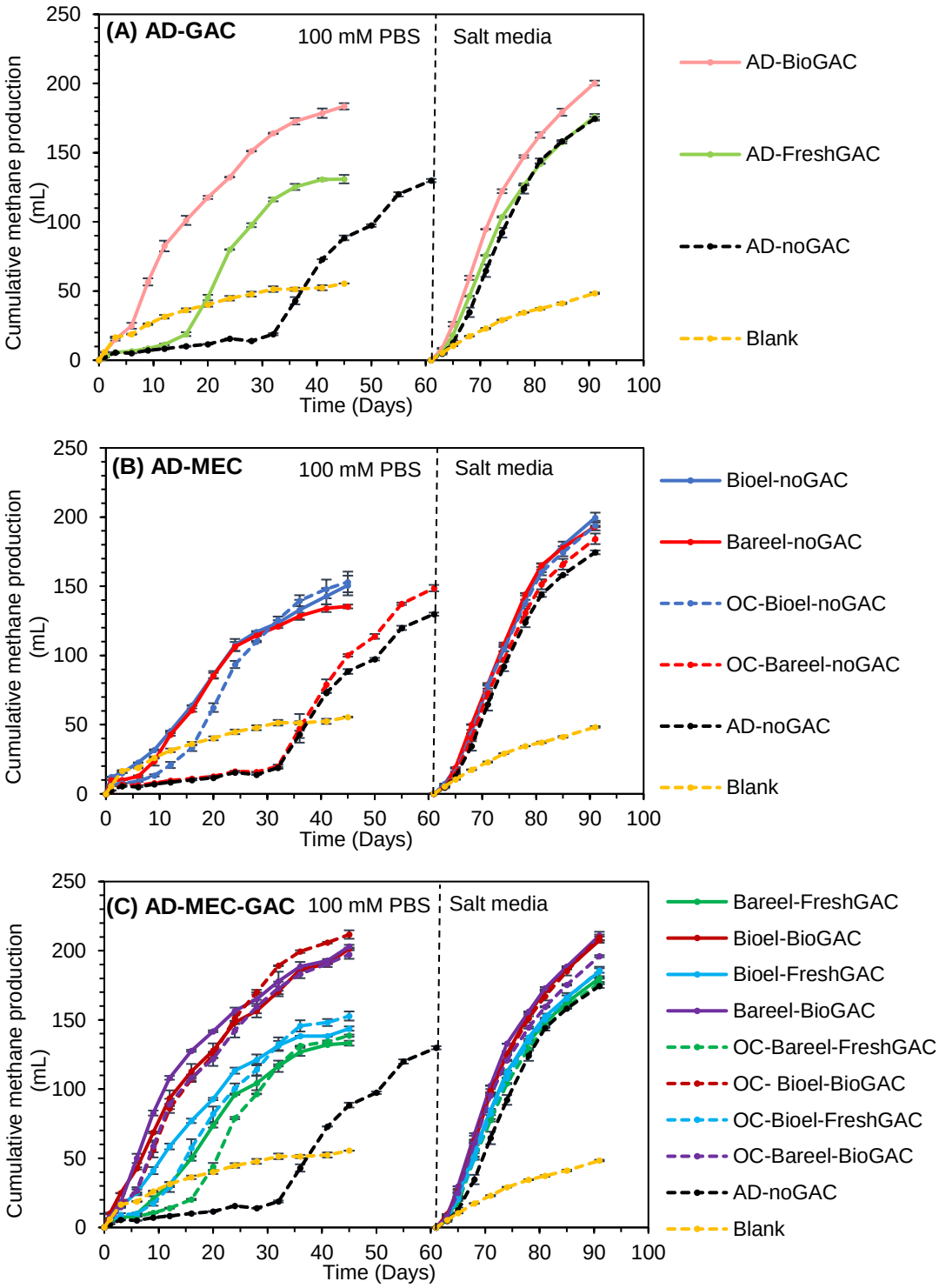

Figure 4.17. Cumulative CH_4 production of A) AD-GAC reactors B) AD-MEC C) AD-MEC-GAC reactors in Set 2

Table 4.4 CH_4 production, kinetics parameters and VS removal (%) of the reactors with 100 mM PBS

	Reactors	Cumulative CH_4 (mL)	Net CH_4yield (ml_{CH4}/gr VS_{added})	Lag Time (Day)	Max CH_4 production rate (mL/d)	Equivalent CH_4 of Current (mL)	VS removal (%)	R^2
AD-GAC	AD-noGAC	129.9±1.2 88.44±1.7*	112.6±1.7 49.9±2.6*	25.49±0.55	4.31±0.16	-	48.9±1.5	0,9863
	AD-FreshGAC	130.9±3.1	114.1±4.6	13.29±0.54	7.29±0.36	-	29.0±4.0	0.9968
	AD-BioGAC	183.5±2.3	193.8±3.4	1.81±0.39	7.01±0.11	-	29.5±1.1	0.9938
AD-MEC	Bioel-noGAC	150.6±7.1	144.0±10.8	2.39±0.26	4.89±0.13	80.3±4.4	21.1±1.1	0.9964
	Bareel-noGAC	135.4±1.4	121.0±2.1	4.56±0.33	5.64±0.01	100.6±3.2	20.2±0.5	0.9966
	OC-Bioel-noGAC	153.1±7.5	147.8±11.3	9.49±0.72	6.17±0.15	-	23.8±1.9	0.9964
	OC-Bareel-noGAC	148.7±2.3 100.1±0.9*	141.1±3.5 67.5±1.3*	26.51±1.09	5.20±0.11	-	46.4±0.4	0.9888
AD-MEC-GAC	Bareel-FreshGAC	133.2±1.7	117.6±2.6	5.96±0.14	5.28±0.14	82.0±2.4	29.1±4.9	0.9983
	Bioel-BioGAC	201.4±0.8	220.9±1.3	0.40±0.01	7.07±5.58	69.4±9.7	33.7±1.6	0.9914
	Bioel-FreshGAC	143.7±1.5	133.6±2.3	1.89±0.46	5.58±0.07	66.1±15.7	24.4±5.3	0.9980
	Bareel-BioGAC	203.1±1.1	223.6±1.7	0.62±0.31	8.66±0.14	69.9±1.7	28.7±2.9	0.9881
	OC-Bareel-FreshGAC	138.6±0.8	125.9±1.2	12.63±0.42	6.67±0.17	-	30.5±5.9	0.9948
	OC-Bioel-BioGAC	211.7±3.0	236.5±4.6	2.36±0.43	7.68±0.04	-	26.4±3.1	0.9956
	OC-Bioel-FreshGAC	152.8±3.3	147.4±5.0	6.71±0.56	6.00±0.15	-	22.3±3.5	0.9978
	OC-Bareel-BioGAC	197.3±3.1	214.7±4.7	1.82±0.09	7.40±0.31	-	29.3±4.1	0.9928

* The results during 45 days of batch operation.

The total CH_4 production in the OC-Bioel-noGAC reactor was similar to Bioel-noGAC and 12% higher than Bareel-noGAC reactors. However, the modified Gompertz results revealed that the required start-up time for this reactor was 120% longer than Bioel-noGAC and 70% longer than Bareel-noGAC. Chen and colleagues stated that applying electrical stimulation could expedite the hydrolysis process (Chen et al.,2016). The CH_4 production yield in the OC-Bareel-noGAC reactor produced was 67.5 ± 1.3 mL CH_4/g VS_{added} as of day 45 and when compared to the other OC reactor (OC-Bioel-noGAC) this amount is less than 50%. The difference between the two OC reactors comes only from the biomass colonized on the electrodes (Ying Chen et al., 2016). The presence of bioelectrodes clearly reduced the lag time of the reactors. Also, in the literature, it is reported that the microorganisms attached to a carrier surface may better tolerate adverse conditions than suspended microorganisms (Falås et al., 2012).

During batch experiments with 100 mM PBS medium, regardless of whether there was applied voltage, all BioGAC amended reactors (AD-BioGAC, Bioel-BioGAC, Bareel-BioGAC, OC-Bioel-BioGAC, OC-Bareel-BioGAC) started CH_4 production after two days. Also, the CH_4 production yields in these reactors were ranked the highest five among all reactors. Between the FreshGAC amended reactors, although the performance of the reactors when the voltage was applied was slightly lower than their OC controls (Bioel-FreshGAC vs. OC-Bioel-FreshGAC) and (Bareel-FreshGAC vs. OC-Bareel-FreshGAC), the modified Gompertz results analysis showed that application of voltage shortened the lag time. The lag time in OC-Bioel-FreshGAC was around 6.6 and dropped to 1.8 days in Bioel-FreshGAC. The lag time in OC-Bareel-FreshGAC was around 12.6 and dropped to 5.9 days in Bareel-FreshGAC. The results of reactors' operation with 100 mM PBS suggest that integrating AD with MEC or amendment of conductive material in AD systems increases the stability of the reactors.

Because there was a significant inhibition in AD reactors via the use of 100 mM PBS, a salt media was used in the second cycle, in this salt media P concentration

was significantly lowered yet the same conductivity level of 8 mS/cm was maintained via various salt additions. (See Figure 3.5 for the experimental design.) The same performance parameters (CH_4 production yield, lag time, CH_4 production rate, etc.) were calculated with salt media and summarized in Table 4.5. In this case, there was no long lag time as opposed to 100 mM PBS. When the modified salt medium was used, the cumulative CH_4 production reached 174.6 ± 1.4 mL in the AD-noGAC reactor with a net CH_4 yield of 247 mL CH_4/g VS_{added} in 30 days of operation. This is more than twice the yield with 100 mM PBS media. The cumulative CH_4 production and CH_4 yield for AD-FreshGAC were around 250 mL CH_4/g $VS_{added.}$ Fresh GAC did not significantly affect CH_4 production, however, it decreased the lag time by 37% in comparison to AD-noGAC. Using the modified medium instead of 100 mM PBS resulted in 298 mL CH_4/g VS_{added} net CH_4 yield during 30 days batch cycle in BioGAC amended AD (AD-BioGAC) reactors. The biomass attached to GAC within the reactors might be responsible for the 15% increase in cumulative CH_4 output (Lee et al., 2016). Besides that, salt medium BioGAC amendment increased the CH_4 production rate by 10.7% as compared to AD-noGAC.

Table 4.5 CH_4 production, modified Gompertz kinetics and VS removal (%) of the reactors with salt media with 100 mM PBS

	Reactors	Cumulative CH_4 (mL)	Net CH_4yield (mL_{CH4}/gr VS_{added})	Lag Time (Day)	Max CH_4 production rate (mL/d)	Equivalent CH_4 of Current (mL)	VS removal (%)	R^2
AD-GAC	AD-noGAC	174.6±1.4	246.9±2.7	3.72±0.37	10.01±0.06	-	29.4±1.5	0.9997
	AD-FreshGAC	176.0±2.0	249.7±3.9	2.53±0.00	9.75±0.03	-	29.0±4.0	0.9973
	AD-BioGAC	200.3±1.7	297.3±3.4	1.95±0.05	11.16±0.09	-	29.5±1.1	0.9962
AD-MEC	Bioel-noGAC	199.6±3.6	296.0±7.0	3.05±0.02	10.76±0.28	22.1±3.9	22.1±1.1	0.9993
	Bareel-noGAC	193.3±0.6	283.6±1.1	2.97±0.01	11.16±0.12	38.0±0.7	20.2±0.5	0.9990
	OC-Bioel-noGAC	193.9±3.5	284.4±6.8	3.19±0.13	10.84±0.25	-	24.4±1.9	0.9988
	OC-Bareel-noGAC	184.3±3.8	266.0±7.5	3.31±0.04	10.24±0.25	-	22.2±0.4	0.9990
AD-MEC-GAC	Bareel-FreshGAC	180.2±0.4	258.0±0.8	2.18±0.08	10.46±0.00	24.9±0.7	24.7±4.9	0.9963
	Bioel-BioGAC	207.5±0.2	311.3±0.5	2.02±0.17	11.64±0.23	20.5±4.5	31.0±1.6	0.9973
	Bioel-FreshGAC	185.0±3.4	267.3±6.7	2.14±0.01	10.45±0.17	15.3±4.2	26.2±5.3	0.9971
	Bareel-BioGAC	210.9±0.7	318.1±1.4	1.82±0.03	12.03±0.01	30.1±0.2	28.1±2.9	0.9950
	OC-Bareel-FreshGAC	176.7±0.7	251.1±1.5	2.44±0.11	9.91±0.14	-	20.5±5.9	0.9975
	OC-Bioel-BioGAC	209.7±4	315.7±7.8	1.88±0.14	11.30±0.34	-	31.0±3.1	0.9946
	OC-Bioel-FreshGAC	185.7±1.6	268.7±3.2	2.36±0.11	10.19±0.05	-	33.3±3.5	0.9973
	OC-Bareel-BioGAC	196.1±0.7	289.0±1.4	1.88±0.05	11.05±0.07	-	29.6±4.1	0.9952

As compared to 45 days of operation with 100 mM PBS medium, the cumulative CH_4 production plateaued after 30 days in the salt medium. Bioel-noGAC reactors

showed an 8% improvement in total CH_4 production and an 11% improvement in net CH_4 yield compared to OC-Bareel-noGAC reactors. External voltage application as well as using biofilm-attached electrodes are responsible for this increase.

Bareel-FreshGAC reactors produced around 180 mL CH_4; yet, with biofilm formed electrodes and bioGAC (Bioel-BioGAC), the amount of CH_4 increased to 208 mL (Table 4.5). The cumulative CH_4 production results suggested that biofilm attached electrodes (Bioel) and GAC (BioGAC) can increase CH_4 production by 14% compared to the Bareel-FreshGAC system. The net CH_4 yield results suggest that using bio-GAC in reactors can increase the net CH_4 yield by more than 28% despite the type of reactor.

The VS removal of the reactors is shown in Tables 4.4 and 4.5. The VS removal of conventional AD reactor (48.9 ± 1.5%) and OC-AD-MEC-Bareel reactors (46.4 ± 0.4%) with 100 mM PBS solution after 61 days batch cycle was highest among all the reactors of the test period. Other than the mentioned reactors, the organic removal of all reactors was similar during the 45 days of batch cycle with 100 mM PBS solution (averaged at 29.8 ± 4.7%). Similarly, when the salt medium was used during the 30 days batch cycle, all reactors had almost identical VS removal (average of 29.6 ± 4.6%). CM has a complex structure (lignin, cellulose, and hemicelluloses), and this complexity slows down its degradation (Font-Palma, 2019). The higher VS removal of conventional AD reactors and OC-Bareel-noGAC reactors could be due to longer incubation times than other reactors. Even though the batch cycle of reactors with 100 mM PBS was a total of 45 days; which is 15 days longer than those with salt medium, their VS removals were similar. Despite the longer batch cycle, the similar organic removals with 100 mM PBS and salt medium suggests that being exposed to high phosphate concentration due to 100 mM PBS media, inhibits the AD mechanism and slows the organic degradation (Carliell-Marquet & Wheatley, 2002).

Current Generation in AD-MEC Reactors during Test Period

During the two cycles, the change in current density in reactors was monitored to evaluate the bioelectrochemical system's contribution to CH_4 production (Figure 4.18) (see Appendix F for duplicate reactors). When utilizing 100 mM PBS instead of the salt medium, exoelectrogenic bacteria function better on the anodic surface, as seen by both the current density and charge accumulation graphs. In the AD-MEC group, the reactors with bioelectrodes (Bioel) produced 0.05 ± 0.002 mA/cm^2 stable current during the first 20 days of the experiment, and then the current density dropped to around 0.02 ± 0.005 mA/cm^2. There was no peak current in these reactors and it is expected as there was already biofilm on the electrodes. On the other hand, the reactors with bare electrodes started the current production after 3 days and reached a peak of 0.18 ± 0.1 mA/cm^2 on day 9, and then on day 17, a second peak around 0.12 ± 0.1 mA/cm^2 was seen. The Current eventually dropped to 0.03 ± 0.003 mA/cm^2 at the end of the batch cycle with 100 mM PBS medium. The second peak was observed in the Bioel reactors as well, but not distinct as in Bareel reactors. According to the research that has been published, the first peaks might be the result of the breakdown of carbohydrates, while the second peaks could be the result of the degradation of crude proteins and lignocelluloses (Xing et al., 2021; C. Zhang et al., 2018).

The charge accumulation graph shows that reactors with bare electrodes produced 3071 ± 99 C, which is 40% higher than reactors with bioelectrodes 2452 ± 134 C. In the second cycle with salt medium, the Bioel reactors produced a stable current density of 0.03 ± 0.002 mA/cm^2 during the first 12 days and then dropped to 0.006 ± 0.002 mA/cm^2 at the end of the experiment. However, the reactors with bare electrodes started the current production after 4 days and reached 0.12 ± 0.03 mA/cm^2 after 6 days and finally dropped to 0.006 ± 0.001 mA/cm^2. The trends in current generations with the two medias for both Bioel-noGAC and Bareel-noGAC were similar yet the generated current was different among all the reactors. Accordingly, the charge accumulation graph shows that the total charge transferred

with 100 mM PBS was ~3.1 times higher than the salt medium. The charge transferred for Bioel reactors was 675 ± 120 C, while for the bare electrode reactors, it was 53% higher with 1162 ± 22 C.

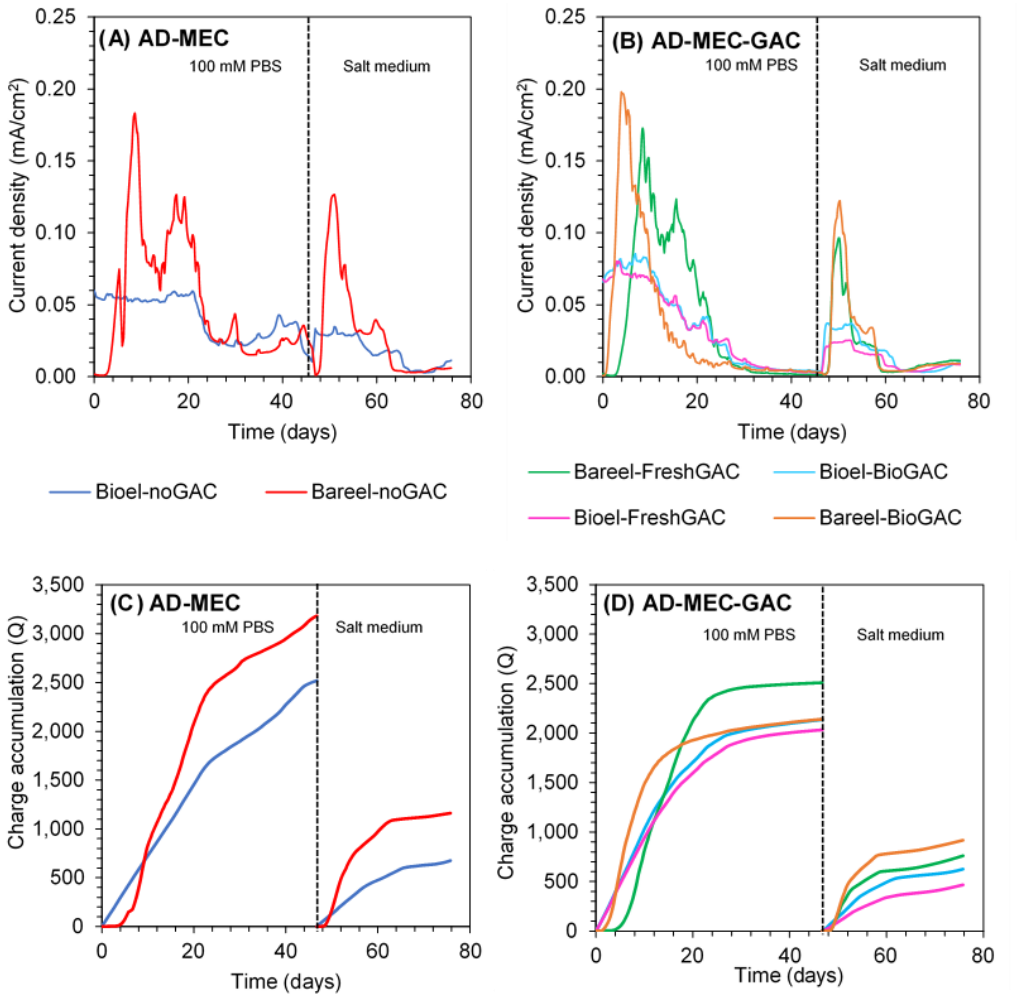

Figure 4.18. A) Current density graph of AD-MEC reactors, B) Current density graph of AD-MEC-GAC reactors, C) Charge accumulation curve of AD-MEC reactors, D) Charge accumulation curve of AD-MEC-GAC

Among the GAC added reactors there was no change with the presence of bioelectrodes. In other words, during the batch cycle with 100 mM PBS, both Bioel-FreshGAC and Bioel-BioGAC produced 0.08 ± 0.005 mA/cm^2 stable current until day 10 and then gradually dropped to 0.003 ± 0.0005 mA/cm^2. The highest current

density between GAC amended reactors belongs to Bareel-BioGAC reactors, which produced the highest peak current of all the reactors of 0.19 ± 0.01 mA/cm^{2,} and also the peak current in this reactor was reached faster than all of the others. In Bareel-BioGAC the peak was reached on day 5 of incubation and then gradually dropped after 1 day. The Bareel-FreshGAC reactor peaked on day 8 with a comparatively high peak current of 0.23 ± 0.05 mA/cm^2. At the end of the first batch cycle, the current density for all the GAC amended reactors was 0.003 ± 0.0005 mA/cm^2.

The GAC amended reactors, with 100 mM PBS Bareel-FreshGAC reactors showed the highest charge transferred with 2503 ± 73 C. The charge transferred for the Bioel-BioGAC, Bioel-FreshGAC, and Bareel-BioGAC reactors were similar; 2119 ± 297 C, 2020 ± 479 C, and 2127 ± 53 C, respectively. During the second cycle with salt medium, the reactors performed similarly to the cycle with 100 mM PBS medium with a lower current density peak as in AD-MECs without any GAC. The highest current density belonged to the Bareel-BioGAC reactor with 0.17 ± 0.03 mA/cm^2 and Bareel-FreshGAC showed a peak of 0.14 ± 0.02 mA/cm^2. The Bioel-BioGAC reactor's peak current density was 0.04 ± 0.08 mA/cm^{2,} and the lowest peak current density was Bioel-FreshGAC with 0.02 ± 0.07 mA/cm^2. Accordingly, Bareel-BioGAC reactors transferred the highest charge between the anode and cathode with 918 ± 5 C. Bareel-FreshGAC, Bioel-BioGAC, and Bioel-FreshGAC transferred 761 ± 21 C, 626 ± 97 C, and 467 ± 128 C, respectively.

The decrease in current production indicates the depletion of available substrate for anodic oxidation (Z. Zhao et al., 2016a). Based on the charge accumulation trend, in 100 mM PBS medium, although the current production did not stop, the rate decreased after 20 days from the start of the batch cycle. On the other hand, with the salt medium, the trend of charge accumulation for both Bioel and Bareel reactors plateaued after 15 days. The reason could be the inhibitory effects of 100 mM PBS which suppress the microorganisms in the bulk solution. Therefore, the electroactive microorganism on the anode surface becomes the main consumer of available organics in the reactor. In the reactors amended with GAC, regardless of buffer medium type, the charge accumulation graph plateaued between 15-20 days after the

start of batch cycles. The reason could be the availability of GAC in the reactors, which decreased the inhibitory effect of 100 mM PBS (Kutlar et al., 2022). Therefore, the available microorganisms in bulk solution also consumed the organics.

The produced current due to the oxidation of organics by exoelectrogenic bacteria is expected to be used by electroactive methanogens on the cathode surface (Cheng et al., 2009). Assuming all the produced currents were converted to CH_4 on the biocathode, the equivalent produced CH_4 is theoretically calculated in Tables 4.4 and 4.5. Comparison of equivalent CH_4 produced from current given in Table 4.4 and 4.5, regardless of reactor type, the 100 mM PBS added reactor produced 67 ± 6% higher than the corresponding reactor with the salt medium. Since the conductivity of both 100 mM PBS and salt media was the same (8 mS/cm), factors other than conductivity also affect the function of exoelectrogenic bacteria. It is stated that PBS decreases the internal resistance of the cell and improves the current production performance (Ruiz et al., 2016). Ruiz and colleagues (2016), operated MECs with PBS, high conductivity, and low conductivity media. The high conductivity media had the same conductivity as PBS media, however, results showed that MEC with PBS had better performance compared to both high conductivity and low conductivity media.

As indicated in Tables 4.4 and 4.5, CH_4 production in AD-MEC reactors was comparable to that of their OC controls (no applied voltage). When equivalent CH_4 from the current was taken into account, these variations (AD-MEC vs. OC) were expected to be higher. As a result, the difference in CH_4 production between AD-MEC reactors and their OC controls is not correlated with equivalent CH_4 production from the current. For example, with 100 mM PBS medium, AD-MEC-Bioeel reactors produced 150.6 ± 7.1 mL, and its open circuit control produced 153.1 ± 7.5 mL of CH_4; however, the equivalented CH_4 based on its produced current was 80.3 ± 4.4 mL. One possible reason could be the slower rate of methanogens compared to the current production rate by exoelectrogenic bacteria (J. Zhang et al., 2013).

Energy recovery efficiencies

The current density graph shown in Figure 4.18 illustrates that in both 100 mM PBS and salt medium, bioelectrode reactors produce less current than reactors with bare electrodes. This has far-reaching implications as the energy requirement due to external voltage addition in these reactors will be much less in comparison to higher current density producing reactors.

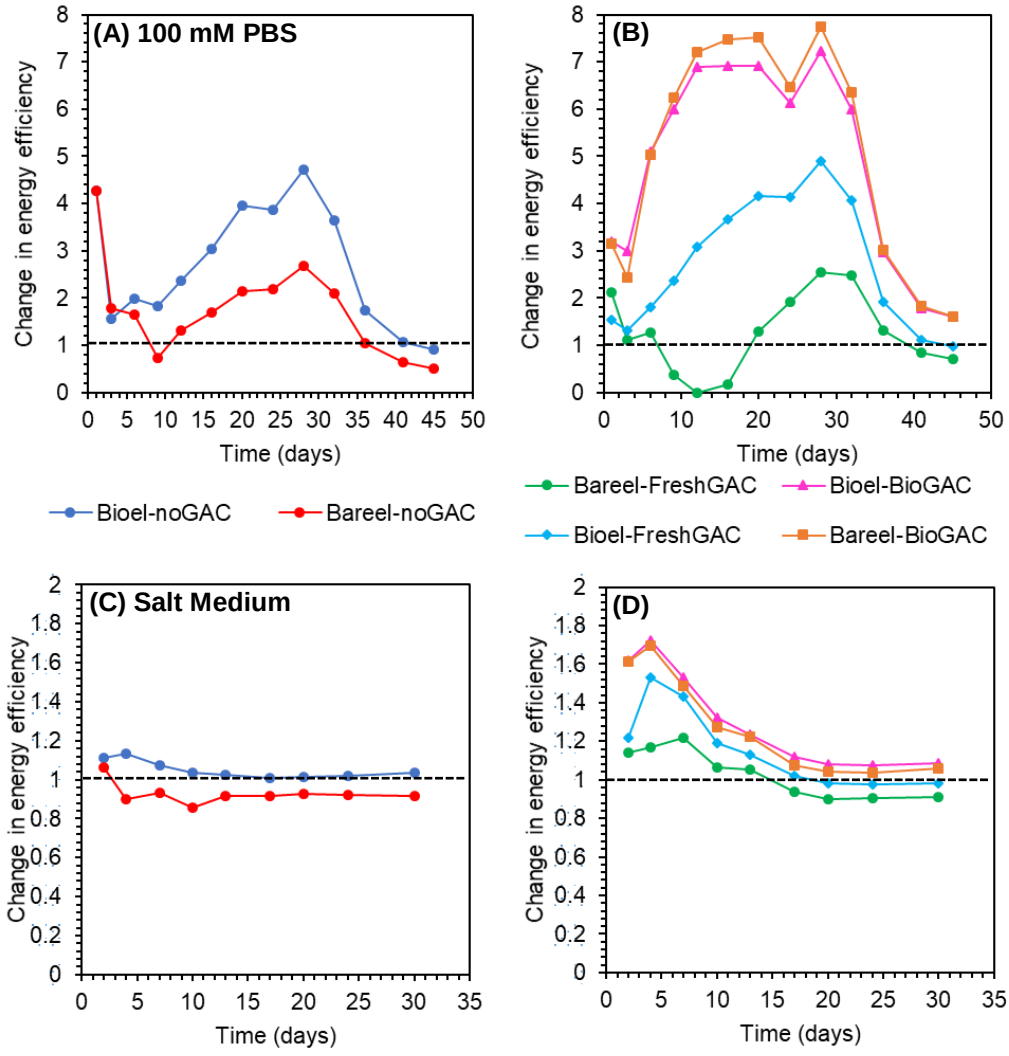

Figure 4.19. Energy efficiency graph of A) AD-MEC reactors with 100 mM PBS, B) AD-MEC-GAC reactors with 100 mM PBS, C) AD-MEC reactors with salt media, D) AD-MEC-GAC reactors with salt media

AD-MEC systems will be regarded energy positive when the energy needed to deliver voltage to them is less than the difference in CH_4 generation between AD and AD-MEC systems. In Figure 4.19, when the change in energy efficiency is greater than 1, it shows the system is energy positive. In 100 mM PBS medium, all the reactors were energy positive, except Bareel-noGAC and Bareel-FreshGAC. Bareel-noGAC and Bareel-FreshGAC had longer lag times, it took 12 and 20 days for them to become energy positive, respectively. As shown in Figure 4.19, the efficiency for all the reactors dropped after day 28, when conventional AD reactors started to produce more CH_4.

Three reactors Bioel-noGAC, Bareel-BioGAC, and Bareel-BioGAC were always energy positive compared to the AD control when the salt medium was used. The Bioel-FreshGAC efficiency fell below 1 after day 17, indicating that running these reactors beyond day 17 was inefficient since the necessary energy for the operation was more than their energy production when compared to conventional AD reactors. Clearly, in continuous system operation, this information may be used to select a retention time. A similar observation was made for Bareel-FreshGAC reactors after day 13. Bareel-noGAC reactors, which surprisingly never became energy efficient, had the lowest performance in terms of energy efficiency. Although the results imply that reactors with 100 mM PBS have substantially better efficiency than those with the salt medium, it should be that the main cause of such a significant difference is the suppression of AD control in the presence of 100 mM PBS.

CHAPTER 5

CONCLUSION

The results of the first part of the experiment revealed that the presence of AD seed minimizes the time required for biofilm development and start-up of CH_4 production from CM as opposed to no inoculum addition. The comparison of peak current density and CH_4 production data at different sCOD concentrations showed that there is no strong relation between peak current and CH_4 production. Instead, charge accumulation graphs provide better tools for comparative analysis, as the total Coulombs transferred is directly linked to the total CH_4 production. There was no clear advantage of using ACE during biofilm formation for CM fed reactors; therefore, using CM instead of ACE decreases the operational cost. Therefore, for biofilm formation in the AD-MEC experiment, CM was used as a substrate.

Comparing the results of the AD-MEC experiment based on the buffer solution type showed that using 100 mM PBS improves the electrochemical characteristic of reactors such as current production and peak current density. However, it negatively affects the net CH_4 yield, CH_4 production rate, and lag time. These negative effects were more pronounced in conventional AD reactors, however: voltage application in AD-MEC coupled system and GAC addition in bulk solution decreased these negative effects. Using biofilm developed electrodes (Bioel) and GACs (BioGAC) positively affected the CH_4 production and kinetics, especially in severe conditions (100 mM PBS) due to microbial aggregation on the surface. However, using bare electrodes without voltage (open circuit) application did not show any significant effect. Regardless of reactor type or buffer solution, BioGAC amended reactors showed the highest CH_4 production performance. This suggests that bioGAC is the most significant factor promoting the AD system. The current density graph illustrated that biofilm formed reactors produce less current than reactors with bare electrodes. This has far-reaching implications as the energy requirement due to

external voltage addition in these reactors will be much less in comparison to higher current density producing AD-MEC reactors. Therefore, the use of bioelectrodes together with bioGAC improves biomethane production from animal wastes both in terms of the yield of CH_4 and from the perspective of energy efficiency. The proposed study revealed the higher effectiveness of the AD system when assisted by MECs with GAC. This result will be useful for future research on improving AD performance by combining diverse BESs.

CHAPTER 6

RECOMMENDATIONS

Electromethanogenesis is a relatively new technology. Similarly, AD-MEC systems have been studied for only ten years. Therefore, they have not been ready for commercialization yet. Despite significant research advancements in fundamental comprehension and bench-scale process development, several recommendations for future research can be summarized as follows:

- The results of this thesis revealed that buffer solution had a great impact on the performance of the reactors. Therefore, further investigation is required to find an optimal buffer solution in order to enhance the AD-MEC system performance from both methane and current generation perspective. For this purpose, it is suggested to run toxicity assays for the AD-MEC system using different buffer solutions.
- The viability of electro-active biofilm during the reactor operation time period has not been assessed in this study. It could be useful to assess the viability of biofilm by employing confocal microscopy to quantify the abundance of the live/ cells that are present on the biofilm.
- In this work, experiments were carried out with batch reactors with < 150 mL active volume. Based on this data, a continuous reactor system at a larger scale may be operated. Finally, executing these systems on a pilot scale might be the next step on this long road toward commercialization.

REFERENCES

Aktaş, Ö., & Çeçen, F. (2007). Bioregeneration of activated carbon: A review. *International Biodeterioration and Biodegradation*, *59*(4), 257–272. https://doi.org/10.1016/j.ibiod.2007.01.003

Amrut Pawar, A., Karthic, A., Lee, S., Pandit, S., & Jung, S. P. (2020). Microbial electrolysis cells for electromethanogenesis: Materials, configurations and operations. *Environmental Engineering Research*, *27*(1), 200484–0. https://doi.org/10.4491/eer.2020.484

An, Z., Feng, Q., Zhao, R., & Wang, X. (2020). Bioelectrochemical methane production from food waste in anaerobic digestion using a carbon-modified copper foam electrode. *Processes*, *8*(4). https://doi.org/10.3390/PR8040416

APHA, Standard Methods for the Examination of Water and Wastewater (21st ed.). (1999). American Public Health Association/American Water Works Association/Water Environment Federation, Washington DC.

Baek, G., Kim, J., Kim, J., & Lee, C. (2020). Individual and combined effects of magnetite addition and external voltage application on anaerobic digestion of dairy wastewater. *Bioresource Technology*, *297*(November 2019), 122443. https://doi.org/10.1016/j.biortech.2019.122443

Bao, H., Yang, H., Zhang, H., Liu, Y., Su, H., & Shen, M. (2020). Improving methane productivity of waste activated sludge by ultrasound and alkali pretreatment in microbial electrolysis cell and anaerobic digestion coupled system. *Environmental Research*, *180*(August 2019), 108863. https://doi.org/10.1016/j.envres.2019.108863

Blasco-Gómez, R., Batlle-Vilanova, P., Villano, M., Balaguer, M. D., Colprim, J., & Puig, S. (2017). On the edge of research and technological application: A critical review of electromethanogenesis. *International Journal of Molecular Sciences*, *18*(4). https://doi.org/10.3390/ijms18040874

Bo, T., Zhu, X., Zhang, L., Tao, Y., He, X., Li, D., & Yan, Z. (2014). A new upgraded biogas production process: Coupling microbial electrolysis cell and anaerobic digestion in single-chamber, barrel-shape stainless steel reactor. *Electrochemistry Communications*, *45*, 67–70. https://doi.org/10.1016/j.elecom.2014.05.026

Bolyen, E., Rideout, J. R., & Dillon, M. R. (2019). Reproducible, interactive, scalable and extensible microbiome data science using QIIME 2. *Nature Biotechnology*, *37*(8), 852–857. https://doi.org/10.1038/s41587-019-0209-9

Bond, D. R., & Lovley, D. R. (2003). Electricity production by Geobacter sulfurreducens attached to electrodes. *Applied and Environmental*

Microbiology, *69*(3), 1548–1555. https://doi.org/10.1128/AEM.69.3.1548-1555.2003

Bougrier, C., Albasi, C., Delgenès, J. P., & Carrère, H. (2006). Effect of ultrasonic, thermal and ozone pre-treatments on waste activated sludge solubilisation and anaerobic biodegradability. *Chemical Engineering and Processing: Process Intensification*, *45*(8), 711–718. https://doi.org/10.1016/j.cep.2006.02.005

Cai, W., Liu, W., Zhang, Z., Feng, K., Ren, G., Pu, C., Sun, H., Li, J., Deng, Y., & Wang, A. (2018). mcrA sequencing reveals the role of basophilic methanogens in a cathodic methanogenic community. *Water Research*, *136*, 192–199. https://doi.org/10.1016/j.watres.2018.02.062

Call, D., & Logan, B. E. (2008). *Hydrogen Production in a Single Chamber Microbial Electrolysis Cell Lacking a Membrane*. *42*(9), 3401–3406.

Callahan, B. J., McMurdie, P. J., Rosen, M. J., Han, A. W., Johnson, A. J. A., & Holmes, S. P. (2016). DADA2: High-resolution sample inference from Illumina amplicon data. *Nature Methods*, *13*(7), 581–583. https://doi.org/10.1038/nmeth.3869

Carliell-Marquet, C. M., & Wheatley, A. D. (2002). Measuring metal and phosphorus speciation in P-rich anaerobic digesters. *Water Science and Technology : A Journal of the International Association on Water Pollution Research*, *45*(10), 305–312. https://doi.org/10.2166/wst.2002.0360

Cayetano, R. D. A., Kim, G. B., Park, J., Yang, Y. H., Jeon, B. H., Jang, M., & Kim, S. H. (2022). Biofilm formation as a method of improved treatment during anaerobic digestion of organic matter for biogas recovery. *Bioresource Technology*, *344*(PB), 126309. https://doi.org/10.1016/j.biortech.2021.126309

Chen, Ye, Cheng, J. J., & Creamer, K. S. (2008). Inhibition of anaerobic digestion process: A review. *Bioresource Technology*, *99*(10), 4044–4064. https://doi.org/10.1016/j.biortech.2007.01.057

Chen, Ying, Yu, B., Yin, C., Zhang, C., Dai, X., Yuan, H., & Zhu, N. (2016). Biostimulation by direct voltage to enhance anaerobic digestion of waste activated sludge. *RSC Advances*, *6*(2), 1581–1588. https://doi.org/10.1039/c5ra24134k

Cheng, S., & Logan, B. E. (2007). Sustainable and efficient biohydrogen production via electrohydrogenesis. *Proceedings of the National Academy of Sciences of the United States of America*, *104*(47), 18871–18873. https://doi.org/10.1073/pnas.0706379104

Cheng, S., Xing, D., Call, D. F., & Logan, B. E. (2009). Direct biological conversion of electrical current into methane by electromethanogenesis. *Environmental Science and Technology*, *43*(10), 3953–3958. https://doi.org/10.1021/es803531g

Choi, J. M., & Lee, C. Y. (2019). Bioelectrochemical enhancement of methane production in anaerobic digestion of food waste. *International Journal of Hydrogen Energy*, *44*(4), 2081–2090. https://doi.org/10.1016/j.ijhydene.2018.08.153

Deaver, J. A., Kerr, C. A., & Popat, S. C. (2022). Primary sludge-based blackwater favors electrical current over methane production in microbial electrochemical cells. *Journal of Water Process Engineering*, *47*(February), 102848. https://doi.org/10.1016/j.jwpe.2022.102848

Ding, A., Yang, Y., Sun, G., & Wu, D. (2015). Impact of applied voltage on methane generation and microbial activities in an anaerobic microbial electrolysis cell (MEC). *Chemical Engineering Journal*, *283*, 260–265. https://doi.org/10.1016/j.cej.2015.07.054

Dou, Z., Dykstra, C. M., & Pavlostathis, S. G. (2018). Bioelectrochemically assisted anaerobic digestion system for biogas upgrading and enhanced methane production. *Science of the Total Environment*, *633*, 1012–1021. https://doi.org/10.1016/j.scitotenv.2018.03.255

Elgrishi, N., Rountree, K. J., McCarthy, B. D., Rountree, E. S., Eisenhart, T. T., & Dempsey, J. L. (2018). A Practical Beginner's Guide to Cyclic Voltammetry. *Journal of Chemical Education*, *95*(2), 197–206. https://doi.org/10.1021/acs.jchemed.7b00361

Falås, P., Baillon-Dhumez, A., Andersen, H. R., Ledin, A., & La Cour Jansen, J. (2012). Suspended biofilm carrier and activated sludge removal of acidic pharmaceuticals. *Water Research*, *46*(4), 1167–1175. https://doi.org/10.1016/j.watres.2011.12.003

Feng, Q., Song, Y. C., & Ahn, Y. (2018). Electroactive microorganisms in bulk solution contribute significantly to methane production in bioelectrochemical anaerobic reactor. *Bioresource Technology*, *259*(January), 119–127. https://doi.org/10.1016/j.biortech.2018.03.039

Feng, Q., Song, Y. C., Li, J., Wang, Z., & Wu, Q. (2020). Influence of electrostatic field and conductive material on the direct interspecies electron transfer for methane production. *Environmental Research*, *188*(July), 109867. https://doi.org/10.1016/j.envres.2020.109867

Feng, Q., Song, Y. C., Yoo, K., Kuppanan, N., Subudhi, S., & Lal, B. (2018). Polarized electrode enhances biological direct interspecies electron transfer for methane production in upflow anaerobic bioelectrochemical reactor. *Chemosphere*, *204*, 186–192. https://doi.org/10.1016/j.chemosphere.2018.03.163

Fricke, K., Harnisch, F., & Schröder, U. (2008). On the use of cyclic voltammetry for the study of anodic electron transfer in microbial fuel cells. *Energy and Environmental Science*, *1*(1), 144–147. https://doi.org/10.1039/b802363h

Fu, Q., Kuramochi, Y., Fukushima, N., Maeda, H., Sato, K., & Kobayashi, H. (2015a). Bioelectrochemical analyses of the development of a thermophilic biocathode catalyzing electromethanogenesis. *Environmental Science and Technology*, *49*(2), 1225–1232. https://doi.org/10.1021/es5052233

Fu, Q., Kuramochi, Y., Fukushima, N., Maeda, H., Sato, K., & Kobayashi, H. (2015b). Bioelectrochemical analyses of the development of a thermophilic biocathode catalyzing electromethanogenesis. *Environmental Science and Technology*, *49*(2), 1225–1232. https://doi.org/10.1021/es5052233

Fujikawa, H., Kai, A., & Morozumi, S. (2004). A new logistic model for Escherichia coli growth at constant and dynamic temperatures. *Food Microbiology*, *21*(5), 501–509. https://doi.org/10.1016/j.fm.2004.01.007

Gao, Y., Sun, D., Dang, Y., Lei, Y., Ji, J., Lv, T., Bian, R., Xiao, Z., Yan, L., & Holmes, D. E. (2017). Enhancing biomethanogenic treatment of fresh incineration leachate using single chambered microbial electrolysis cells. *Bioresource Technology*, *231*, 129–137. https://doi.org/10.1016/j.biortech.2017.02.024

Giang, H., Zhang, J., Zhu, Z., Suni, I. I., & Liang, Y. (2018). Single-chamber microbial electrochemical cell for CH4 production from CO2 utilizing a microbial consortium. In *International Journal of Energy Research* (Vol. 42, Issue 3, pp. 1308–1315). https://doi.org/10.1002/er.3931

Guo, Z., Thangavel, S., Wang, L., He, Z., Cai, W., Wang, A., & Liu, W. (2017). Efficient methane production from beer wastewater in a membraneless microbial electrolysis cell with a stacked cathode: The effect of the cathode/anode ratio on bioenergy recovery. *Energy and Fuels*, *31*(1), 615–620. https://doi.org/10.1021/acs.energyfuels.6b02375

Hamelers, H. V. M., Ter Heijne, A., Sleutels, T. H. J. A., Jeremiasse, A. W., Strik, D. P. B. T. B., & Buisman, C. J. N. (2010). New applications and performance of bioelectrochemical systems. *Applied Microbiology and Biotechnology*, *85*(6), 1673–1685. https://doi.org/10.1007/s00253-009-2357-1

Hara, M., Onaka, Y., Kobayashi, H., Fu, Q., Kawaguchi, H., Vilcaez, J., & Sato, K. (2013). Mechanism of electromethanogenic reduction of CO2 by a thermophilic methanogen. *Energy Procedia*, *37*, 7021–7028. https://doi.org/10.1016/j.egypro.2013.06.637

Herrmann, C., Sánchez, E., Schultze, M., & Borja, R. (2021). Comparative effect of biochar and activated carbon addition on the mesophilic anaerobic digestion of piggery waste in batch mode. *Journal of Environmental Science and Health - Part A Toxic/Hazardous Substances and Environmental Engineering*, *56*(9), 946–952. https://doi.org/10.1080/10934529.2021.1944833

Hou, Y., Zhang, R., Luo, H., Liu, G., Kim, Y., Yu, S., & Zeng, J. (2015). Microbial

electrolysis cell with spiral wound electrode for wastewater treatment and methane production. *Process Biochemistry*, *50*(7), 1103–1109. https://doi.org/10.1016/j.procbio.2015.04.001

Huang, Q., Liu, Y., & Dhar, B. R. (2022). A critical review of microbial electrolysis cells coupled with anaerobic digester for enhanced biomethane recovery from high-strength feedstocks. *Critical Reviews in Environmental Science and Technology*, *52*(1), 50–89. https://doi.org/10.1080/10643389.2020.1813065

Ivanov, I., Ren, L., Siegert, M., & Logan, B. E. (2013). A quantitative method to evaluate microbial electrolysis cell effectiveness for energy recovery and wastewater treatment. *International Journal of Hydrogen Energy*, *38*(30), 13135–13142. https://doi.org/10.1016/j.ijhydene.2013.07.123

Jang, H. M., Choi, Y. K., & Kan, E. (2018). Effects of dairy manure-derived biochar on psychrophilic, mesophilic and thermophilic anaerobic digestions of dairy manure. *Bioresource Technology*, *250*(November 2017), 927–931. https://doi.org/10.1016/j.biortech.2017.11.074

Kas, A., & Yilmazel, Y. D. (2022). High current density via direct electron transfer by hyperthermophilic archaeon, Geoglobus acetivorans, in microbial electrolysis cells operated at 80 °C. *Bioelectrochemistry*, *145*, 108072. https://doi.org/10.1016/j.bioelechem.2022.108072

Klindworth, A., Pruesse, E., Schweer, T., Peplies, J., Quast, C., Horn, M., & Glöckner, F. O. (2013). Evaluation of general 16S ribosomal RNA gene PCR primers for classical and next-generation sequencing-based diversity studies. *Nucleic Acids Research*, *41*(1), 1–11. https://doi.org/10.1093/nar/gks808

Kobayashi, H., Saito, N., Fu, Q., Kawaguchi, H., Vilcaez, J., Wakayama, T., Maeda, H., & Sato, K. (2013). Bio-electrochemical property and phylogenetic diversity of microbial communities associated with bioelectrodes of an electromethanogenic reactor. *Journal of Bioscience and Bioengineering*, *116*(1), 114–117. https://doi.org/10.1016/j.jbiosc.2013.01.001

Kuramochi, Y., Fu, Q., Kobayashi, H., Ikarashi, M., Wakayama, T., Kawaguchi, H., Vilcaez, J., Maeda, H., & Sato, K. (2013). Electromethanogenic CO2 conversion by subsurface-reservoir microorganisms. *Energy Procedia*, *37*(3), 7014–7020. https://doi.org/10.1016/j.egypro.2013.06.636

Kutlar, F. E., Tunca, B., & Yilmazel, Y. D. (2022). Carbon-based conductive materials enhance biomethane recovery from organic wastes: A review of the impacts on anaerobic treatment. *Chemosphere*, *290*(November 2021), 133247. https://doi.org/10.1016/j.chemosphere.2021.133247

LaBarge, N., Yilmazel, Y. D., Hong, P. Y., & Logan, B. E. (2017a). Effect of pre-acclimation of granular activated carbon on microbial electrolysis cell startup and performance. *Bioelectrochemistry*, *113*, 20–25.

https://doi.org/10.1016/j.bioelechem.2016.08.003

LaBarge, N., Yilmazel, Y. D., Hong, P. Y., & Logan, B. E. (2017b). Effect of pre-acclimation of granular activated carbon on microbial electrolysis cell startup and performance. *Bioelectrochemistry*, *113*, 20–25. https://doi.org/10.1016/j.bioelechem.2016.08.003

Lee, J. Y., Lee, S. H., & Park, H. D. (2016). Enrichment of specific electro-active microorganisms and enhancement of methane production by adding granular activated carbon in anaerobic reactors. *Bioresource Technology*, *205*, 205–212. https://doi.org/10.1016/j.biortech.2016.01.054

Li, X., Zeng, C., Lu, Y., Liu, G., Luo, H., & Zhang, R. (2019). Development of methanogens within cathodic biofilm in the single-chamber microbial electrolysis cell. *Bioresource Technology*, *274*(November 2018), 403–409. https://doi.org/10.1016/j.biortech.2018.12.002

Li, Y., Zhao, J., Krooneman, J., & Euverink, G. J. W. (2021). Strategies to boost anaerobic digestion performance of cow manure: Laboratory achievements and their full-scale application potential. *Science of the Total Environment*, *755*. https://doi.org/10.1016/j.scitotenv.2020.142940

Liang, M., Luo, B., & Ã, L. Z. (2009). *Application of graphene and graphene-based materials in clean energy-related devices*. *July*, 1161–1170. https://doi.org/10.1002/er

Liu, F., Rotaru, A. E., Shrestha, P. M., Malvankar, N. S., Nevin, K. P., & Lovley, D. R. (2012). Promoting direct interspecies electron transfer with activated carbon. *Energy and Environmental Science*, *5*(10), 8982–8989. https://doi.org/10.1039/c2ee22459c

Liu, W., Piao, Y., Zhang, F., Liu, L., Meng, D., Nan, J., Deng, Y., & Wang, A. (2018). Hydrogen consumption and methanogenic community evolution in anodophilic biofilms in single chamber microbial electrolysis cells under different startup modes. *Environmental Science: Water Research and Technology*, *4*(11), 1839–1850. https://doi.org/10.1039/c8ew00357b

Logan, B. E., Call, D., Cheng, S., Hamelers, H. V. M., Sleutels, T. H. J. A., Jeremiasse, A. W., & Rozendal, R. A. (2008). Microbial electrolysis cells for high yield hydrogen gas production from organic matter. *Environmental Science and Technology*, *42*(23), 8630–8640. https://doi.org/10.1021/es801553z

Lovley, D. R. (2011). Live wires: Direct extracellular electron exchange for bioenergy and the bioremediation of energy-related contamination. *Energy and Environmental Science*, *4*(12), 4896–4906. https://doi.org/10.1039/c1ee02229f

Lovley, D. R. (2017). Happy together: Microbial communities that hook up to

swap electrons. *ISME Journal*, *11*(2), 327–336. https://doi.org/10.1038/ismej.2016.136

Macaskill, J. B., & Bates, R. G. (1978). *Activity Coefficient of Hydrochloric Acid in the System HCI-KCI-H20 at 25 ~ and Ionic Strengths from 0 . 1 to 3 Moles-kg- ’*. *6*, 433–442.

Mancipe-Jiménez, D. C., Costa, C., & Márquez, M. C. (2017). Methanogenesis inhibition by phosphorus in anaerobic liquid waste treatment. *Waste Treatment and Recovery*, *2*(1), 1–8. https://doi.org/10.1515/lwr-2017-0001

Marshall, C. W., Ross, D. E., Fichot, E. B., Norman, R. S., & May, H. D. (2012). Electrosynthesis of commodity chemicals by an autotrophic microbial community. *Applied and Environmental Microbiology*, *78*(23), 8412–8420. https://doi.org/10.1128/AEM.02401-12

Martins, G., Salvador, A. F., Pereira, L., & Alves, M. M. (2018). Methane Production and Conductive Materials: A Critical Review. *Environmental Science and Technology*, *52*(18), 10241–10253. https://doi.org/10.1021/acs.est.8b01913

Mayer, F., Enzmann, F., Lopez, A. M., & Holtmann, D. (2019). Performance of different methanogenic species for the microbial electrosynthesis of methane from carbon dioxide. *Bioresource Technology*, *289*(June), 121706. https://doi.org/10.1016/j.biortech.2019.121706

Mir, M. A., Hussain, A., & Verma, C. (2016). Design considerations and operational performance of anaerobic digester: A review. *Cogent Engineering*, *3*(1). https://doi.org/10.1080/23311916.2016.1181696

Moreno, R., Escapa, A., & Mor, A. (2016). *Domestic wastewater treatment in parallel with methane production in a microbial electrolysis cell n*. *93*, 442–448. https://doi.org/10.1016/j.renene.2016.02.083

Ou, S., Kashima, H., Aaron, D. S., Regan, J. M., & Mench, M. M. (2017). Full cell simulation and the evaluation of the buffer system on air-cathode microbial fuel cell. *Journal of Power Sources*, *347*, 159–169. https://doi.org/10.1016/j.jpowsour.2017.02.031

Park, J. G., Lee, B., Park, H. R., & Jun, H. B. (2019). Long-term evaluation of methane production in a bio-electrochemical anaerobic digestion reactor according to the organic loading rate. *Bioresource Technology*, *273*(September 2018), 478–486. https://doi.org/10.1016/j.biortech.2018.11.021

Park, J. H., Park, J. H., Je Seong, H., Sul, W. J., Jin, K. H., & Park, H. D. (2018). Metagenomic insight into methanogenic reactors promoting direct interspecies electron transfer via granular activated carbon. *Bioresource Technology*, *259*(December 2017), 414–422. https://doi.org/10.1016/j.biortech.2018.03.050

Peng, H., Zhao, Z., Xiao, H., Yang, Y., Zhao, H., & Zhang, Y. (2019). A strategy for enhancing anaerobic digestion of waste activated sludge: Driving anodic oxidation by adding nitrate into microbial electrolysis cell. *Journal of Environmental Sciences (China)*, *81*, 34–42. https://doi.org/10.1016/j.jes.2019.02.009

Piao, D. M., Song, Y. C., Oh, G. G., Kim, D. H., & Bae, B. U. (2019). Contribution of yeast extract, activated carbon, and an electrostatic field to interspecies electron transfer for the bioelectrochemical conversion of coal to methane. *Energies*, *12*(21). https://doi.org/10.3390/en12214051

Poirier, S., Madigou, C., Bouchez, T., & Chapleur, O. (2017). Improving anaerobic digestion with support media: Mitigation of ammonia inhibition and effect on microbial communities. *Bioresource Technology*, *235*, 229–239. https://doi.org/10.1016/j.biortech.2017.03.099

Rago, L., Ruiz, Y., Baeza, J. A., Guisasola, A., & Cortés, P. (2015). Microbial community analysis in a long-term membrane-less microbial electrolysis cell with hydrogen and methane production. *Bioelectrochemistry*, *106*, 359–368. https://doi.org/10.1016/j.bioelechem.2015.06.003

Ren, G., Hu, A., Huang, S., Ye, J., Tang, J., & Zhou, S. (2018). Graphite-assisted electro-fermentation methanogenesis: Spectroelectrochemical and microbial community analyses of cathode biofilms. *Bioresource Technology*, *269*(August), 74–80. https://doi.org/10.1016/j.biortech.2018.08.078

Rognes, T., Flouri, T., Nichols, B., Quince, C., & Mahé, F. (2016). VSEARCH: A versatile open source tool for metagenomics. *PeerJ*, *2016*(10), 1–22. https://doi.org/10.7717/peerj.2584

Rotaru, A. E., Shrestha, P. M., Liu, F., Markovaite, B., Chen, S., Nevin, K. P., & Lovley, D. R. (2014). Direct interspecies electron transfer between Geobacter metallireducens and Methanosarcina barkeri. *Applied and Environmental Microbiology*, *80*(15), 4599–4605. https://doi.org/10.1128/AEM.00895-14

Rotaru, A. E., Shrestha, P. M., Liu, F., Shrestha, M., Shrestha, D., Embree, M., Zengler, K., Wardman, C., Nevin, K. P., & Lovley, D. R. (2014). A new model for electron flow during anaerobic digestion: Direct interspecies electron transfer to Methanosaeta for the reduction of carbon dioxide to methane. *Energy and Environmental Science*, *7*(1), 408–415. https://doi.org/10.1039/c3ee42189a

Ruiz, Y., Baeza, J. A., & Guisasola, A. (2016). Microbial electrolysis cell performance using non-buffered and low conductivity wastewaters. *Chemical Engineering Journal*, *289*, 341–348. https://doi.org/10.1016/j.cej.2015.12.098

Ryue, J., Lin, L., Liu, Y., Lu, W., McCartney, D., & Dhar, B. R. (2019). Comparative effects of GAC addition on methane productivity and microbial community in mesophilic and thermophilic anaerobic digestion of food waste.

Biochemical Engineering Journal, *146*(November 2018), 79–87. https://doi.org/10.1016/j.bej.2019.03.010

Sasaki, K., Morita, M., Sasaki, D., Hirano, S. ichi, Matsumoto, N., Ohmura, N., & Igarashi, Y. (2011). Methanogenic communities on the electrodes of bioelectrochemical reactors without membranes. *Journal of Bioscience and Bioengineering*, *111*(1), 47–49. https://doi.org/10.1016/j.jbiosc.2010.08.010

Siegert, M., Li, X. F., Yates, M. D., & Logan, B. E. (2015). The presence of hydrogenotrophic methanogens in the inoculum improves methane gas production in microbial electrolysis cells. *Frontiers in Microbiology*, *5*(DEC), 1–12. https://doi.org/10.3389/fmicb.2014.00778

Siegert, M., Yates, M. D., Spormann, A. M., & Logan, B. E. (2015). Methanobacterium Dominates Biocathodic Archaeal Communities in Methanogenic Microbial Electrolysis Cells. *ACS Sustainable Chemistry and Engineering*, *3*(7), 1668–1676. https://doi.org/10.1021/acssuschemeng.5b00367

Sun, M., Zhang, Z., Lv, M., Liu, G., & Feng, Y. (2020). Enhancing anaerobic digestion performance of synthetic brewery wastewater with direct voltage. *Bioresource Technology*, *315*(June), 123764. https://doi.org/10.1016/j.biortech.2020.123764

Sun, R., Zhou, A., Jia, J., Liang, Q., Liu, Q., Xing, D., & Ren, N. (2015). Characterization of methane production and microbial community shifts during waste activated sludge degradation in microbial electrolysis cells. *Bioresource Technology*, *175*, 68–74. https://doi.org/10.1016/j.biortech.2014.10.052

Syed, Z., Sonu, K., & Sogani, M. (2022). Cattle manure management using microbial fuel cells for green energy generation. *Biofuels, Bioproducts and Biorefining*, *16*(2), 460–470. https://doi.org/10.1002/bbb.2293

Villano, M., Aulenta, F., Ciucci, C., Ferri, T., Giuliano, A., & Majone, M. (2010). Bioelectrochemical reduction of CO2 to CH4 via direct and indirect extracellular electron transfer by a hydrogenophilic methanogenic culture. *Bioresource Technology*, *101*(9), 3085–3090. https://doi.org/10.1016/j.biortech.2009.12.077

Villano, M., Monaco, G., Aulenta, F., & Majone, M. (2011). Electrochemically assisted methane production in a biofilm reactor. *Journal of Power Sources*, *196*(22), 9467–9472. https://doi.org/10.1016/j.jpowsour.2011.07.016

Villano, M., Ralo, C., Zeppilli, M., Aulenta, F., & Majone, M. (2016). Influence of the set anode potential on the performance and internal energy losses of a methane-producing microbial electrolysis cell. *Bioelectrochemistry*, *107*, 1–6. https://doi.org/10.1016/j.bioelechem.2015.07.008

Villano, M., Scardala, S., Aulenta, F., & Majone, M. (2013). Carbon and nitrogen removal and enhanced methane production in a microbial electrolysis cell. *Bioresource Technology*, *130*, 366–371. https://doi.org/10.1016/j.biortech.2012.11.080

Vu, M. T., Noori, M. T., & Min, B. (2020). Conductive magnetite nanoparticles trigger syntrophic methane production in single chamber microbial electrochemical systems. *Bioresource Technology*, *296*(August 2019), 122265. https://doi.org/10.1016/j.biortech.2019.122265

Wang, L., He, Z., Guo, Z., Sangeetha, T., Yang, C., Gao, L., Wang, A., & Liu, W. (2019). Microbial community development on different cathode metals in a bioelectrolysis enhanced methane production system. *Journal of Power Sources*, *444*(September), 227306. https://doi.org/10.1016/j.jpowsour.2019.227306

Wang, R., Li, Y., Wang, W., Chen, Y., & Vanrolleghem, P. A. (2015). Effect of high orthophosphate concentration on mesophilic anaerobic sludge digestion and its modeling. *Chemical Engineering Journal*, *260*, 791–800. https://doi.org/10.1016/j.cej.2014.09.050

Wang, W., Lee, D. J., & Lei, Z. (2022). Integrating anaerobic digestion with microbial electrolysis cell for performance enhancement: A review. *Bioresource Technology*, *344*(PB), 126321. https://doi.org/10.1016/j.biortech.2021.126321

Xing, T., Yun, S., Li, B., Wang, K., Chen, J., Jia, B., Ke, T., & An, J. (2021). Coconut-shell-derived bio-based carbon enhanced microbial electrolysis cells for upgrading anaerobic co-digestion of cow manure and aloe peel waste. *Bioresource Technology*, *338*(July), 125520. https://doi.org/10.1016/j.biortech.2021.125520

Yin, C., Shen, Y., Yuan, R., Zhu, N., Yuan, H., & Lou, Z. (2019). Sludge-based biochar-assisted thermophilic anaerobic digestion of waste-activated sludge in microbial electrolysis cell for methane production. *Bioresource Technology*, *284*(March), 315–324. https://doi.org/10.1016/j.biortech.2019.03.146

Yin, Q., Zhu, X., Zhan, G., Bo, T., Yang, Y., Tao, Y., He, X., Li, D., & Yan, Z. (2016). Enhanced methane production in an anaerobic digestion and microbial electrolysis cell coupled system with co-cultivation of Geobacter and Methanosarcina. *Journal of Environmental Sciences (China)*, *42*(Daping Li), 210–214. https://doi.org/10.1016/j.jes.2015.07.006

Yu, J., Kim, S., & Kwon, O. S. (2019). Effect of applied voltage and temperature on methane production and microbial community in microbial electrochemical anaerobic digestion systems treating swine manure. *Journal of Industrial Microbiology and Biotechnology*, *46*(7), 911–923. https://doi.org/10.1007/s10295-019-02182-6

Zakaria, B. S., & Dhar, B. R. (2019). Progress towards catalyzing electro-methanogenesis in anaerobic digestion process: Fundamentals, process optimization, design and scale-up considerations. *Bioresource Technology*, *289*(June), 121738. https://doi.org/10.1016/j.biortech.2019.121738

Zeppilli, M., Villano, M., Aulenta, F., Lampis, S., Vallini, G., & Majone, M. (2015). Effect of the anode feeding composition on the performance of a continuous-flow methane-producing microbial electrolysis cell. *Environmental Science and Pollution Research*, *22*(10), 7349–7360. https://doi.org/10.1007/s11356-014-3158-3

Zhang, C., Yun, S., Li, X., Wang, Z., Xu, H., & Du, T. (2018). Low-cost composited accelerants for anaerobic digestion of dairy manure: Focusing on methane yield, digestate utilization and energy evaluation. *Bioresource Technology*, *263*(March), 517–524. https://doi.org/10.1016/j.biortech.2018.05.042

Zhang, J., Zhang, Y., Quan, X., & Chen, S. (2013). Effects of ferric iron on the anaerobic treatment and microbial biodiversity in a coupled microbial electrolysis cell (MEC) - Anaerobic reactor. *Water Research*, *47*(15), 5719–5728. https://doi.org/10.1016/j.watres.2013.06.056

Zhao, L., Wang, X. T., Chen, K. Y., Wang, Z. H., Xu, X. J., Zhou, X., Xing, D. F., Ren, N. Q., Lee, D. J., & Chen, C. (2021). The underlying mechanism of enhanced methane production using microbial electrolysis cell assisted anaerobic digestion (MEC-AD) of proteins. *Water Research*, *201*(December 2020), 117325. https://doi.org/10.1016/j.watres.2021.117325

Zhao, Z., Zhang, Y., Quan, X., & Zhao, H. (2016a). Evaluation on direct interspecies electron transfer in anaerobic sludge digestion of microbial electrolysis cell. *Bioresource Technology*, *200*, 235–244. https://doi.org/10.1016/j.biortech.2015.10.021

Zhao, Z., Zhang, Y., Quan, X., & Zhao, H. (2016b). Evaluation on direct interspecies electron transfer in anaerobic sludge digestion of microbial electrolysis cell. *Bioresource Technology*, *200*, 235–244. https://doi.org/10.1016/j.biortech.2015.10.021

Zhen, G., Lu, X., Kobayashi, T., Kumar, G., & Xu, K. (2016). Promoted electromethanosynthesis in a two-chamber microbial electrolysis cells (MECs) containing a hybrid biocathode covered with graphite felt (GF). *Chemical Engineering Journal*, *284*, 1146–1155. https://doi.org/10.1016/j.cej.2015.09.071

Zhen, G., Zheng, S., Lu, X., Zhu, X., Mei, J., Kobayashi, T., Xu, K., Li, Y. Y., & Zhao, Y. (2018). A comprehensive comparison of five different carbon-based cathode materials in CO2 electromethanogenesis: Long-term performance, cell-electrode contact behaviors and extracellular electron transfer pathways. *Bioresource Technology*, *266*(June), 382–388.

https://doi.org/10.1016/j.biortech.2018.06.101

APPENDICES

A. Supplementary information for the Figure 2.2

Figure 2.2. Figure 2.2 Scientific publications investigating MMECs published from 2013 to 2021. This data was extracted from Scopus database using the keywords “microbial electrolysis cell”, and “methane” (Search date: 27 July 2022) (Appendix A).

Search criteria:

KEY (microbial AND electrolysis AND cell AND methane) AND (LIMIT-TO (DOCTYPE , "ar")) AND (LIMIT-TO (EXACTKEYWORD , "Methane") OR LIMIT-TO (EXACTKEYWORD , "Microbial Electrolysis Cell"))

B. Example calculations

Modified Gompertz kinetic parameter calculations:

$$P_p = P_\infty \times exp\left\{-exp\left[\frac{R_m \times e}{P_\infty}(\lambda - t) + 1\right]\right\}$$

P is cumulative CH_4 production (mL), P_∞ is CH_4 production potential (mL), R_m is the maximum specific CH_4 production rate (mL/d), and λ is the lag phase period to produce CH_4 (days) (Fujikawa et al., 2004).

Predicted methane production using modified Gompertz formula was calculated for each sampling. The difference between actual methane and predicted methane for each sampling squared and then sum of all of them calculated as below.

$$SSR = \sum_n (P_p - P_{actual})^2$$

Using solver in excel then minimum of value SSR with initial value of 1 for P_∞, R_m, λ calculated. Later the R^2 value for finding the correlation between predicted and actual methane for each reactor calculated.

Coulombs transferred calculations:

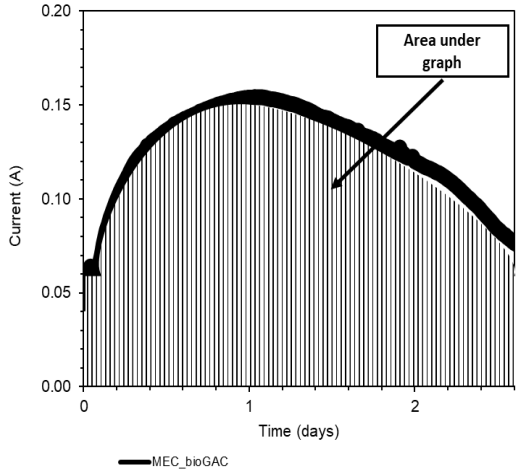

Figure B.1 Example of current graph for MEC-BioGAC

The moles of electrons (Coulombs) that transferred from anode is calculated as below

$C = \int_{t=0}^{t} Idt = 406.1$

$A_{surface\ area} = 15.5\ cm^2$

$normalized\ coulombs = \frac{406.1}{15.5} = 26.6\ {}^{C}/_{cm^2}$

Converting transferred Coulombs to mL methane:

First, we convert moles of electrons to the moles of methane using the formula below:

$CH_4 = \frac{\int_{t=0}^{t} Idt}{8F} = \frac{406.1}{8 \times 96485} = 5.2 \times 10^{-4}$

Then using ideal gas formula, we convert moles of methane to the ml methane as below:

$PV = nRT$

$P = 1.01325$ atm

$T = 308$ K

$R = 0.08314$

$V = \frac{5.2 \times 10^{-4} \times 308 \times 1000}{1.01325} = 13.29\ mL_{\ CH_4}$

C. Current density graphs for triplicates in Set 1

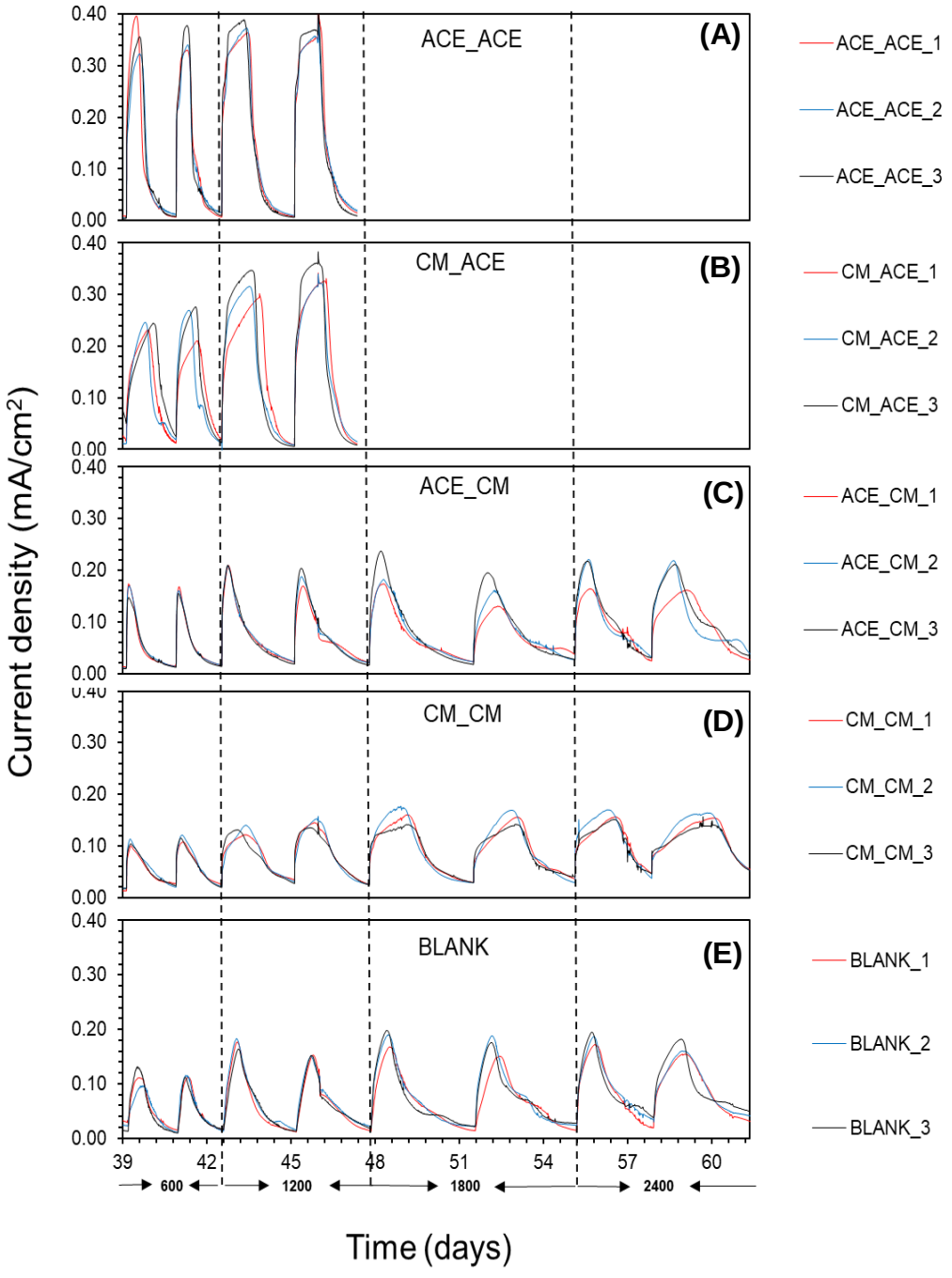

Figure C.1 Current density graphs for triplicates in Set 1 (A) ACE_ACE (B) CM_ACE (C) ACE_CM (D) CM_CM (E) Blank

D. The Modified Gompertz Fittings of Charge Accumulation in Set 1

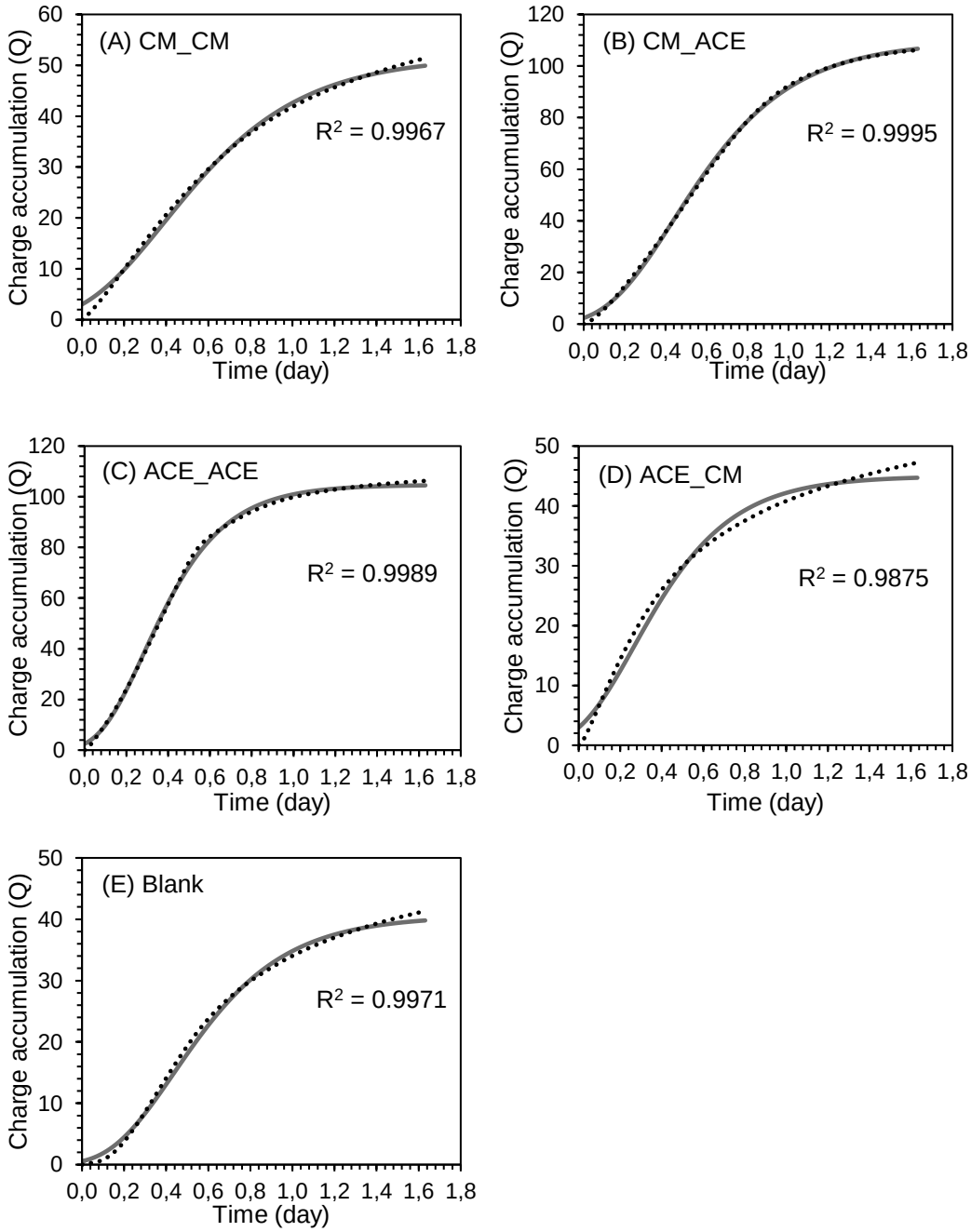

Figure D.1. The modifed Gompertz model fittings of charge accumulation at 600 mg/L sCOD concentration during Set 1 (A) CM_CM, (B) CM_ACE, (C)

ACE_ACE, (D) ACE_CM and (E) Blank (Dashed line: experimental results, Solid line: model results)

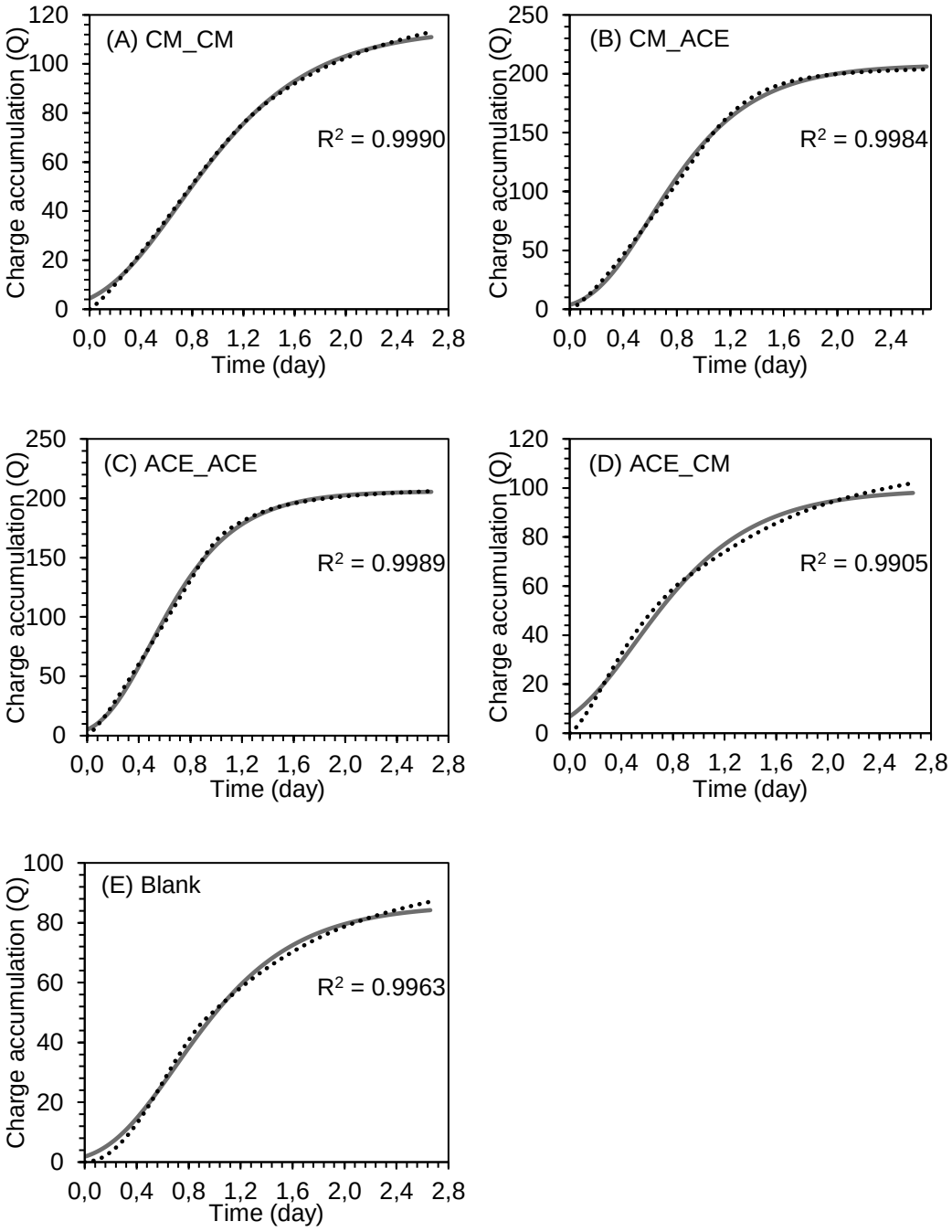

Figure D.2. The modifed Gompertz model fittings of charge accumulation at 1200 mg/L sCOD concentration during Set 1 (A) CM_CM, (B) CM_ACE, (C)

ACE_ACE, (D) ACE_CM and (E) Blank (Dashed line: experimental results, Solid line: model results)

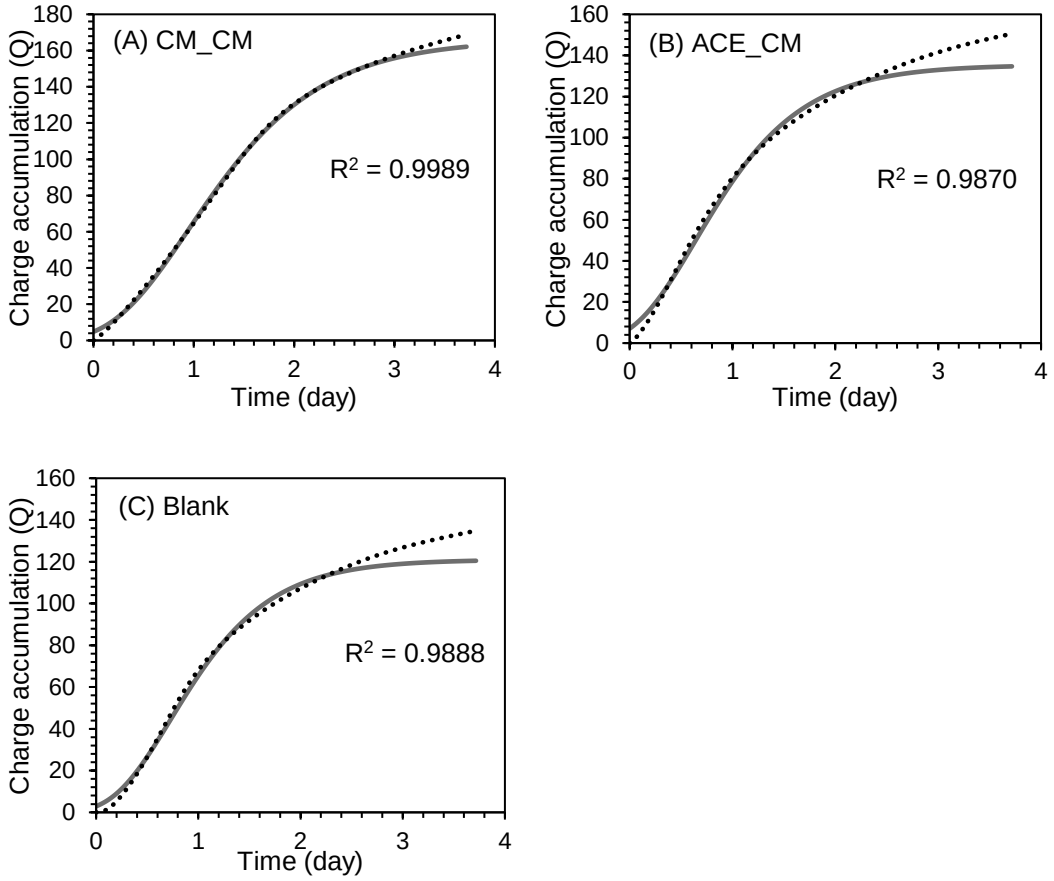

Figure D.3. The modifed Gompertz model fittings of charge accumulation at 1800 mg/L sCOD concentration during Set 1 (A) CM_CM, (B) ACE_CM, (C) Blank, (Dashed line: experimental results, Solid line: model results)

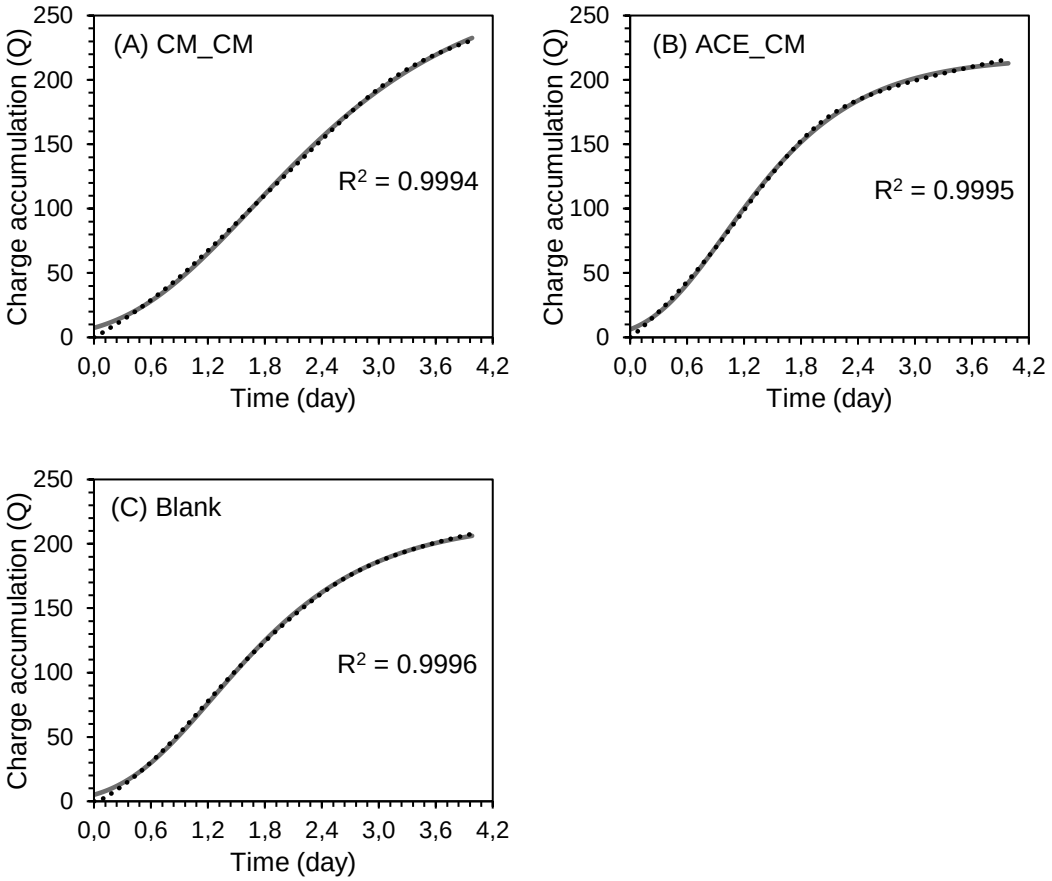

Figure D.4. The modifed Gompertz model fittings of charge accumulation at 2400 mg/L sCOD concentration during Set 1 (A) CM_CM, (B) ACE_CM, (C) Blank, (Dashed line: experimental results, Solid line: model results)

E. The Modified Gompertz Fittings of Methane Production in Set 2

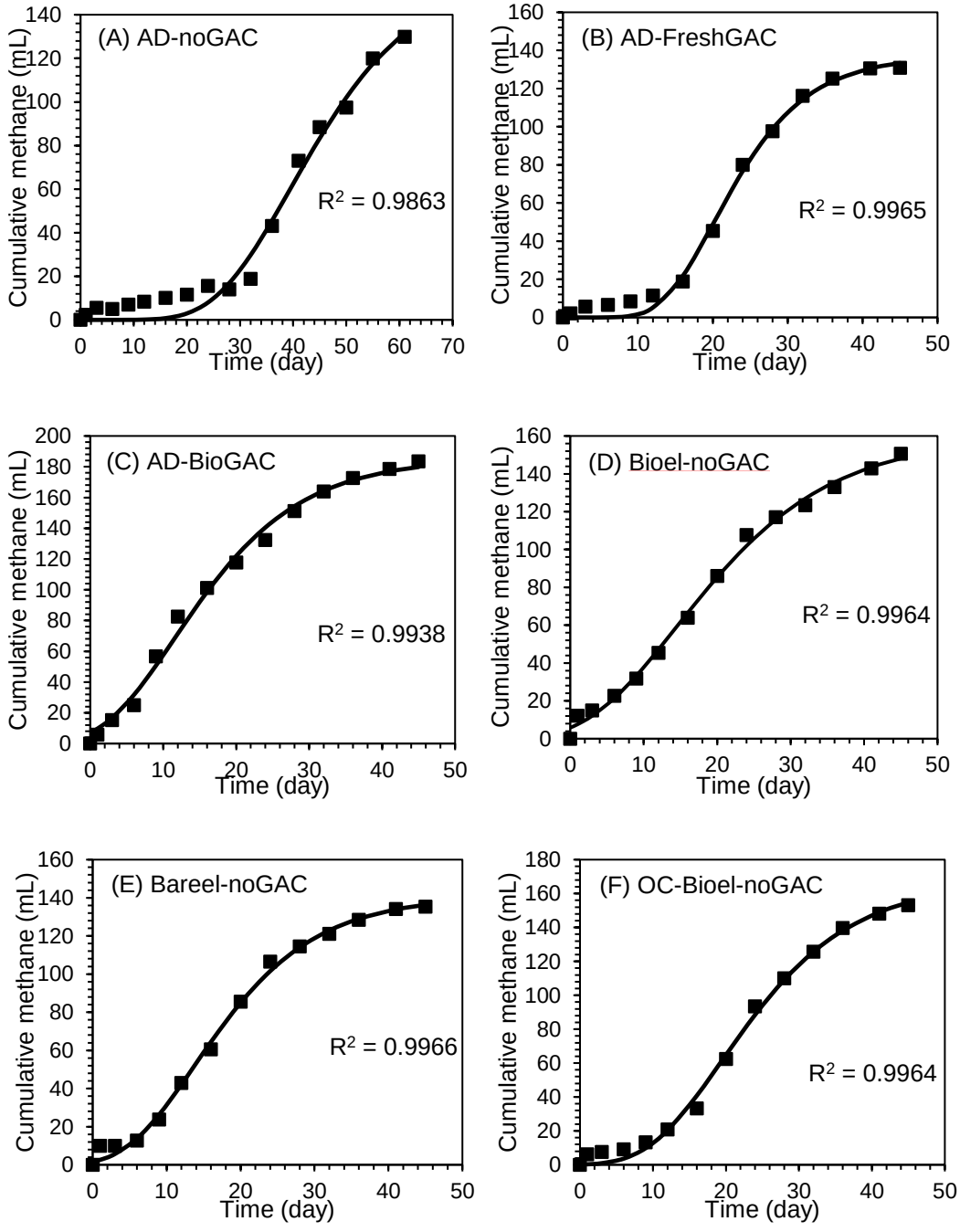

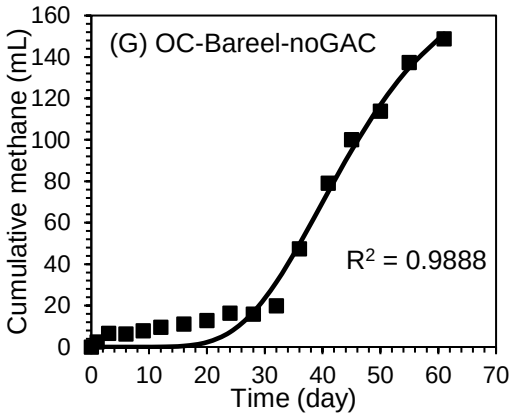
(G) OC-Bareel-noGAC
Cumulative methane (mL)
Time (day)
R2 = 0.9888

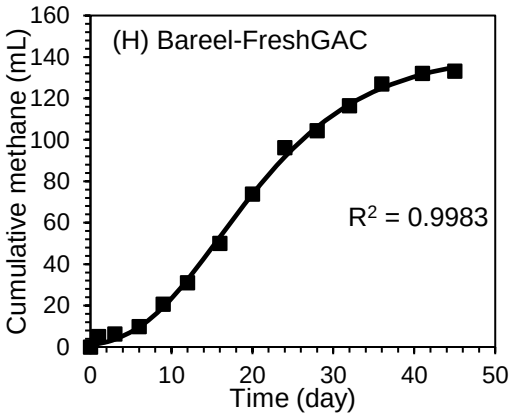
(H) Bareel-FreshGAC
Cumulative methane (mL)
Time (day)
R2 = 0.9983

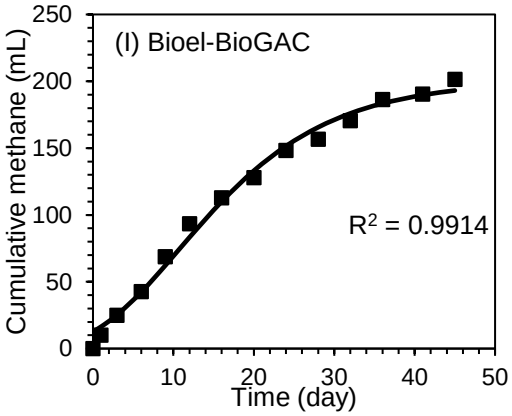
(I) Bioel-BioGAC
Cumulative methane (mL)
Time (day)
R2 = 0.9914

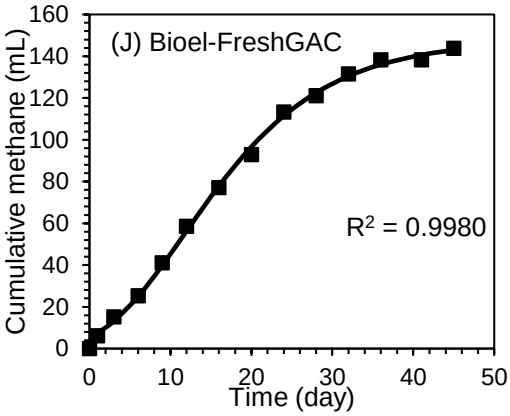
(J) Bioel-FreshGAC
Cumulative methane (mL)
Time (day)
R2 = 0.9980

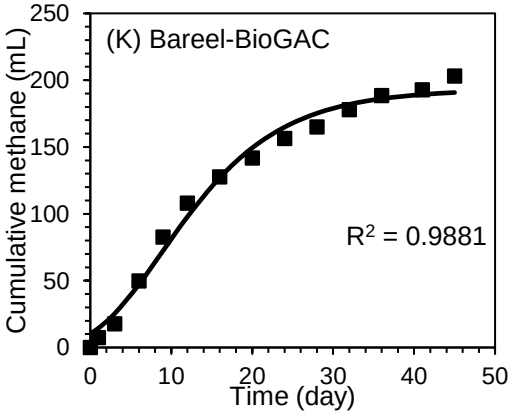
(K) Bareel-BioGAC
Cumulative methane (mL)
Time (day)
R2 = 0.9881

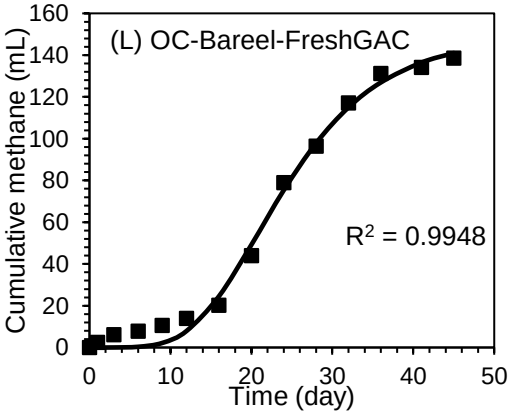
(L) OC-Bareel-FreshGAC
Cumulative methane (mL)
Time (day)
R2 = 0.9948

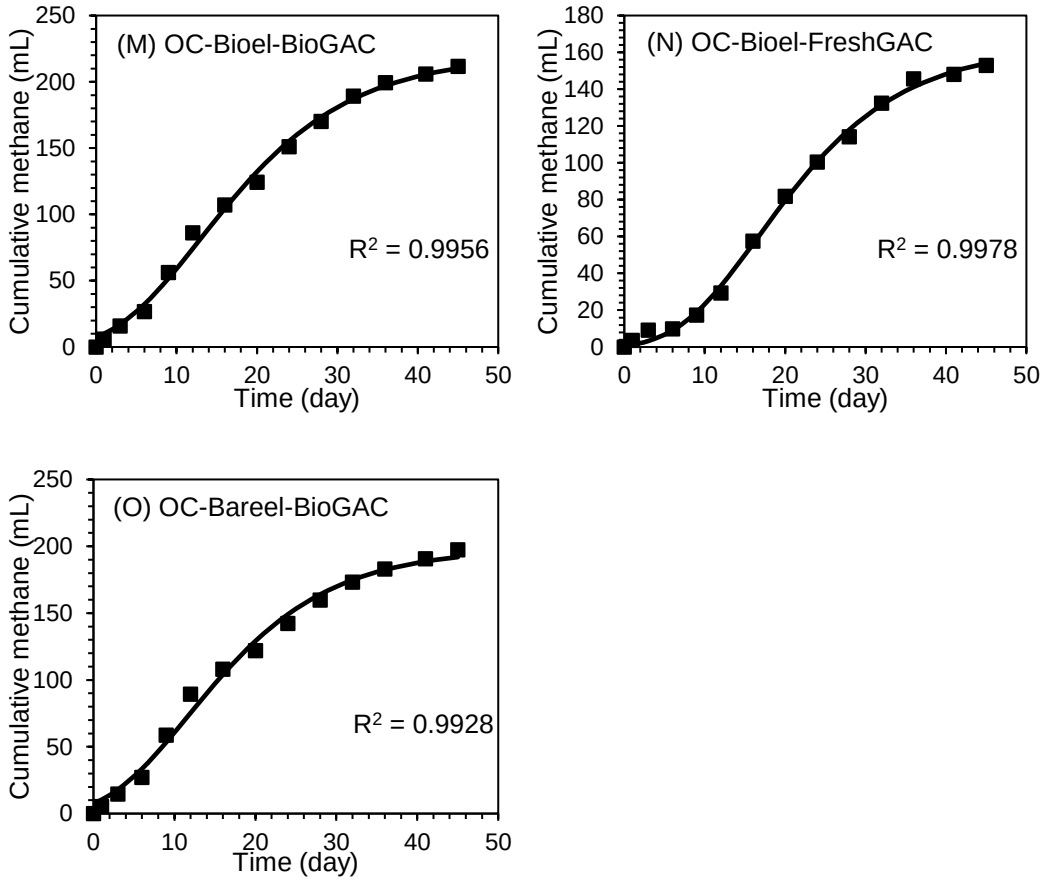

Figure E.1. The modifed Gompertz model fittings of cumulative methane production with 100 mM PBS media during Set 2 (Dots: experimental results, Solid line: model results)

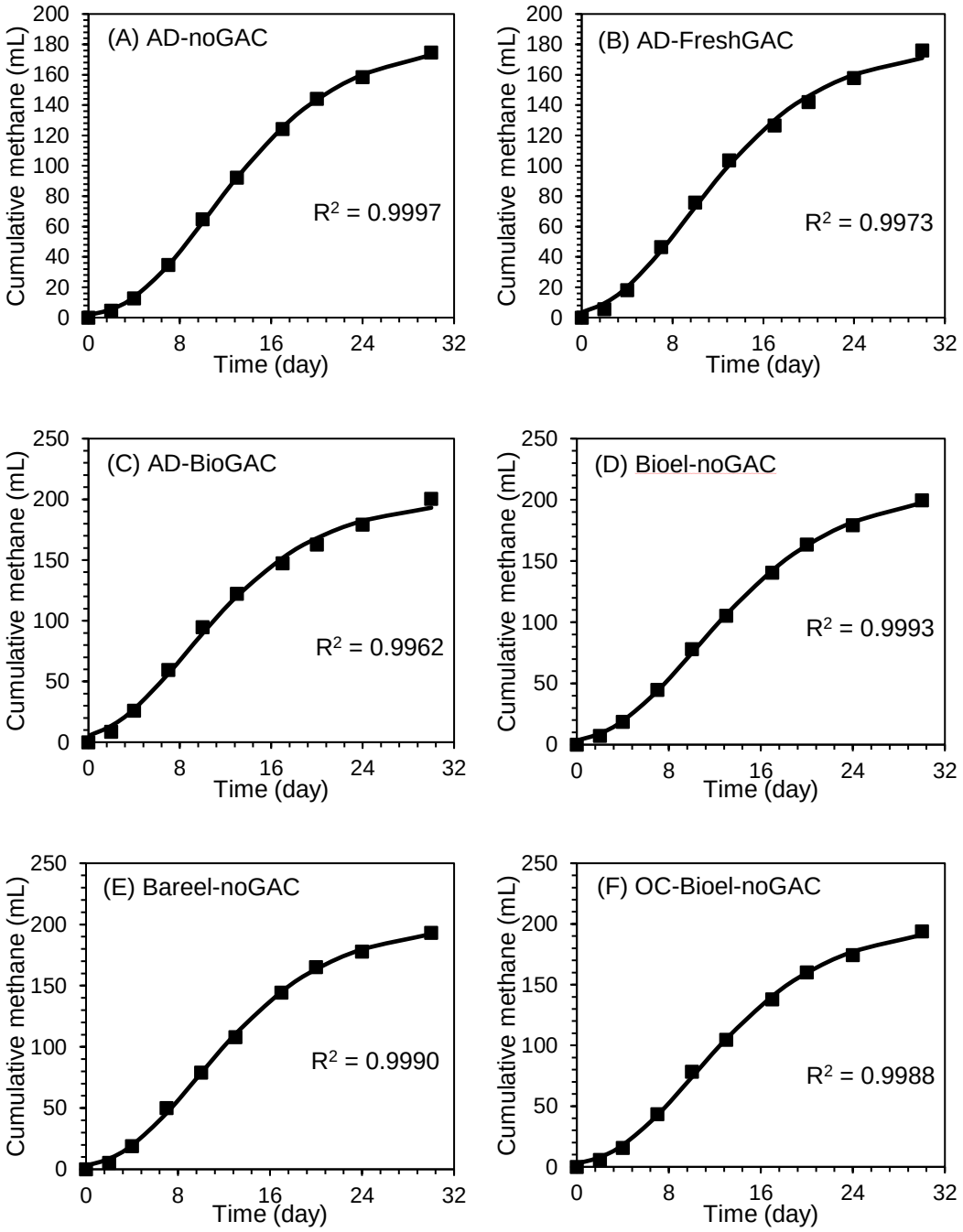
(A) AD-noGAC
R2 = 0.9997
(B) AD-FreshGAC
R2 = 0.9973
(C) AD-BioGAC
R2 = 0.9962
(D) Bioel-noGAC
R2 = 0.9993
(E) Bareel-noGAC
R2 = 0.9990
(F) OC-Bioel-noGAC
R2 = 0.9988
Cumulative methane (mL)
Time (day)

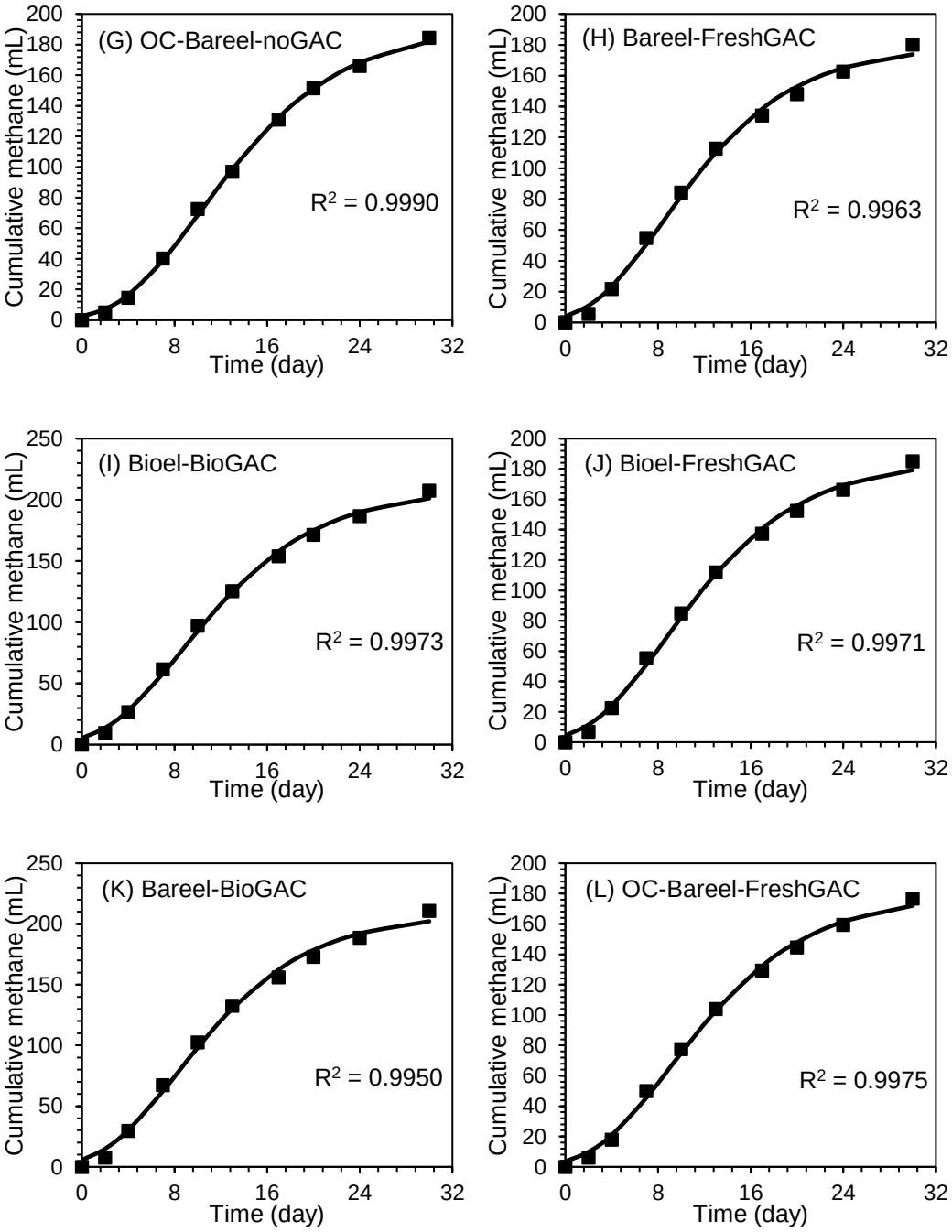
(G) OC-Bareel-noGAC
R2 = 0.9990
(H) Bareel-FreshGAC
R2 = 0.9963
(I) Bioel-BioGAC
R2 = 0.9973
(J) Bioel-FreshGAC
R2 = 0.9971
(K) Bareel-BioGAC
R2 = 0.9950
(L) OC-Bareel-FreshGAC
R2 = 0.9975
Cumulative methane (mL)
Time (day)

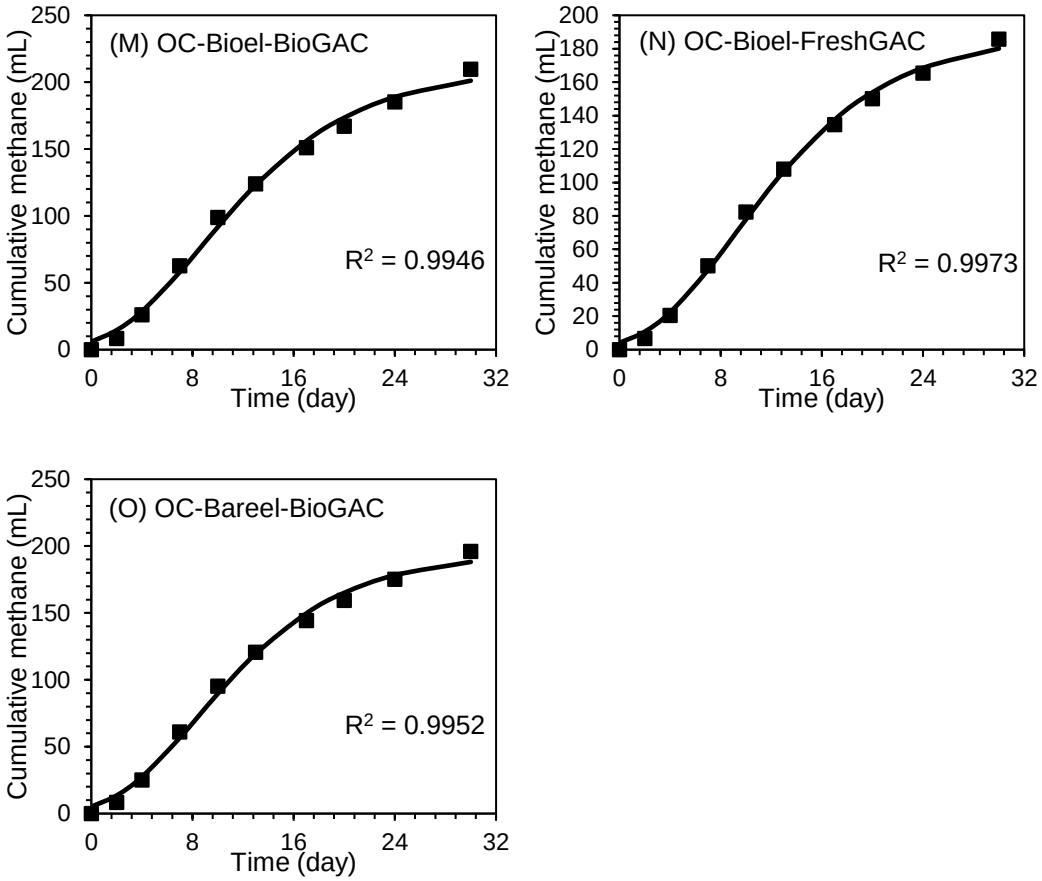

Figure E.2. The modifed Gompertz model fittings of cumulative methane production with salt media during Set 2 (Dots: experimental results, Solid line: model results)

F. Current density graphs for duplicates in Set 2

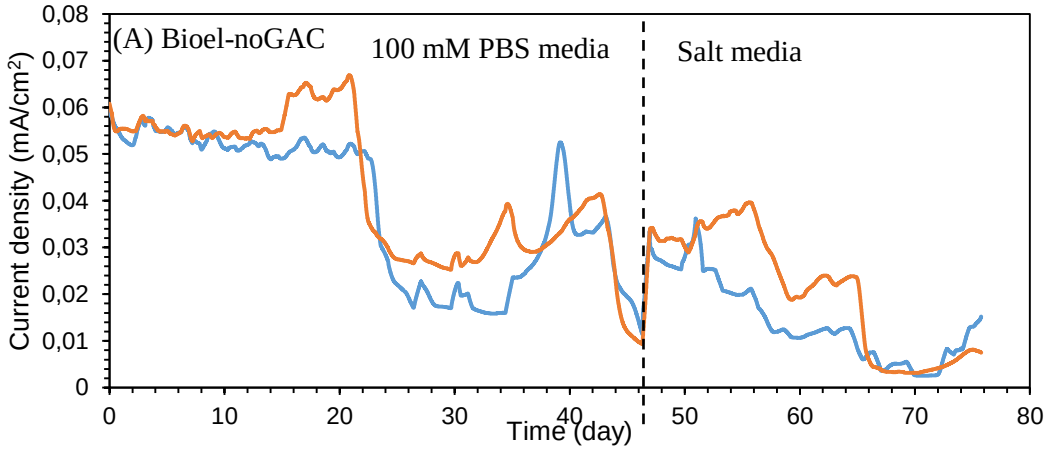

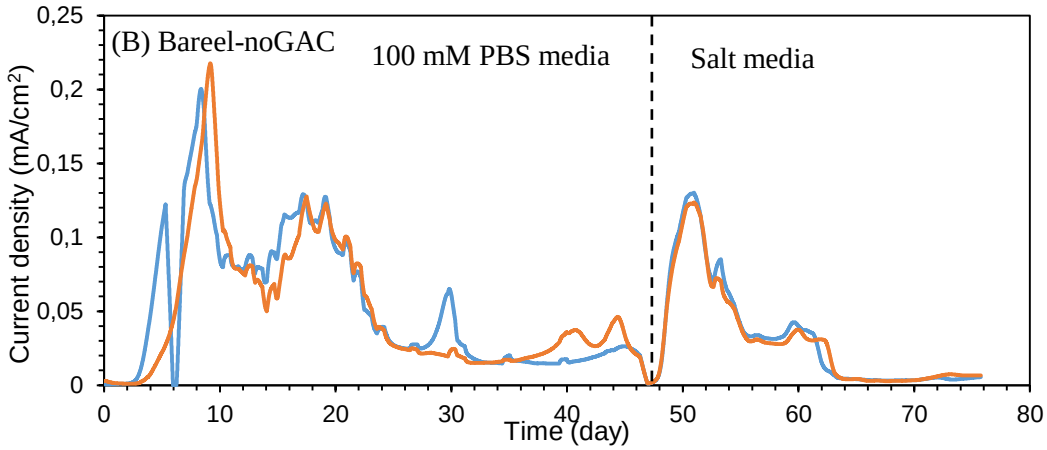

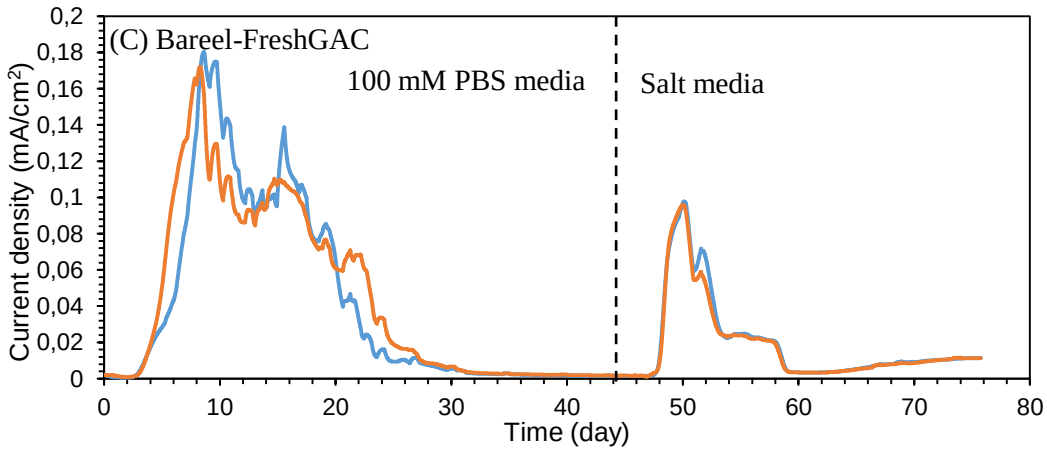

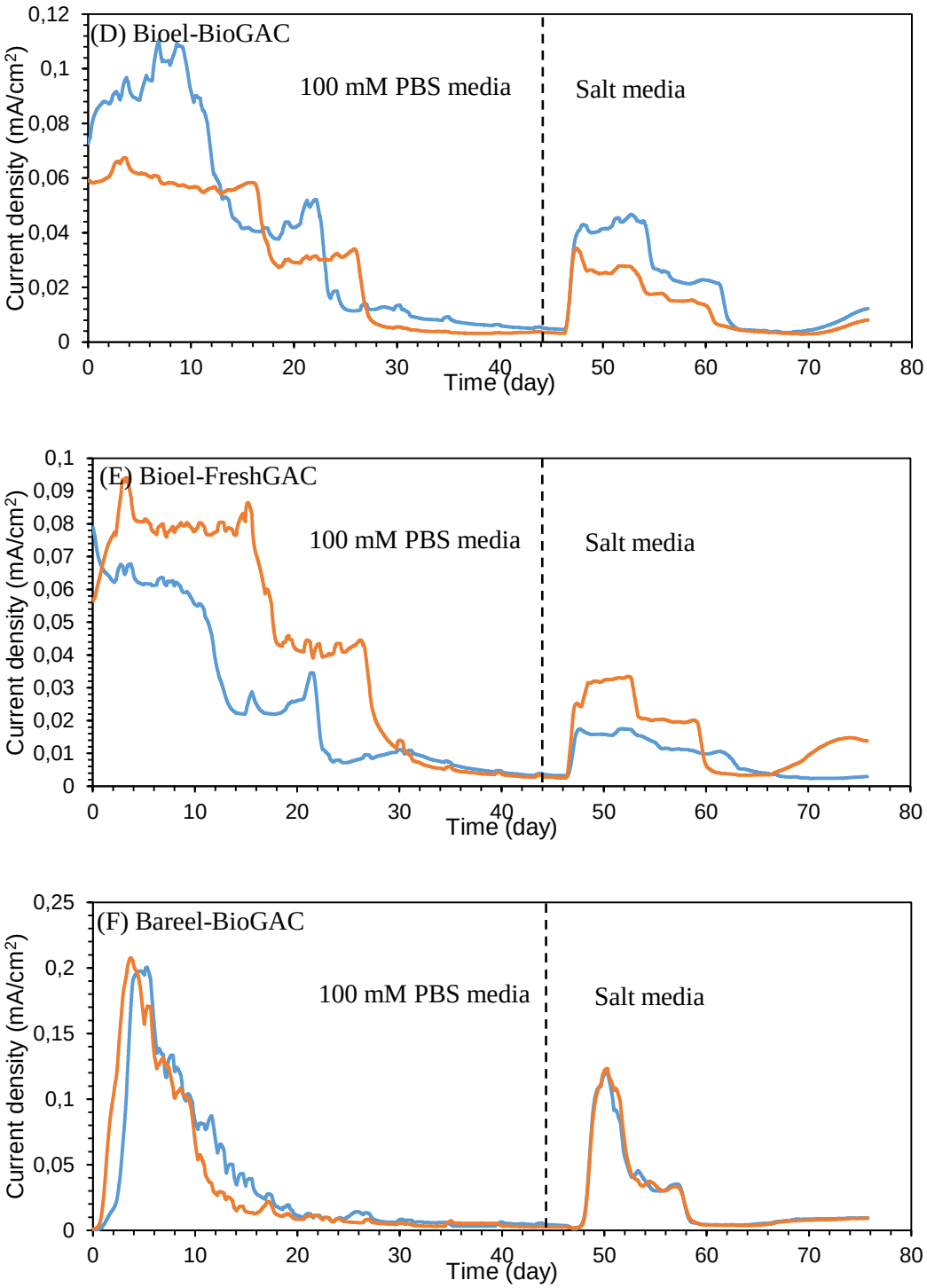

Figure F.1 Current density graphs for duplicates in Set 2 (A) Bioel-noGAC, (B) Bareel-noGAC, (C) Bareel-FreshGAC, (D) Bioel-BioGAC, (E) Bioel-FreshGAC, and (F) Bareel-BioGAC